INFORMATION TO USERS

This manuscript has been reproduced from the microfilm master. UMI films the text directly from the original or copy submitted. Thus, some thesis and dissertation copies are in typewriter face, while others may be from any type of computer printer.

The quality of this reproduction is dependent upon the quality of the copy submitted. Broken or indistinct print, colored or poor quality illustrations and photographs, print bleedthrough, substandard margins, and improper alignment can adversely affect reproduction.

In the unlikely event that the author did not send UMI a complete manuscript and there are missing pages, these will be noted. Also, if unauthorized copyright material had to be removed, a note will indicate the deletion.

Oversize materials (e.g., maps, drawings, charts) are reproduced by sectioning the original, beginning at the upper left-hand corner and continuing from left to right in equal sections with small overlaps.

Photographs included in the original manuscript have been reproduced xerographically in this copy. Higher quality 6" x 9" black and white photographic prints are available for any photographs or illustrations appearing in this copy for an additional charge. Contact UMI directly to order.

ProQuest Information and Learning
300 North Zeeb Road, Ann Arbor, MI 48106-1346 USA
800-521-0600



Downloaded from SHAREOK. Persistent Handle URL: https://hdl.handle.net/11244/359

UNIVERSITY OF OKLAHOMA

GRADUATE COLLEGE

MAGNETIC MINERALS – UNDERSTANDING THE PROCESSES OF FORMATION IN SOILS AND CLAYS AND IDENTIFYING THEIR PRESENCE IN THE ROCK RECORD

A Dissertation

SUBMITTED TO THE GRADUATE FACULTY

in partial fulfillment of the requirements for the

degree of

Doctor of Philosophy

By

MONIKA COGOINI
Norman, Oklahoma
2001

UMI Number: 3023441

Copyright 2001 by
Cogoini, Monika

All rights reserved.



UMI Microform 3023441
Copyright 2001 by Beii & Howeil Information and Learning Company.
All rights reserved. This microform edition is protected against
unauthorized copying under Title 17, United States Code.

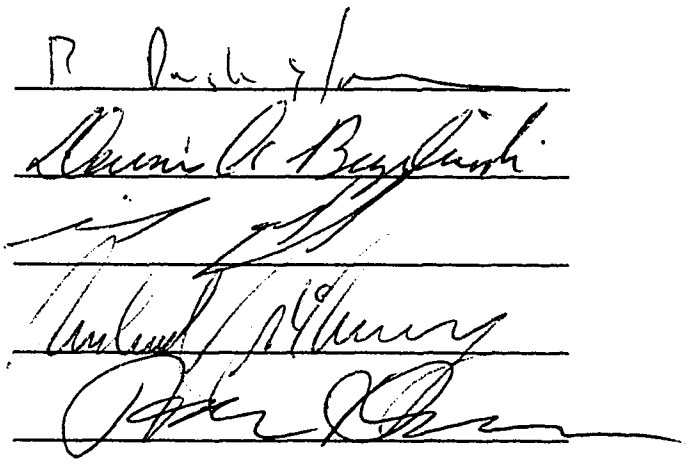
Beli & Howeii Information and Learning Company
300 North Zeeb Road
P.O. Box 1346
Ann Arbor, MI 48106-1346

© Copyright by MONIKA COGOINI 2001
All Rights Reserved.

MAGNETIC MINERALS – UNDERSTANDING THE PROCESSES OF FORMATION IN SOILS AND CLAYS AND IDENTIFYING THEIR PRESENCE IN THE ROCK RECORD

A Dissertation APPROVED FOR THE
SCHOOL OF GEOLOGY AND GEOPHYSICS

BY



DEDICATION

In Liebe und Dankbarkeit

für meine Eltern

und Brüder

ACKNOWLEDGEMENTS

So many people helped during the process of developing ideas, conducting research, and with the write up of this dissertation that it would probably take an entire chapter to mention everyone. I am grateful to all people involved, but I would like to mention some people by name for their special contributions. I wish to thank my advisor Dr. R. D. Elmore for the support he provided despite my excursions into other fields and for the many things he taught me during my years in the Ph.D. program. The research on the first chapter would not have been possible without the devotion of Dr. M. J. McInerney to patiently teach a geologist an understanding of the world of microbes and the like. I am grateful for his guidance and discussions concerning the development of the project involving microbiological aspects. The benefits reached far beyond the research of the first chapter. I wish to express my appreciation to Dr. M. H. Engel for many helpful suggestions concerning the clay diagenesis project and for allowing me to use his laboratory facilities and for providing valuable resources. Special thanks to Dr. D. A. Bazylinski (Iowa State University) for his encouragement and for never getting tired of answering my questions. I also wish to thank Dr. T. Dewers for reviewing this dissertation and for his helpful comments and suggestions along the way. In addition to my committee members, I would like to extend my thanks to Dr. G. S. Soreghan for the original idea and her collaboration on the fourth chapter of this dissertation. I thank Dr. W. Harrison (Colorado School of Mines) for the XRD analyses.

For all the good things he has brought to my life for the past decade and for his encouragement, friendship, and tremendous support in all aspects of this work – I wish to express my sincere gratitude to my fiancé, Dr. Bodo Katz. I would also like to thank Dr. Ann M. Hirt (ETH Zurich,

Switzerland) for her friendship and many interesting and helpful discussions we have had since we met. Many thanks to the people at the Institute for Rock Magnetism at the University of Minnesota who made this work possible with their kind support and for numerous discussions - special thanks to Dr. Mike Jackson and Dr. Stefanie Brachfeld.

I am very grateful to Neil Wofford for his exceptional willingness to help and teach me the microbiological laboratory techniques necessary to conduct the work for chapter 1 - even at the most impossible times. Many other people have helped with field and laboratory work or other aspects of the research on the different projects: my appreciation to Jesus Maza, Dr. Antonio Acosta-Vigil, Kristy Tramp, Kulwadee Lawwongnam-Pigott, Dr. Barbara J. Smallwood, Rick Meinhardt, Mike Hsieh, Dr. Vladimir Andrusevich, Aisha Ragas, Eric Cox, Dr. Mark Nanny, Michelle Abraham. I would like to extend my thanks to my friends in the U.S. and those across the Atlantic for their encouragement and moral support throughout my time at this university. To the wonderful people who make every students' life easier: for their kindness, extraordinary readiness to help, and competence in all sorts of areas ranging from bureaucratic, financial to such important issues like sharing cakes – a big praise for every member of the office staff.

Financial support for the project of the first chapter was provided by two student grants (GSA and AAPG) and a fellowship from the University of Minnesota to conduct rock magnetic analyses at the Institute for Rock Magnetism. The clay diagenesis project was funded through a DOE grant to Dr. R. D. Elmore. The project written up in the last chapter was supported by NSF grant EAR-9805130 (made out to Dr. G. S. Soreghan) and a GSA student grant.

TABLE OF CONTENTS

	Foreword	1
	References Foreword	3
Chapter 1	**Magnetite Formation by Biological Processes in a Soil Profile Under Different Laboratory Conditions**	**5**
1	Abstract	6
1.1	Introduction	7
1.2	Methods and Materials	11
1.2.1	Sample Collection and Microcosm Preparation	11
1.2.2	Bulk Magnetic Susceptibility Measurements	16
1.2.3	Rock Magnetic Analyses	17
1.2.4	Organic Matter Content	18
1.3	Results and Interpretations	18
1.3.1	Bulk Magnetic Susceptibility – Shallow Core	18
1.3.2	Bulk Magnetic Susceptibility – Deep Core	22
1.3.3	Bulk Magnetic Susceptibility – Comparison of Cores	25
1.3.4	Rock Magnetism	25
1.3.5	Total Organic Carbon (TOC)	33
1.4	Discussion and Summary	33
1.5	Conclusions	37
	References Chapter 1	38
Chapter 2	**Magnetic Enhancements Associated with Low Temperature Heating of Smectites**	**44**
2	Abstract	45
2.1	Introduction	46
2.2	Materials and Methods	49
2.3	Results and Interpretations	52
2.3.1	Bulk Magnetic Susceptibility – Initial Values	52
2.3.2	Bulk Magnetic Susceptibility – Smectites	52
2.3.3	Bulk Magnetic Susceptibility – Other Clays	54
2.3.4	Magnetic Mineralogy	60
2.3.4.1	Smectites	60
2.3.4.2	Other Clays	62
2.4	Discussion	68
2.5	Conclusions	72
	References Chapter 2	74

Chapter 3	**Rock Magnetic Evidence for the Authigenesis of Remanence Carrying Magnetite in Thermally Treated Smectites – An Analogy to Low Burial Conditions**	**78**
3	Abstract	79
3.1	Introduction	80
3.2	Materials and Methods	82
3.3	Results and Interpretations	86
3.3.1	Bulk Magnetic Susceptibility	86
3.3.2	Hysteresis	92
3.3.3	Low Temperature Analysis	97
3.3.4	IRM_{200}, SIRM, ARM	102
3.3.5	X-ray Diffraction	107
3.4	Discussion	109
3.5	Conclusions	112
	References Chapter 3	114
Chapter 4	**Contrasting Rock-Magnetic Characteristics of Two Upper Paleozoic Loessite-Paleosol Profiles**	**116**
4	Abstract	117
4.1	Introduction	118
4.2	Geologic Setting	119
4.3	Methods	122
4.4	Results and Interpretations	123
4.4.1	Bulk Magnetic, Paramagnetic, and Ferrimagnetic Susceptibility	123
4.4.2	Low Temperature Analyses	125
4.4.3	IRM Acquisition and Thermal Decay of IRM	128
4.4.4	Curie Balance, Mössbauer Spectroscopy, Petrography	129
4.5	Discussion and Summary	129
	References Chapter 4	132
	Concluding Remarks	136

LIST OF TABLES

Chapter 1

1.1	Experimental design for the two soil cores	13
1.2	Summary of bulk magnetic susceptibility results	21

Chapter 2

2.1	Experimental design for all investigated clays	51
2.2	Mean bulk magnetic susceptibility – comparison of initial and after progression of the experiments	55

Chapter 3

3.1	Summary of statistics for bulk magnetic susceptibility trends of the three smectites	89

LIST OF ILLUSTRATIONS

Chapter 1

1.1 a-c	Bulk magnetic susceptibility of the shallow core	20
1.2 a-c	Bulk magnetic susceptibility of the deep core	24
1.3 a-b	Thermal demagnetization of low-temperature SIRMs	27
1.4 a-b	Representative IRM acquisition (a) and thermal decay (b)	30
1.5	ARM spectra	32
1.6	Hysteresis loop for live incubation sample	32

Chapter 2

2.1 a-e	Bulk magnetic susceptibility of clays heated to 98°C over time	56
2.2 a-e	Bulk magnetic susceptibility of clays heated to 62°C over time	58
2.3 a-e	IRM acquisition for clay samples before and after heating	64
2.4 a-e	Thermal demagnetization of tri-axial IRM for clay samples after heating	66

Chapter 3

3.1	Bulk magnetic susceptibility of dry smectites heated to 62°C over time	90
3.2	Bulk magnetic susceptibility of wet smectites heated to 62°C over time	91
3.3 a-c	Hysteresis loops for smectites after heating with and without paramagnetic slope correction	93
3.4	Ferrimagnetic susceptibility and saturation magnetization versus bulk magnetic susceptibility	96
3.5 a-c	Thermal demagnetization of low temperature SIRM and cooling of room temperature SIRM for 3 heated smectites	99
3.6	Estimation of remanence and SP contents	101
3.7 a-c	Remanence of smectites before and after heating, IRM_{200}, SIRM-IRM_{200}, and ARM	105
3.8 a-b	X-ray Diffraction of NAu-2 nontronite	108

Chapter 4

4.1	Location and paleogeographic map	121
4.2 a-c	Magnetic susceptibilities and saturation magnetization of loessite-paleosol couplets	124
4.3 a-d	Thermal demagnetization of low-temperature SIRM for loessitic and paleosol samples	127

Foreword

Magnetic minerals form authigenically in soils and sediments, but the processes involved in their formation can be complex and are often a matter of debate. For example, anomalous concentrations in magnetic minerals have been described in soils and their origin has been ascribed to processes including inorganic (Maher & Taylor, 1988) and biological precipitation (e.g., Stanjek et al., 1994). Also, the presence of secondary magnetic minerals in sedimentary rocks has been described and their origin has been related to a variety of geologic processes such as orogenic fluid migration (e.g., McCabe & Elmore, 1989), presence of hydrocarbons (Banerjee et al., 1997), and clay diagenesis (Katz et al., 1998). Developing a better understanding for the conditions by which magnetic minerals form is important because of the information they can provide to decipher the geologic past on Earth and potentially on other planets. Firstly, variations in the magnetic mineral content in loessite-paleosol deposits have been linked to climate (e.g., Zhou et al., 1990; Begét et al., 1990; Liu et al., 1992) and various hypotheses exist concerning their origin such as pedogenic formation of ultra-fine magnetite (Xiuming et al., 1993). Secondly, authigenic formation of magnetite, which can be dated paleomagnetically, is common in the rock record (Elmore & McCabe, 1991) but the origin of the secondary magnetic phase is generally unclear. Thirdly, the presence of magnetic minerals may provide clues towards the recognition of processes and environmental conditions during their time of formation. For instance, the presence of nm-scale magnetite crystals in the meteorite ALH84001 was proposed to be a remnant of life once thriving on Mars based partially on its morphological similarities with magnetite formed by magnetotactic bacteria on Earth (McKay et al., 1996). A biologic origin of the SP magnetite in the meteorite is, however, controversial.

The first chapter of this dissertation investigates the formation of magnetic minerals under a variety of laboratory conditions in a soil profile exposed to hydrocarbons. Magnetite was formed only in biological samples but not in the abiotic counterparts suggesting biological processes may be more important in the formation of magnetic minerals in soils than previously thought. The second chapter is devoted to testing whether changes can be observed in the magnetic signal in a variety of clays heated at temperatures of 62 and 98°C. Bulk magnetic susceptibility (χ_b) increased only in some smectites but not in any of the other tested clays potentially suggesting clay diagenetic processes occurring at low temperature heating can alter the magnetic characteristics of clays. The third chapter takes a closer look at smectites heated to temperatures equivalent to low burial conditions and rock magnetically characterizes the magnetic grains formed. The findings suggest that clay diagenetic processes occurring at low temperatures can lead to the formation of magnetite capable of carrying remanence and thus, provide a viable mechanism for the acquisition of secondary magnetizations in sedimentary rocks. The last chapter deals with a rock magnetic comparison of two Paleozoic loessite-paleosol couplets to investigate whether enhanced χ_b trends in recent paleosols as compared to the loessite can be confirmed in ancient deposits. The results for one couplet are similar to those from the Chinese Loess Plateau, with an enrichment of ferrimagnetic material in the paleosol. The second couplet, however, reveals that the variations in the χ_b can be more complex and shows the importance of combining rock magnetic with sedimentologic evidence in order to identify the origin and preservation of χ_b patterns in geologic deposits.

References Foreword

Banerjee, S., R.D. Elmore, and M.H. Engel, Chemical remagnetization caused by burial diagenesis: Testing the hypothesis in the Pennsylvanian Belden formation, Colorado, *Journal of Geophysical Research, 102*, 24825-24842, 1997.

Begét, J.E., D.B. Stone, and D.B. Hawkins, Paleoclimatic forcing of magnetic susceptibility variations in Alaskan loess during the late Quaternary, *Geology, 18*, 40-43, 1990.

Elmore, R.D., and C.R. McCabe, The occurrence and origin of remagnetization in the sedimentary rocks of North America, in *Contributions in Geomagnetism and Paleomagnetism*, pp. 377-383, U.S. Nat. Rep. Int. Union Geod. Geophys. 1987-1990, 1991.

Katz, B., R.D. Elmore, M. Cogoini, and S. Ferry, Widespread chemical remagnetization: Orogenic fluids or burial diagenesis of clays? *Geology, 26*, 603-606, 1998.

Liu, X.M., J. Shaw, T.S. Liu, F. Heller, and B. Yuan, Magnetic mineralogy of Chinese loess and its significance, *Geophysical Journal International, 108*, 301-308, 1992.

Maher, B.A., and R.M. Taylor, Formation of ultra-fine-grained magnetite in soils, *Nature, 336*, 368-371, 1988.

McCabe, C., and R.D. Elmore, The occurrence and origin of late Paleozoic remagnetization in the sedimentary rocks of North America, *Reviews of Geophysics, 27*, 471-494, 1989.

McKay, D.S., E.K. Jr. Gibson, K.L. Thomas-Keprta, H. Vali, C.S. Romaneck, S.J. Clemett, X.D.F. Chillier, C.R. Mächling, and R.N. Zare, Search for past life on Mars: Possible relic biogenic activity in Martian meterorite ALH84001, *Science, 273*, 924-930, 1996.

Stanjek, H., J.W.E. Fassbinder, H. Vali, H. Wägele, and W. Graf, Evidence of biogenic greigite (ferrimagnetic Fe_3S_4) in soil, European Journal of Soil Science, 45, 97-103, 1994.

Xiuming, L., J. Shaw, L. Tungsheng, and F. Heller, Magnetic susceptibility of the Chinese loess-palaeosol sequence: environmental change and pedogenesis, *Journal of the Geological Society, 150*, 583-588, 1993.

Zhou, L.P., F. Oldfield, A.G. Wintle, S.G. Robinson, and J.T. Wang, Partly pedogenic origin of magnetic variations in Chinese loess, *Nature, 346*, 737-739, 1990.

CHAPTER 1

Magnetite Formation by Biological Processes in a Soil Profile Under Different Laboratory Conditions

1 Abstract

Authigenesis of magnetite occurred due to biological factors but not in abiotic controls in a laboratory-treated hydrocarbon-exposed silty clay loam collected near Clearview, Oklahoma. Bulk magnetic susceptibility (χ_b) increased with time in live incubations from a shallow core (5-12 cm depth) with hydrogen, methane, oxygen, methane plus oxygen or no amendment (nitrogen atmosphere). Results from a deeper core (15-22 cm depth) confirmed a biological origin of increases in χ_b which was observed in live incubations that did not receive oxygen. In addition, an increase in χ_b in positive controls (inoculated with *Geobacter metallireducens*) similar to that observed in the live incubation samples suggested that bacterial iron reduction is a viable mechanism of magnetic mineral formation in these soils. Thermal demagnetization of low temperature saturation remanence indicated the presence of multi-domain and/or single-domain magnetite and superparamagnetic grains. An increase in the Verwey transition and higher room temperature remanence after treatment to enhance the amount of iron-reducing bacteria indicated an increasing amount and/or growth of magnetite grains. Based on acquisition and thermal decay patterns of isothermal remanent magnetizations, magnetite was the dominant remanence carrier in the soil, but pyrrhotite and goethite were present as well. Hysteresis measurements confirmed an increase in the ferrimagnetic material in the live incubations. This study shows that a hydrocarbon exposed soil has the biological potential to form magnetite of a broad grain size spectrum. Biogenic formation of magnetic minerals in some soils may be a common process and thus, maybe more important than abiotic reactions alone in soils similar to the one examined.

1.1 Introduction

Previous researchers have documented the presence of magnetic minerals in some soils (e.g., Fassbinder & Stanjek, 1994) and an up-profile increase in the magnetic mineral content possibly related to the age of the soil has also been reported (Maher & Taylor, 1988). The types of magnetic minerals present can be diverse and their origins may be difficult to identify.

While some of the magnetic material in soils may be detrital in origin, others may be formed authigenically via inorganic/abiological (e.g., Maher & Taylor, 1988) or biological processes (e.g., Stanjek et al., 1994). The chemical conditions characterizing an environment, such as E_h and pH as well as the activity of chemical species, determine whether a milieu is thermodynamically favorable for magnetic mineral formation. However, natural environments are often not at equilibrium and microbiological factors may prevent or enable reactions, for example by changing local E_h and pH conditions (Bell et al., 1987).

Taylor et al. (1987) were able to create magnetite inorganically under conditions comparable to soil formation and found the magnetic grains to be similar to those found in soils. Circumstantial evidence for the inorganic formation of authigenic superparamagnetic (SP) magnetite was found in two brown earth soils from the UK (Maher & Taylor, 1988).

Machel and Burton (1991) and Machel (1995) suggested that prevailing conditions in hydrocarbon-exposed environments are conducive to the formation of minerals such as magnetite, pyrrhotite, pyrite, and siderite. The authors describe E_h-pH stability fields that are thermodynamically favorable for these minerals and are based on the presence of petroleum contamination. Machel (1996) proposed that knowledge of thermodynamic constraints and

microbiological factors in areas of hydrocarbon seepage may allow for the prediction of magnetic phases that form near the surface and in the subsurface. The applicability of this idea however, has not been explored in natural samples.

Besides chemical conditions, various groups of microorganisms can cause the formation of magnetic minerals. Iron-reducing bacteria form magnetic minerals in a process referred to as "biologically induced", i.e. the magnetic minerals form extracellularly as a byproduct resulting from the reduction of ferric iron (Lovley et al., 1987; Lovley, 1990; Stolz et al., 1990). Iron reducers release the ferrous iron into their surroundings where the ions react with compounds such as ferric oxyhydroxides to form a new magnetic phase. The magnetic grains produced by iron-reducing bacteria are dominantly SP magnetite and resemble those that are formed inorganically (Moskowitz et al., 1989; Sparks et al., 1990).

Magnetotactic bacteria create chains of magnetic crystals internally, i.e. biologically controlled and utilize them for navigation (e.g., Frankel et al., 1985; Bazylinski et al., 1993; Bazylinski, 1996). The magnetic grains produced can be uniquely characterized via a combination of rock magnetic and spectroscopic methods due to their specific grain shapes and size range (Moskowitz et al., 1989, 1993; Bazylinski & Moskowitz, 1997).

Sulfate-reducing bacteria are also capable of creating iron biominerals. These bacteria may use ferric iron instead of sulfate as their terminal electron acceptor and release the reduced iron into the environment (Coleman et al., 1993; Lovley et al., 1993) where a reaction with iron oxyhydroxides in the surroundings could lead to the formation of a new magnetic phase. Sakaguchi et al. (1993) described the synthesis of intracellular magnetite in a dissimilatory

sulfate-reducing organism that is also capable of causing external precipitation of iron sulfides. Sulfate-reducing bacteria may also be involved in a more indirect formation of iron sulfides by releasing H_2S into the environment, which chemically reduces iron oxyhydroxides (Morse et al., 1987).

All three types of bacteria occur in a variety of environments. Iron-reducing bacteria are common in soils and sediments. They have been reported in freshwater systems (Lovley & Phillips, 1986; Bell et al., 1987; Lovley, 1991) and have also been found at hydrocarbon-contaminated sites (e.g., Anderson et al., 1999). Magnetotactic bacteria have been described in freshwater environments (e.g., Blakemore et al., 1979; Hawthorne & McKenzie, 1993) as well as in marine settings (e.g., Bazylinski et al., 1988; Karlin et al., 1987; Stolz et al., 1986). Konhauser (1998) listed a variety of environments providing suitable habitats for magnetotactic bacteria. Some sulfate-reducing bacteria were found in freshwater habitats (Sakaguchi et al., 1993), while others were isolated from a salt-marsh (Coleman et al., 1993). Sulfate reducers are also capable of thriving under hydrocarbon-contaminated conditions (e.g., Weiner & Lovley, 1998; Lovley et al., 1995).

The most common biogenically formed magnetic mineral is magnetite (e.g., Karlin et al., 1987; Lovley et al., 1987; Bazylinski et al., 1988; Sparks et al., 1990; Sakaguchi et al., 1993), but iron sulfides like greigite (Mann et al., 1990; Stanjek et al., 1994; Pósfai et al., 1998) and pyrrhotite (Farina et al., 1990) may also be produced. The resemblance of inorganically formed magnetic minerals to those produced by some organisms like iron-reducing bacteria makes it

difficult to determine the origin of a variety of magnetic phases present within soils and sediments.

Understanding the magnetic mineral forming mechanisms in soils is important. Deciphering the role of microorganisms may help elucidate their potential contribution to the magnetic signal in soils and paleosols. In particular, conditions under which magnetic minerals may be biologically produced, for example by iron-reducing bacteria, need to be understood. Most studies mentioned above dealt with optimized laboratory conditions promoting growth of bacteria or addressed theoretical considerations. The aim of this study was to explore the possibility of formation of iron biominerals in a hydrocarbon-contaminated soil profile under a variety of laboratory conditions and without specifically inducing microbial growth. Several conditions, including some involving the addition of oxygen and others that did not receive oxygen, were tested on the soil profile by measuring χ_b over time. Additionally, positive controls using a *Geobacter metallireducens* culture, and abiotic control samples were measured to test biologic feasibility and a possible chemical origin of magnetic changes, respectively. Furthermore, a variety of rock magnetic techniques were applied to identify, characterize and compare biologically active, positive and chemical controls with respect to their magnetic mineral content.

1.2 Methods and Materials

1.2.1 Sample Collection and Microcosm Preparation

Samples from a soil profile were collected near Clearview, Oklahoma under aseptic conditions using autoclaved teflon liners that were capped with sterilized teflon tape. The soils of the profile were retrieved above a depleted oil field with a recent history of contamination with hydrocarbons (Pyle, 1996). The soil was sampled along two horizontal cores of 33 cm length taken at depths of 5-12 cm and 15-22 cm. The shallow core consisted of a dark, grayish-brown, silty clay loam that contained abundant decomposing plant material. This decaying organic matter was commonly surrounded by a halo of soil (usually less than 1 mm) where the coloration changed to a yellowish tint. The soil contained in the deep core was a silty clay loam, dark grayish- to greenish-brown in color, with noticeably less plant material and fewer yellowish lenses than the shallow core. Both cores were placed inside an anaerobic chamber (Balch & Wolfe, 1976) immediately after returning from the study site in order to minimize changes in the redox conditions. Prior to weighing the soil in sterilized serum bottles, each core was homogenized in a sterilized beaker using aseptic teflon and porcelain tools. To each serum bottle, 20 g of moist soil were added, which was equivalent to approximately 18.6 g of air-dried mass. The latter value was used for mass normalization purposes in the χ_h measurements described below. Each serum bottle was closed with a rubber stopper and crimped with an aluminum seal prior to taking it outside the chamber for further treatment.

Replicate serum bottles from each core were exposed to a variety of experimental conditions. A summary of the experimental design including the different conditions and number of

replicates is provided in Table 1.1. The headspace of all of the serum bottles was exchanged by evacuation with vacuum and repressurization 3 times with 100 % N_2 (approximately 30 kPa) using sterile syringes with sterile cotton filters (Balch & Wolfe, 1976). Four serum bottles inoculated with soil of the shallow core received one of the following treatments: 446 μmol of CH_4; 450 μmol of CH_4 plus 180 μmol of O_2; 900 μmol of O_2 or no treatment (unamended control). The headspace of four serum bottles inoculated with soil from the shallow cores was exchanged as described above with 100 % H_2 (35 kPa). The same treatments were applied to three serum bottles inoculated with the soil of the deep core. Gases were added using sterile syringes, needles, and microfilters. Syringes were flushed repeatedly with the gas before insertion into the serum bottles. Nitrogen amended soil served as the unamended control to test if magnetic mineral formation occurred without significant alteration of the chemical conditions. Methane was amended to investigate whether light hydrocarbons that easily seep into soils overlying hydrocarbon reservoirs can cause authigenesis of magnetic minerals. The addition of methane plus oxygen was used to test if microaerophilic conditions – which are favorable for some magnetotactic bacteria (Bazylinski & Moskowitz, 1997) – could be responsible for magnetic mineral formation. Hydrogen was used because most known iron reducers are able to use it as an electron donor for Fe(III) reduction. By adding only oxygen to serum bottles, magnetic mineral formation under potentially aerobic conditions was tested.

Core	Condition → / Set ↓	other conditions	N_2	H_2	CH_4	$CH_4 + O_2$	O_2
Shallow	**Live Incubation**	no medium	2	2	2	2	2
		with medium	2	2	2	2	2
Shallow	**Positive Control**	no medium	2	2	2	2	2
		with medium	2	2	2	2	2
Shallow	**Abiotic Control**	no medium	2	2	2	2	2
		with medium	2	2	2	2	2
Deep	**Live Incubation**	no medium	2	2	2	2	2
		with medium	1	1	1	1	1
Deep	**Positive Control**	no medium	2	2	2	2	2
		with medium	1	1	1	1	1
Deep	**Abiotic Control**	no medium	2	2	2	2	2
		with medium	1	1	1	1	1

Table 1.1: Experimental design indicating the number of replicates for each treatment. Positive control samples were inoculated with a *Geobacter metallireducens* culture. Some samples received a mineral medium with acetate and either a bicarbonate or PIPES buffer which contains no bicarbonate.

One replicate of each treatment received 10 ml of a bicarbonate-buffered, acetate mineral medium (Lovley & Phillips, 1988) to determine if nutrient addition stimulated magnetic mineral formation. Since high concentrations of bicarbonate may lead to siderite precipitation, another replicate of serum bottles inoculated with soil of the shallow core received 10 ml of the acetate mineral medium buffered with 50 mM PIPES (piperazine-N,N'-bis 2-ethanesulfonic acid) and was adjusted to circumneutral pH. A second set of serum bottles inoculated with soil from both cores was prepared as above and then each bottle received 4 ml of a culture of *Geobacter metallireducens* strain GS 15 and served as positive controls. A third set of serum bottles inoculated with soil from each core was prepared as described above and then autoclaved twice (121°C, 20 minutes each cycle) and served as abiotic controls.

The mineral medium contained the following reagents: sodium acetate (0.82 g/l), $CaCl_2$ (0.1 g/l), NaCl (0.1 g/l), KH_2PO_4 (0.6 g/l), NH_4Cl (1.5 g/l), yeast extract (0.1 g/l), a trace mineral (10 ml) and a vitamin solution (10 ml) (Tanner, 1997), and sodium bicarbonate (2.5 g/l) as a pH buffer. The pH of the medium was adjusted to 6.9-7.0. The medium was boiled under an 80 % N_2: 20 % CO_2 gas phase, stoppered, sealed with an aluminum seal, and autoclaved (121°C; 15 minutes). The same recipe was used for the PIPES-buffered medium (50 mM).

Geobacter metallireducens was grown in the above mineral medium with 10 mM sodium acetate and iron-nitrilo-triacetic acid (NTA) as the electron acceptor. Iron-NTA solution was prepared by adding 1.64 g $NaHCO_3$, 2.56 g nitrilo-triacetic acid (NTA), and 2.70 g $FeCl_3$ to 100 ml of deionized H_2O. The pH was adjusted to 6.3 to 6.9. The suspension was filtered using a 0.45 and 0.25 μm Nalgene filter apparatus. The filtrate was then passed through a 0.2 μm syringe filter

into a sterile serum bottle with 100 % N_2. The solution was degassed by evacuation under vacuum and repressurization with 100 % N_2. Ten ml of the sterile iron-NTA solution was added to 90 ml of 10 mM sterile acetate mineral medium in serum bottles using degassed sterile syringes and needles (Balch & Wolfe, 1976). The serum bottles were inoculated with 40 ml of a *Geobacter metallireducens* culture grown with the same medium. The cultures were incubated at 34°C without shaking for 36 hours prior to adding them as positive controls for the soil samples.

A methane-treated live incubation after 180 days of incubation was used to determine if enhancing the growth of iron-reducing bacteria would increase magnetic mineral formation. The sample was split into 6 sterile vials inside the anaerobic chamber. Nine millilitres of acetate mineral medium with bicarbonate buffer and 1 ml of a ferric oxyhydroxide solution were added to each vial. The vials were stoppered and crimped with an aluminum seal and removed from the anaerobic chamber. The headspace of each vial was aseptically exchanged with 80 % H_2 : 20 % CO_2 as described above. Three of them were then autoclaved and served as abiotic controls.

The ferric oxyhydroxide solution was prepared by dissolving 108 g for $FeCl_3$ in 1 l deionized water. The pH was adjusted to 7.0 and excess Cl^- was removed by washing the solution 6 times and by centrifugation each for 30 minutes after resuspension of the ferric precipitate. The χ_b could not be utilized to monitor the magnetic signal because of the small sample size, but the samples were used in low-temperature analyses described below.

1.2.2 Bulk Magnetic Susceptibility Measurements

In order to monitor the magnetic mineral content of the samples, the χ_b was measured for each sample within a few hours after inoculation and periodically thereafter for up to 350 days. Mass normalized χ_b was measured three times at each time interval with a Sapphire SI-2 Instrument. The mean and standard deviation was calculated for each time interval for each sample and if the standard deviation was greater than 12.5 % of the mean χ_b the data were not used in further analyses. The average measurement standard deviation was 4.3 % and 4.1 % of the mean sample χ_b for the shallow and deep cores, respectively. Occasionally, means deviated significantly from the overall average for an individual sample probably due to fluctuations in the instrument performance. These outliers were graphically identified and eliminated. For both cores, the measurements of χ_b at different times were averaged for each sample using all post-initial χ_b measurements. The means of each of the replicates for each treatment were then used to determine the overall mean and standard deviation of the treatment for each core. Since there were no apparent differences in χ_b between samples that received medium or those that did not contain medium, the statistical analyses were conducted on the grouped samples treated under the same experimental condition (e.g., live incubations amended with nitrogen). In order to determine if there were statistically significant differences of the χ_b between live incubations, positive and abiotic control sets, a paired t-test (e.g., Sall & Lehman, 1996) was applied to the means within each set and compared to the Null hypothesis that the mean of the group χ_b is equal to the initial χ_b. An F-test (e.g., Sall & Lehman, 1996) was performed for comparison of the different environmental conditions between groups (live incubation, positive control, and abiotic

control). All χ_b measurements taken after the initial measurements were calculated as percentages of the initial χ_b of each individual sample.

1.2.3 Rock Magnetic Analyses

Representative samples of each horizontal core were chosen for rock magnetic characterization of the magnetic mineralogy and magnetic grains prior to and after the experiment. Prior to conducting the analyses, the soils were freeze-dried. The presence of superparamagnetic (SP) grains and coarser (single-domain [SD] and multi-domain [MD]) magnetite was investigated for ten samples. For this purpose, the thermal decay of a low-temperature saturation isothermal remanent magnetization (SIRM) acquired at 5 or 10°K was recorded on a Magnetic Property Measurement System (MPMS) at the Institute for Rock Magnetism at the University of Minnesota. Hysteresis studies were conducted at the Institute for Rock Magnetism on a Vibrating Sample Magnetometer (VSM) in order to determine the ferrimagnetic portion of the χ_b of live incubations and abiotic soil on three selected samples of the deep core.

For additional measurements, the freeze-dried samples were mixed with a matrix of kaolin and silica and were measured on a 2G, three-axes, cryogenic magnetometer located in a magnetically shielded room. To gain knowledge about the magnetic mineralogy of the soil, a stepwise increase in the isothermal remanent magnetization (IRM) was produced by applying direct fields via an impulse magnetizer and the remanences were recorded on the magnetometer for fourteen samples. In addition, IRMs were acquired along three perpendicular axes in direct

fields of 120, 400, and 2500 mT and were subsequently thermally demagnetized in a magnetically shielded Schonstedt TSD-1 oven (Lowrie, 1990). In order to develop an understanding for the distribution of grain sizes of low coercivity magnetic material, eight selected samples were demagnetized by alternating field (AF) demagnetization at 100 mT in a 2G Automated Degaussing System and the anhysteretic remanent magnetization (ARM) acquisition behavior of these samples was determined. This was accomplished by subjecting the samples to a direct field of 0.1 mT while applying stepwise increases in AFs up to 100 mT. The AF-decay pattern of ARM acquired at 100 mT was also recorded.

1.2.4 Organic Matter Content

To estimate the organic matter present within the two cores, the total organic carbon (TOC) content was measured on a Solid Sample Module (SSM) 5000 A for three original samples from each horizontal core. The instrument measures total carbon and inorganic carbon and the total organic carbon was calculated as the difference between the two.

1.3 Results and Interpretations

1.3.1 Bulk Magnetic Susceptibility - Shallow Core

Monitoring of the χ_b signal with time for each set of samples of the five treatments revealed an increase in χ_b after the first measurement (taken after 18 days) and thereafter in many live incubation and positive control samples but not in abiotic control samples (Figure 1.1a-c, Table 1.2). The live samples of the shallow core all showed statistically significant (99 % confidence

interval) increases in χ_b compared to the initial measurement, which was defined as 100 % (Figure 1.1a, Table 1.2). In some cases, such as the methane-treated samples, increases occurred very gradually up to 100 days. Subsequently, the χ_b dropped slightly by approximately 5 % after prolonged incubation (Figure 1.1a). The largest increases in χ_b were observed in serum bottles that did not receive oxygen.

For the positive control samples from the shallow core, the χ_b increased with time for all environmental conditions with a confidence interval of 99 % (Figure 1.1b, Table 1.2). Unlike the live incubations, the positive control samples showed similar increases in χ_b whether oxygen was present or not and a drop in χ_b after prolonged incubation was occasionally observed, particularly in CH_4 amended samples.

The χ_b of the abiotic control samples of the shallow core closely resembled their initial levels even after prolonged exposure to the different experimental conditions (Figure 1.1c, Table 1.2). In general, there was less variance in the signal as compared to the live incubations and positive control samples. For all conditions, except the methane plus oxygen amended samples, there was a 99 % probability that the mean χ_b did not change significantly from its original value (Table 1.2). In the case of the methane plus oxygen treatment, the 99 % confidence interval for the mean χ_b is slightly below the initial value. The slight drop in the χ_b signal in the bottles with methane and oxygen may indicate that a small portion of the magnetic material that was initially present in the soil had transformed.

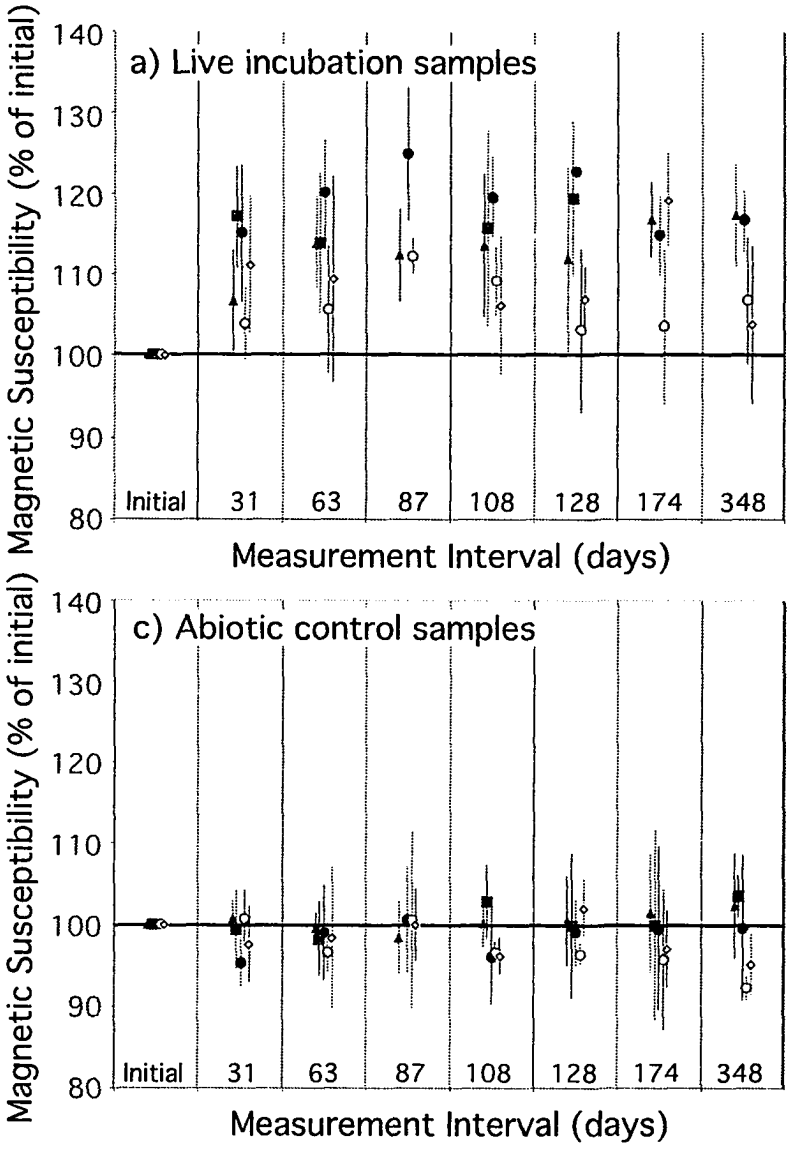


Figure 1.1: Bulk magnetic susceptibility of the shallow core expressed as a proportion of the initial value measured at discrete time intervals. Live incubations (a), positive controls (b), and autoclaved controls (c). Different experimental treatments are indicated by different symbols. Solid triangle: nitrogen, solid square: hydrogen, solid circle: methane, open circle: methane plus oxygen, open diamond: oxygen. Vertical bars represent standard deviations.

Sample Type ↓	χ_b is given in % of initial ↓	Treat-ment →	SHALLOW CORE (5-12 cm)				
			N_2	H_2	CH_4	$CH_4 + O_2$	O_2
Live Incubation	Mean χ_b (Standard deviation)		113.2 (3.5)	114.7 (3.0)	119.1 (3.9)	106.3 (3.4)	109.3 (4.98)
Positive Control	Mean χ_b (Standard deviation)		116.4 (4.1)	111.8 (2.5)	116.2 (1.8)	112.2 (2.4)	116.6 (4.1)
Abiotic control	Mean χ_b (Standard deviation)		100.5 (1.3)	100.8 (1.9)	98.5 (2.0)	97.1 (2.9)	98.1 (2.4)
Sample Type ↓	**χ_b is given in % of initial ↓**	**Treat-ment →**	**DEEP CORE (15-22 cm)**				
			N_2	H_2	CH_4	$CH_4 + O_2$	O_2
Live Incubation	Mean χ_b (Standard deviation)		107.9 (2.5)	115.4 (3.3)	111.0 (2.5)	101.1 (3.6)	101.5 (2.7)
Positive Control	Mean χ_b (Standard deviation)		109.1 (3.0)	106.1 (3.8)	102.4 (4.2)	103.1 (2.1)	107.1 (3.0)
Abiotic control	Mean χ_b (Standard deviation)		101.0 (2.5)	102.4 (2.44)	102.5 (2.5)	101.0 (1.8)	98.6 (4.5)

Table 1.2: Average bulk magnetic susceptibility (χ_b) results of both cores showing values as a percentage of the initial χ_b (initial χ_b = 100 %) and standard deviations as percentages of the corresponding mean χ_b. The underlined numbers indicate treatments where the means of the samples were significantly different from their initial χ_b at a 99 % confidence interval.

There was a statistically significant difference between the two biological sets and the abiotic control with a confidence interval of 99 %. The means for the live incubations and the positive controls were not significantly different if oxygen was absent. When oxygen was present, the χ_b mean for the positive control was significantly higher than that of live incubations. These results, particularly the similarities between live incubations and positive controls, may suggest that within the shallow core, similar biological factors could have been responsible for the enhancement in χ_b in the absence of oxygen. Furthermore, chemical/abiological processes alone were not capable of producing magnetic minerals under the given experimental conditions.

1.3.2 Bulk Magnetic Susceptibility - Deep Core

The χ_b results of the deep core showed statistically significant increases over time (confidence interval of 99 %) in live incubations that did not receive oxygen and in non-methane treated positive controls (Figure 1.2a, b, Table 1.2). Abiotic controls revealed no variations in the χ_b with time. The χ_b for the live incubations of the deep core gradually increased for all treatments without oxygen added (Figure 1.2a). An initial gradual rise and then a slight drop after prolonged incubation were observed for the hydrogen and the nitrogen amended samples and only for a few individual methane amended samples. The largest increase in χ_b occurred in samples that were exposed to hydrogen (Figure 1.2a, Table 1.2).

The positive control samples of the deep core showed somewhat different results compared to the live incubations. For the three experimental conditions that did not contain methane, the calculated means of data collected after the initial measurement were significantly greater than

the initial χ_b with a probability of 99 % (Figure 1.2, Table 1.2). Although the means for the methane and methane plus oxygen samples were slightly above the respective initial χ_b measurements, the differences were not significant. The mean χ_b of abiotic samples from the deep core generally were not significantly different from the initial χ_b signal with a probability of 99 % (Figure 1.2c, Table 1.2).

When comparing the different groups, significant differences were found between the means of χ_b for live incubations and abiotic control samples for treatments with nitrogen, hydrogen, and methane with a confidence interval of 99 %. In the presence of oxygen, with or without methane, the means were not significantly different. For the positive and abiotic control samples significant differences were only found in nitrogen and oxygen treatments. There were significant differences between the means of the live incubations and positive control groups for the hydrogen and methane treatments, but not for any of the other condition. The different results between treatments for the live incubations and positive control samples suggest that, within the deep core, different biological factors may be responsible for the formation of magnetic minerals. But since authigenesis of magnetic phases did not occur in abiotic controls, chemical processes alone can be excluded as the cause for the magnetic mineral addition.

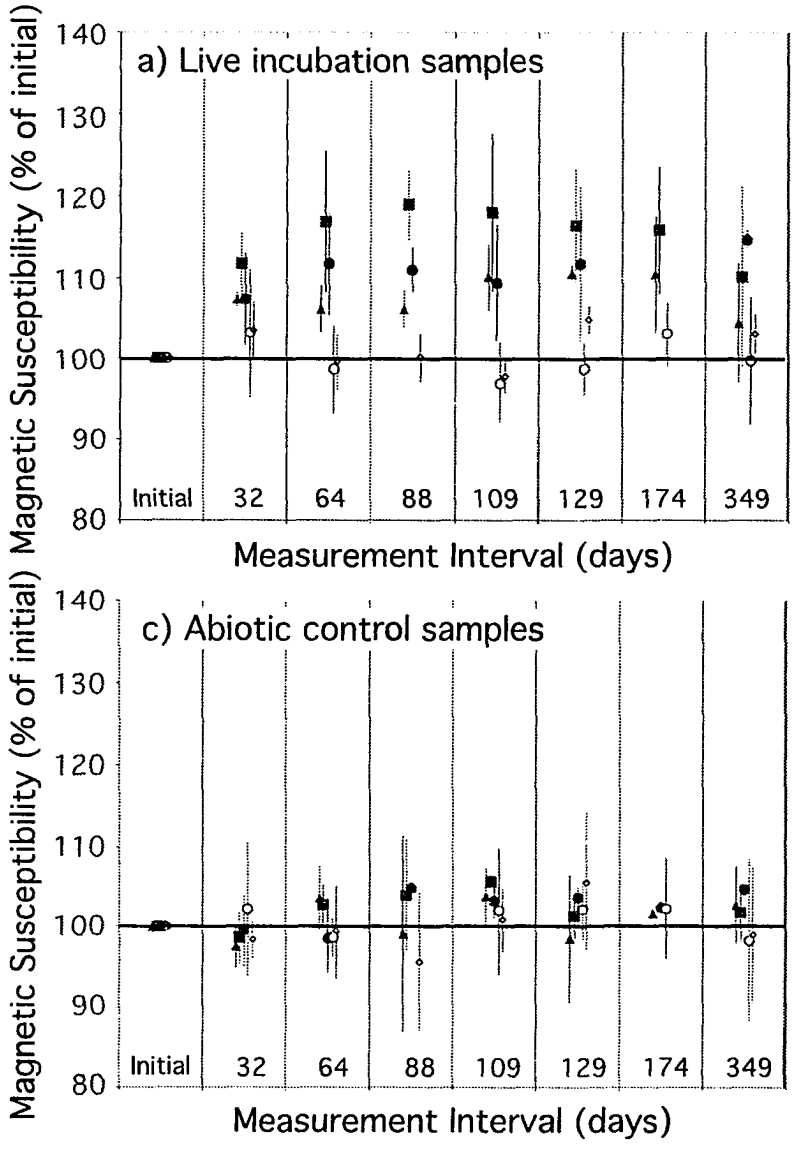


Figure 1.2: Bulk magnetic susceptibility of the deep core expressed as a proportion of the initial value measured at discrete time intervals. Live incubations (a), positive control samples (b), and abiotic controls (c). Laboratory conditions are indicated by different symbols: solid triangle: nitrogen, solid square: hydrogen, solid circle: methane, open circle: methane plus oxygen, open diamond: oxygen. Vertical bars represent standard deviations.

1.3.3 Bulk Magnetic Susceptibility - Comparison of Cores

In general, the live incubation samples of the shallow core showed greater increases in χ_b (expressed as percentages of the initial χ_b) compared to those of the deep core under all conditions except when treated with hydrogen (Table 1.2). In the latter case, relative enhancement of χ_b was comparable in both cores for the live incubation samples. The positive controls for the two cores differed in that the shallow core showed increases in the magnetic mineral content for all conditions, whereas for samples of the deep core, an increase in the magnetic signal was only recorded for samples in which no methane was added. Abiotic control samples of each core showed essentially no variation in χ_b and thus, chemical processes did not appear to cause any changes in the magnetic mineralogy. The comparison of the two cores indicates that although biological factors are responsible for the potential magnetic mineral authigenesis in both, it is interpreted that the processes responsible for the augmentation of the χ_b differ for the different depth intervals.

1.3.4 Rock Magnetism

To investigate the magnetic mineralogy of the soil and in particular whether different grain sizes of magnetite were present, the thermal decay patterns of low-temperature SIRMs were measured. When several samples were measured after three weeks of incubation, there were small differences between live incubations and abiotic control samples as shown for hydrogen-treated samples from the deep core (Figure 1.3a). The results were also representative for the shallow core and methane-amended samples. The remanence decreased rapidly at temperatures

up to 40 to 45°K and then continued to drop gradually during warming to room temperature for samples from both cores. This demagnetization behavior is indicative of the presence of superparamagnetic (SP) grains, which are commonly inferred to be ultra-fine grained magnetite or maghemite (e.g., Hunt et al., 1995). The presence of a weakly developed Verwey transition around 115°K was noted particularly in the live incubation samples and is indicative of magnetite grains that are capable of carrying remanence at room temperature (Figure 1.3a, b) (e.g., Özdemir et al., 1993). The Verwey transition was even less developed in the abiotic samples and was only detected by plotting the first derivative of the decay (Figure 1.3a). A positive control sample treated under the same conditions revealed a decay pattern similar to that of the live incubation sample.

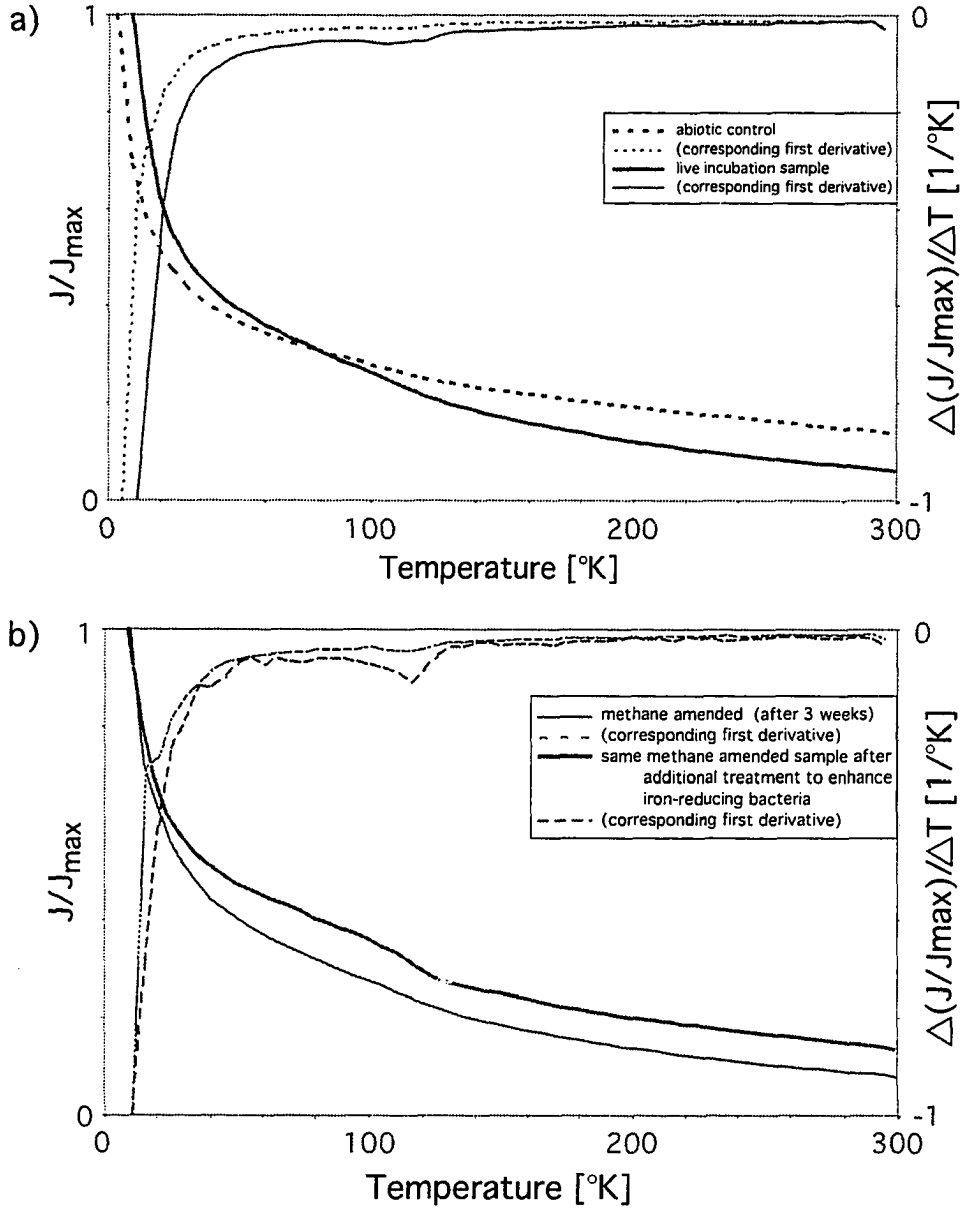


Figure 1.3: Thermal demagnetization of low-temperature SIRMs. Two hydrogen treated samples (live incubation and abiotic control) of the deep core (a) showed the presence of superparamagnetic (SP) grains and coarse magnetite (Verwey transition) particularly in the live incubation sample. A live incubation sample of the deep core after three weeks of exposure to methane and after additional treatment to enhance growth of iron-reducing bacteria (b). The demagnetization patterns showed the presence of SP material in both measurements and an increase in coarse magnetite after the additional treatment suggesting an increase and/or growth of remanence-carrying magnetite.

The low-temperature SIRM of a live incubation sample exposed to methane was measured after three weeks of treatment as described above and again after it underwent nutrient additions to enhance the amount of iron-reducing bacteria (Figure 1.3b). In the live incubation samples from this additional experiment, the occurrence of small areas that had turned black within the soil was observed. However, the iron gel in media generally appeared to remain spatially separated from the soil and retained its orange/orange-brownish color, which was due to the presence of ferric iron. There was no color change observed in the autoclaved controls. After three weeks of methane exposure, the demagnetization pattern of the sample was similar to that of the other live incubation samples (compare to Figure 1.3a) indicating that it contained SP grains, probably ultrafine-grained magnetite and coarser magnetite. After the additional treatment to enhance the growth of iron-reducing bacteria, the demagnetization behavior revealed that slightly higher temperatures were needed to demagnetize the low-temperature SIRM in comparison to when the sample was measured prior to the extra treatment. In addition, a more developed Verwey transition was present and a greater remanence at room temperature was observed compared to the sample before nutrient amendment. These observations are interpreted as reflecting growth of the magnetite grains that were present in the initial sample.

Measurements of IRM acquisition revealed the presence of low and medium to high coercivity minerals (Figure 1.4a). The results are representative for the original soil of both cores, live incubation and abiotic control samples treated with hydrogen (shallow core) or nitrogen (deep core). The interpretation was based on the observation of a rapid initial increase in remanence up to approximately 200 mT (IRM_{200}) followed by a gradual increase to large applied

fields. The ratio of IRM_{200} over SIRM was on average 84 % and there were no major differences between any of the samples or between the two cores. The high ratio indicates a predominance of a low coercivity phase in all soil samples.

Subsequent thermal demagnetization of tri-axial IRMs identified a low, an intermediate and a high coercivity phase (Figure 1.4b). The axis representing the low coercivity phase indicated a relatively continuous gradual decay with a commonly observed change in slope around 350°C and complete loss of remanence up to a maximum of 580°C. The low coercivity phase made up the bulk of the total remanence in both cores. The remanence loss at 580°C suggested the presence of magnetite. The intermediate coercivity axis showed a steep drop at around 350°C. The loss of remanence on the intermediate coercivity component and the slight drop at the same temperature range on the low coercivity axis indicated the presence of pyrrhotite. The continued decay on the intermediate coercivity axis up to 580°C may indicate oxidation of some of the pyrrhotite at elevated temperatures to magnetite. Only a very small portion of the remanence was carried by a high coercivity phase, which, based on a drop in intensity at 100°C (Figure 1.4b), was likely due to the presence of goethite (Dekkers, 1989). There were no major differences observed in original samples from either core or between live incubations and abiotic samples of either core under any of the different experimental conditions. Based on these room temperature remanence studies, the overall magnetic mineralogy consisted of predominantly magnetite, some pyrrhotite and goethite and was the same for all samples investigated. No new remanence-carrying magnetic phase was created under the experimentally tested conditions.

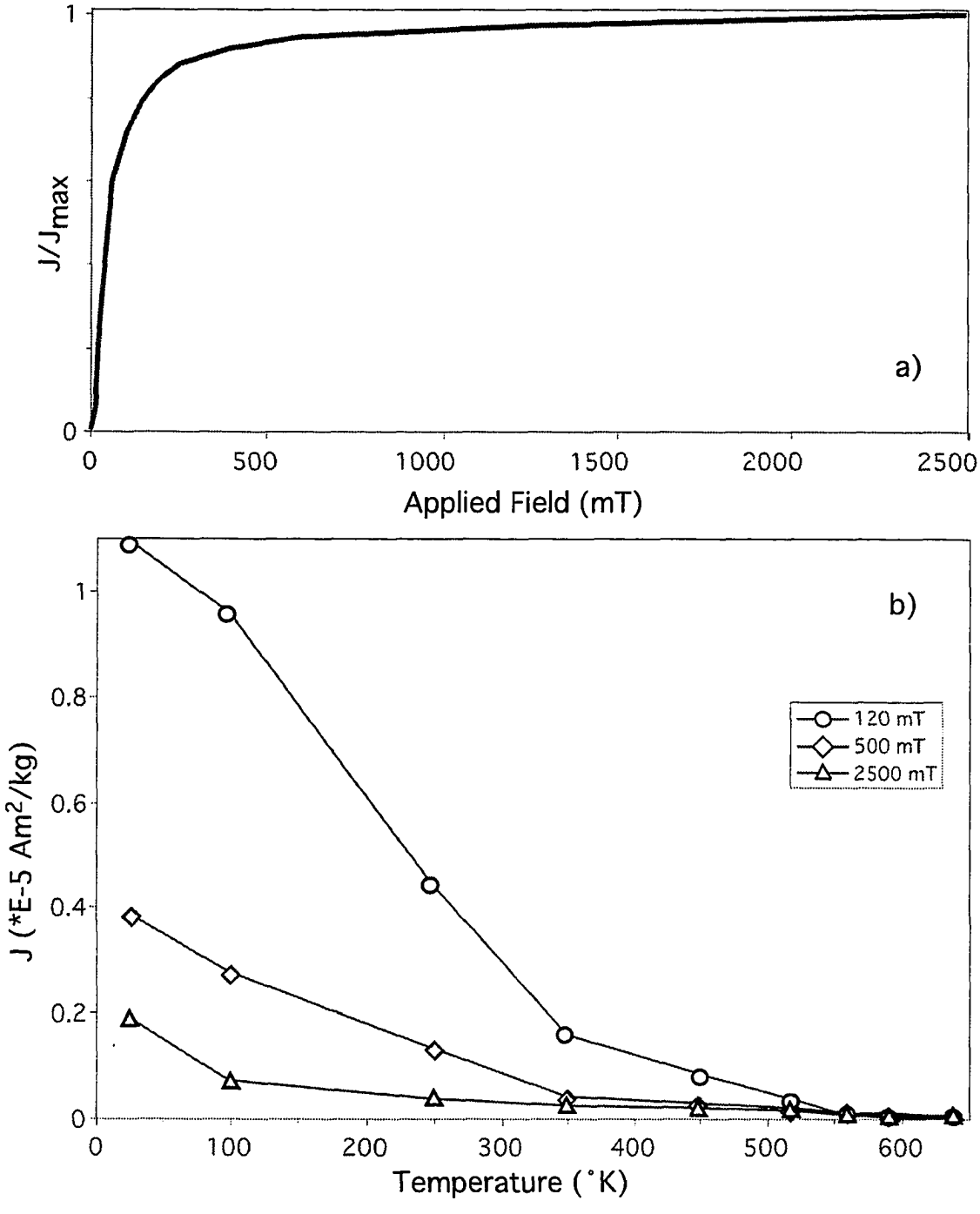


Figure 1.4: Acquisition of an IRM (a) and thermal demagnetization of a tri-axial IRM (b) of a hydrogen-treated live incubation sample of the shallow core. The IRM acquisition pattern suggested the presence and dominance of a low coercivity phase. Thermal demagnetization of the low coercivity axis (120 mT) identified this component as magnetite which decayed at about 570°C. The drop in remanence up to 350°C in the low and intermediate (500 mT) coercivity axes characterized pyrrhotite. A third magnetic mineral was identified as goethite which was carried by the high coercivity axis (2500 mT) and decayed up to 100°C.

The ARM spectra indicated essentially no variations between samples from either of the cores (example for the deep core in Figure 1.5). The ARM spectra between original soil, live incubations and abiotic controls for both cores and three experimental conditions (methane, hydrogen, and nitrogen) were also similar for all samples. The spectra indicated a wide size range of magnetite grains as indicated by the broad peak and relatively gentle decrease in intensity at greater applied AFs (Figure 1.5). The total ARMs measured on original untreated soil from both cores as well as samples of live incubations and abiotic samples treated with hydrogen (shallow core) and methane (deep core) were similar and ranged from 1.02 to 1.59xE-5 Am^2/kg.

Hysteresis experiments were conducted mainly to investigate the influence of ferri- and paramagnetic minerals on the χ_b in live incubation and abiotic control samples (Figure 1.6). The hysteresis measurements indicated that the χ_b was dominated by a ferrimagnetic component, which made up 97.7 % of the χ_b in a live incubation sample of the deep core amended with hydrogen. In contrast, the ferrimagnetic susceptibility (χ_f) of the abiotic equivalent sample accounted for only 84.8 % of the χ_b. Although only measured for one sample pair, these results may suggest that there was an increase in ferrimagnetic material in the live incubation samples concurrent with the increase in χ_b. A methane-amended, live incubation sample of the deep core showed a 95.4 % contribution of the χ_f to χ_b which again indicated the extremely large proportion of χ_f in live incubation samples. Hysteresis loops of all measured samples indicated the predominance of the low coercivity phase that was previously identified as magnetite.

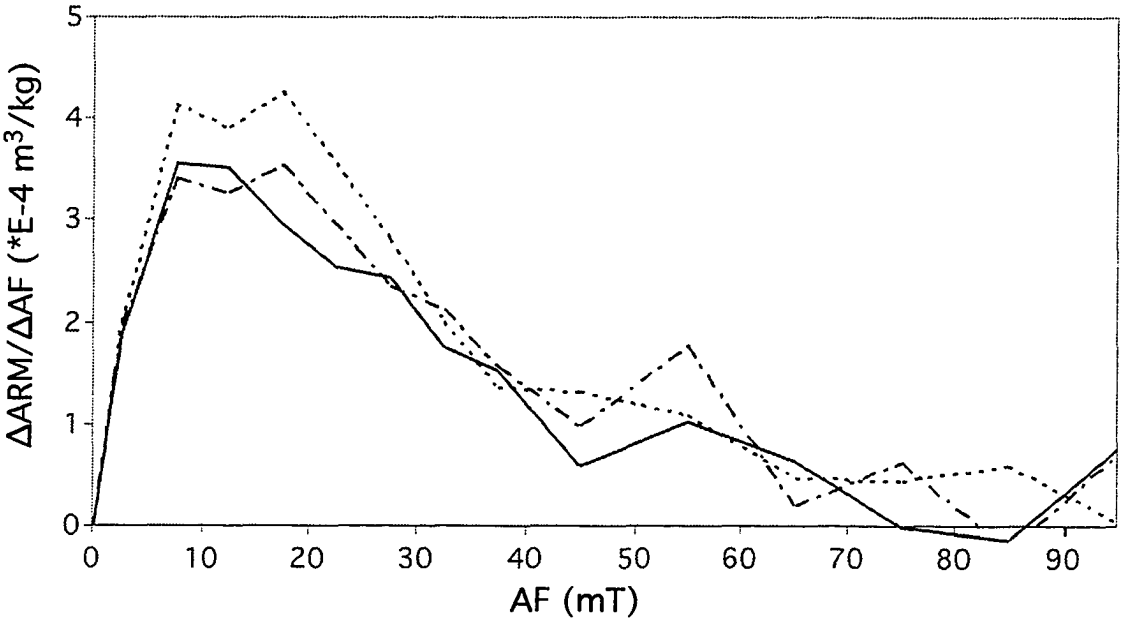


Figure 1.5: ARM spectra of three samples of the deep core: an original soil sample as taken from the study site (dotted line), a live incubation sample treated with nitrogen (solid line), and a nitrogen treated abiotic control sample (dashed line). ARMs were similar for all samples indicating no significant variations in the remanence carrying grain sizes.

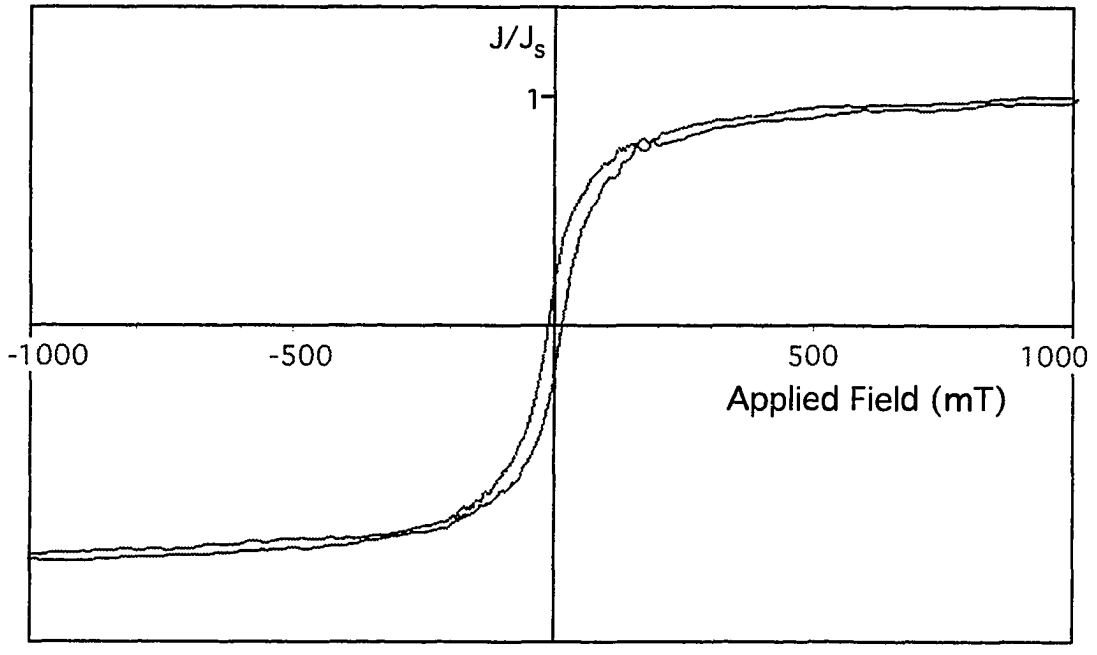


Figure 1.6: Hysteresis loop for a methane treated live incubation sample of the deep core. The loop was slope corrected (high field slope = 1.82×10^{-8} m^3/kg), which represented the para-magnetic susceptibility used to calculate the ferrimagnetic component. The steep initial rise and near closure at low applied fields indicated the predominance of a low coercivity phase.

1.3.5 Total Organic Carbon (TOC)

Analyses of TOC indicated that the shallow core contained an average of 0.7 mg/l of organic carbon (ranging from 0.59 to 0.91 mg/l) whereas the deeper core had on average TOC of 0.33 mg/l (ranging from 0.30 to 0.34 mg/l). Both cores did not contain any inorganic carbon within the detection limits of the instrument. A larger abundance of organic material in the shallow core is consistent with greater increases in χ_b in samples from this core compared to the deep core.

1.4 Discussion and Summary

Increases in the χ_b in live incubation samples of both cores are interpreted to be caused by authigenesis of magnetite as a result of microbial activity. In the shallow core, formation of magnetite occurred under all experimental conditions, but was more favorable when oxygen was absent. In the deep core, magnetite formation occurred only in the absence of oxygen. Since the abiotic controls did not show alteration of the magnetic signal, it is unlikely that the chemical conditions prevailing in either of the soil cores alone play a role. Instead, it is likely that biological factors are responsible for the formation of additional magnetite.

Thermal demagnetization of low-temperature SIRM suggests that SP and coarser (SD and/or MD) magnetite are present. Although Hunt et al. (1995) state that SP grains could be magnetite or maghemite, there is no evidence for the presence of maghemite and thus, the SP grains are inferred to be magnetite. Variability in SP amounts between live incubations and abiotic controls could not be determined because the SIRMs were acquired at two different temperatures. The low-temperature data indicates, however, that there is a difference between biological and abiotic

samples in the remanence-carrying grain size fraction of magnetite. In the initial stages of the experiments, there was no major distinction between the live incubations and abiotic control samples. The fact that the Verwey transition is almost absent in the abiotic controls but somewhat more expressed, albeit weak, in the live incubations and positive controls could indicate a greater presence of SD and/or MD magnetite in the biological samples. While a small amount of coarse magnetite was initially present, the grain size distribution of magnetite changed towards a larger proportion of coarse grains. This was based on the low-temperature analyses of a methane-amended sample during the early stages of the experiment and after efforts to enhance iron-reducing bacteria. The growth of magnetite grains is also suggested based on a slight drop in χ_b after prolonged incubation (particularly in methane and hydrogen amended samples) for a number of live incubation and positive control samples of both cores. The χ_b measurements are influenced most strongly by SP grains, thus, once the grains grow beyond the SP threshold (20-40 nm [e.g., Dunlop, 1973]), the χ_b could be expected to show a slight decrease with time. Hysteresis measurements offer supporting evidence that the ferrimagnetic mineral content increased in live incubations compared to abiotic controls. The presence and dominance of remanence-carrying magnetite is confirmed by ARM, IRM acquisition and subsequent thermal demagnetization analyses.

Different types of microorganisms could be responsible for the formation of magnetite under the different conditions or even within samples. Iron-reducing bacteria, which commonly produce relatively large amounts of magnetite are one option (e.g., Lovley & Phillips, 1988). Among the magnetite they produce, only a minor proportion is larger than SP grains (Moskowitz

et al., 1993). A masking or suppression of the Verwey transition due to swamping by the presence of SP grains has been previously suggested to occur in the low-temperature analysis of magnetite produced by iron-reducing bacteria (Bazylinski & Moskowitz, 1997). The results presented herein would be consistent with such an observation. The fact that positive control samples, particularly those of the shallow core, show similar results to those of the live incubations may suggest that iron reducers are present in the soil and could be responsible for the addition of magnetic material at least in the shallow core. As for the deep core, the fact that the inoculated samples with methane and methane plus oxygen showed no magnetic mineral formation is surprising. It suggests that some factor, perhaps another type of microorganism, is present in the deep core that possibly inhibits precipitation of magnetic minerals either directly by altering chemical conditions or indirectly by preventing or slowing the growth of iron-reducing bacteria. Thus, it may be expected that iron-reducing bacteria are, at least not entirely, responsible for the magnetite formation in the live incubations that showed increases in the magnetic mineral content despite the presence of methane.

Alternatively, magnetotactic bacteria could be present in both cores; some of the known bacteria are microaerophilic, i.e. they thrive in the oxic-anoxic transition zone (e.g., Bazylinski & Moskowitz, 1997), which could explain the increases in χ_b under conditions with and without oxygen added. These microorganisms commonly produce SD magnetite of a narrow grain size distribution, which cause the presence of the Verwey transition in low-temperature experiments (Moskowitz et al., 1989). The increase in coarse magnetite observed in the live incubation samples became obvious after enhancing growth of iron-reducing bacteria. However,

magnetotactic bacteria also require iron to produce magnetite and thus, growth of both organisms can not be excluded. Since both SP and coarser magnetite are present, it is not possible to identify if only one of the bacterial types is responsible for magnetite authigenesis under the tested conditions. A third type of microorganisms, sulfate-reducers, are a possible factor for the formation of magnetic phases, although the presence of sulfur in the soil is mainly in the form of sulfide as may be suggested by the presence of iron-sulfides like pyrrhotite. It could be the concerted action of different microorganisms living in the soil or a combination of biological reactions followed by some unidentified chemical process that caused additional magnetite to precipitate and grow.

Augmentation of χ_b is generally more apparent in the shallow core than in the deeper core and also more likely to occur in the former under all five tested conditions. This could be due to a greater availability of ferric iron for reduction and incorporation into magnetic mineral authigenesis in the shallow core. Alternatively, a greater variety of microorganisms capable of producing magnetite could be present based on the observation that all laboratory treatments resulted in magnetite authigenesis within the shallow core but only in the non-oxygen treated samples of the deep core.

The role of pyrrhotite and how it was formed remains unclear. It is likely that the presence of hydrocarbons provided some of the sulfide necessary for the formation of this magnetic mineral, but whether it formed merely due to the chemical conditions or because of an interaction with microorganisms was beyond the scope of this investigation. Machel (1996) describes several possible scenarios involving hydrocarbons under which different magnetic minerals may form

and shows the thermodynamic stability diagrams accordingly. The coexistence of pyrrhotite and magnetite as well as small amounts of goethite may, however, be coincidental and suggests the investigated soil system is far from being at a chemical equilibrium. Hence, theoretical stability diagrams may only be applicable to some limited degree.

1.5 Conclusions

Evidence was presented that indicates the importance of microorganisms in the authigenesis of magnetic minerals in soils and suggests that chemical processes alone are not sufficient for the creation of new magnetic material. Although abiologic factors may play some role, they probably require microorganisms to expel compounds necessary for magnetic mineral formation or magnetic minerals themselves prior to any abiologic reaction. Furthermore, it appears that there is a great variability in the factors causing magnetic mineral formation within a soil profile and authigenesis may not be attributed to only one biological factor but to a variety of biological factors. Lastly, the fact that detectable differences in amounts of magnetite were formed within a relatively short period of time reveals the potential importance of biological magnetic mineral formation. Future research is necessary to investigate other soil types and in particular soils that were not exposed to hydrocarbons to confirm or refute the importance of microbially formed magnetic phases in soils in general.

References Chapter 1

Anderson, R.T., and D.R. Lovley, Naphthalene and benzene degradation under Fe(III)-reducing conditions in petroleum-contaminated aquifers, *Bioremediation Journal, 3*, 121-135, 1999.

Balch, W.E., and R.S. Wolfe, New approach to the cultivation of methanogenic bacteria: 2-mercaptoethanesulfonic acid (HS-CoM)-dependent growth of *Methanobacterium ruminantium* in a pressurized atmosphere, *Applied and Environmental Microbiology, 32*, 781-791, 1976.

Bazylinski, D.A., R.B. Frankel, and H.W. Jannasch, Anaerobic magnetite production by a marine, magnetotactic bacterium, *Nature, 334*, 518-519, 1988.

Bazylinski, D.A., B.R. Heywood, S. Mann, and R.B. Frankel, Fe_3O_4 and Fe_3S_4 in a bacterium, *Nature, 366*, 218, 1993.

Bazylinski, D.A., Controlled biomineralization of magnetic minerals by magnetotactic bacteria, *Chemical Geology, 132*, 191-198, 1996.

Bazylinski, D.A., and B.M. Moskowitz, Microbial biomineralization of magnetic iron minerals, *Reviews in Mineralogy, 35*, 181-223, 1997.

Bell, P.E., A.L. Mills, and J.S. Herman, Biogeochemical conditions favoring magnetite formation during anaerobic iron reduction, *Applied and Environmental Microbiology, 53*, 2610-2616, 1987.

Blakemore, R.P., D. Maratea, and R.S. Wolfe, Isolation and pure culture of a freshwater magnetic spirillum in chemically defined medium, *Journal of Bacteriology, 140*, 720-729, 1979.

Coleman, M.L., D.B. Hedrick, D.R. Lovley, D.C. White, and K. Pye, Reduction of Fe(III) in sediments by sulphate-reducing bacteria, *Nature, 361*, 436-438, 1993.

Dearing, J.A., K.L. Hay, S.M.J. Baban, A.S. Huddleston, E.M.H. Wellington, and P.J. Loveland, Magnetic susceptibility of soil: an evaluation of conflicting theories using a national data set, *Geophysical Journal International, 127*, 728-734, 1996.

Dekkers, M.J., Magnetic properties of natural goethite - II. TRM behaviour during thermal and alternating field demagnetization and low-temperature treatment, *Geophysical Journal, 97*, 341-355, 1989.

Dunlop, D.J., Superparamagnetic and single domain threshold sizes in magnetite, *Journal of Geophysical Research, 78*, 1780-1793, 1973.

Dunlop, D.J., and Ö. Özdemir, Rock magnetism - Fundamentals and frontiers, editor: D. Edwards, Cambridge University Press, pp. 573, 1997.

Farina, M., D.M.S. Esquivel, and H.G.P. Lins de Barros, Magnetic iron-sulphur crystals from a magnetotactic microorganism, *Nature, 343*, 256-258, 1990.

Fassbinder, J.W.E., and H. Stanjek, Magnetic properties of biogenic soil greigite (Fe_3S_4), *Geophysical Research Letters, 21*, 2349-2352, 1994.

Frankel, R.B., G.C. Papaefthymiou, R.P. Blakemore, and W. O'Brien, Fe_3O_4 precipitation in magnetotactic bacteria, *Biochem. Biophys. Acta, 763*, 147-159, 1985.

Hawthorne, T.B., and J.A. McKenzie, Biogenic magnetite: authigenesis and diagenesis with changing redox conditions in Lake Greifen, Switzerland, Applications of Paleomagnetism to Sedimentary Geology, SEPM Special Publication, 49, 3-15, 1993.

Jones, J.G., S. Gardener, and B.M. Simon, Bacterial reduction of ferric iron in a stratified eutrophic lake, *Journal of General Microbiology, 129*, 131-139, 1983.

Karlin, R., M. Lyle, and G.R. Heath, Authigenic magnetite formation in suboxic marine sediments, *Nature, 326, 490-493*, 1987.

Konhauser, K.O., Diversity of bacterial iron mineralization, *Earth-Science Reviews, 43*, 91-121, 1998.

Lovley, D.R., and E.J.P. Phillips, Availability of ferric iron for microbial reduction in bottom sediments of the freshwater tidal Potomac River, *Applied and Environmental Microbiology, 52*, 751-757, 1986.

Lovley, D.R., J.F. Stolz, G.L. Nord, Jr., and E.J.P. Phillips, Anaerobic production of magnetite by a dissimilatory iron-reducing microorganism, *Nature, 330*, 252-254, 1987.

Lovley, D.R., and E.J.P. Phillips, Novel mode of microbial energy metabolism: Organic carbon oxidation coupled to dissimilatory reduction of iron or manganese, *Applied and Environmental Microbiology, 54*, 1472-1480, 1988.

Lovley, D.R., Magnetite formation during microbial dissimilatory iron reduction, in Iron Biominerals, edited by R.B. Frankel, and R.P. Blakemore, pp. 151-166, Plenum Press, New York, 1990.

Lovley, D.R., Dissimilatory Fe(III) and Mn(IV) reduction, *Microbiological Reviews, 55*, 259-287, 1991.

Lovley, D.R., E.E. Roden, E.J.P. Phillips, and J.C. Woodward, Enzymatic iron and uranium reduction by sulfate-reducing bacteria, *Marine Geology, 113*, 41-53, 1993.

Lovley, D.R., J.D. Coates, J.C. Woodward, E.J.P. Phillips, Benzene oxidation coupled to sulfate reduction, *Applied and Environmental Microbiology, 61*, 953-958, 1995.

Lowrie, W., Identification of ferromagnetic minerals in a rock by coercivity and unblocking temperature properties, *Geophysical Research Letters, 17*, 159-162, 1990.

Machel, H.G., and E.A. Burton, Chemical and microbial processes causing anomalous magnetization in environments affected by hydrocarbon seepage, *Geophysics, 56*, 598-605, 1991.

Machel, H.G., Magnetic mineral assemblages and magnetic contrasts in diagenetic environments - with implications for studies of palaeomagnetism, hydrocarbon migration and exploration, in Palaeomagnetic applications in hydrocarbon exploration and production, edited by P. Turner, and A. Turner, pp. 9-29, Geological Society Special Publication, 1995.

Machel, H.G., Magnetic contrasts as a result of hydrocarbon seepage and migration, in Hydrocarbon migration and its near-surface expression, edited by D. Schumacher, and M.A. Abrams, pp. 99-109, AAPG Memoir, 1996.

Maher, B.A., and R.M. Taylor, Formation of ultrafine-grained magnetite in soils, *Nature, 336*, 368-370, 1988.

Mann, S., N.H.C. Sparks, R.B. Frankel, D.A. Bazylinski, and H.W. Jannasch, Biomineralization of ferrimagnetic greigite (Fe_3S_4) and iron pyrite (FeS_2) in a magnetotactic bacterium, *Nature, 343*, 258-261, 1990.

Morse, J.W., F.F. Millero, J.C. Cornwall, and D. Rickard, *Earth Science Review, 24*, 1-42, 1987.

Moskowitz, B.M., R.B. Frankel, D.A. Bazylinski, H.W. Jannasch, and D.R. Lovley, A comparison of magnetite particles produced anaerobically by magnetotactic and dissimilatory iron-reducing bacteria, *Geophysical Research Letters, 16*, 665-668, 1989.

Moskowitz, B.M., R.B. Frankel, and D.A. Bazylinski, Rock magnetic criteria for the detection of biogenic magnetite, *Earth and Planetary Science Letters, 120*, 283-300, 1993.

Pósfai, M., P.R. Buseck, D.A. Bazylinski, and R.B. Frankel, Iron sulfides from magnetotactic bacteria: structure, composition, and phase transitions, *American Mineralogist, 83*, 1469-1481, 1998.

Pyle, T.A., Investigation of a brine disturbed land: A proposed reclamation strategy, The University of Oklahoma, Thesis, pp. 139, 1996.

Sakaguchi, T., J.G. Burgess, and T. Matsunaga, Magnetite formation by a sulphate-reducing bacterium, *Nature, 365*, 47-49, 1993.

Sparks, N.H.C., S. Mann, D.A. Bazylinski, D.R. Lovley, H.W. Jannasch, and R.B. Frankel, Structure and morphology of magnetite anaerobically-produced by a marine magnetotactic bacterium and a dissimilatory iron-reducing bacterium, *Earth and Planetary Science Letters, 98*, 14-22, 1990.

Stanjek, H., J.W.E. Fassbinder, H. Vali, H. Wägele, and W. Graf, Evidence of biogenic greigite (ferrimagnetic Fe_3S_4) in soil, *European Journal of Soil Science*, 45, 97-103, 1994.

Stolz, J.F., D.R. Lovley, and S.E. Haggerty, Biogenic magnetite and the magnetization of sediments, *Journal of Geophysical Research, 95*, 4355-4361, 1990.

Tanner, R.S., Cultivation of bacteria and fungi, in Manual of Environmental Microbiology, edited by C.J. Hurst, G.R. Knudsen, M.J. McInerney, L.D. Stetzenbach, and M.V. Walter, pp. 894, American Society for Microbiology, Washington, D.C., ASM Press, 1997.

Taylor, R.M., B.A. Maher, and P.G. Self, Magnetite in soils: I. The synthesis of single-domain and superparamagnetic magnetite, *Clay Minerals, 22*, 411-422, 1987.

Weiner, J., and D.R. Lovley, Anaerobic benzene degradation in petroleum-contaminated sediments after inoculation with a benzene-oxidizing enrichment, *Applied and Environmental Microbiology, 64*, 775-778, 1998.

CHAPTER 2

Magnetic Enhancements

Associated with Low Temperature Heating

of Smectites

2 Abstract

Widespread chemical remanent magnetizations (CRMs) are a common occurrence in sedimentary rocks and several mechanisms such as migration of orogenic fluids or the presence of hydrocarbons have been previously proposed to cause their formation. One other possible mechanism causing magnetite authigenesis and CRMs is the low temperature diagenetic conversion of smectite to illite during burial in sedimentary rocks. Although empirical evidence supports such a connection, genetic links between low temperature diagenesis (below 100°C) and changes in the magnetic signal have not been tested. In this study, bulk magnetic susceptibility (χ_b) of heated (62 and 98°C) clays, i.e. different smectites, illite-smectite, illites, and chlorite was monitored over time under a variety of experimental conditions (presence of potassium, hydrocarbons, and/or pyrite). Gradual increases in the magnetic signal in a nontronite were identified under all temperatures, and there were no differences between experimental conditions. Room temperature control samples, however, did not show an increase in the χ_b. Another smectite, a Na-montmorillonite, showed an augmentation in the χ_b signal but with a more complex response between conditions. Alterations to the magnetic signal were not found in any of the other clays, including one smectite (iron-sodium nontronite). The dominant remanence-carrying magnetic phase that is present before and after heating was identified as magnetite, but pyrrhotite is also found in all clay types. These results suggest that changes in the remanence-carrying fraction potentially occur in some smectites due to low temperature heating. In addition, the results indicated that the other hypothesized conditions are not needed to accomplish enhancements of the magnetic signal. Furthermore, this study suggests that the processes causing

an augmentation of the magnetic signal may not only depend on the presence of smectite, but also on the specific type of smectite. Furthermore, the process of enhancing the magnetic signal occurs very rapidly. The low temperatures that are necessary to alter the magnetic signal and the apparent insensitivity to boundary conditions may indicate that magnetic mineral alteration by smectite diagenesis could be a common mechanism in sedimentary rocks. Additional studies are needed to characterize the magnetic changes.

2.1 Introduction

Secondary magnetic minerals such as magnetite have been proposed to form due to a variety of processes in sedimentary rocks. These authigenic magnetic minerals are capable of recording ancient but post-depositional magnetic directions by acquiring a chemical remanent magnetization (CRM) at the time of their formation. Such CRMs can be found throughout stratigraphic units of sedimentary basins (e.g., Elmore & McCabe, 1991) and many reside in magnetite (e.g., Jackson, 1990; Katz et al., 1998). The processes causing the formation of secondary magnetite may be diverse and several mechanisms have been proposed in the literature such as fluids expelled during orogeny, maturation of hydrocarbons, and burial diagenesis of clays.

In many previous studies, the spatial and temporal association between orogenic belts and CRMs has led to the hypothesis that the discharge and migration of tectonic fluids during orogeny (Oliver, 1986; 1992; Miller & Kent, 1988) may cause authigenesis of magnetic phases and resulting CRMs (e.g., McCabe & Elmore, 1989). This could explain the CRMs in some

sedimentary rocks and the pervasive nature of some CRMs (e.g., McCabe et al., 1989; Jackson, 1990; Stamatakos et al., 1996). Some studies have suggested that during burial, smectites may release iron (Boles & Franks, 1979) which is necessary for magnetic mineral formation (Lu et al., 1991) but that orogenic fluids are needed as a source of potassium during the process of diagenetic formation of illite (Jackson et al., 1988; McCabe et al., 1989).

Alternatively, hydrocarbon maturation and/or migration could cause some of the CRMs present in sedimentary rocks (Banerjee et al., 1997). Authigenesis of magnetite may occur due to chemical conditions prevailing in hydrocarbon-exposed deposits (Machel & Burton, 1991; Machel, 1995). An empirical connection between hydrocarbon migration and the acquisition of a CRM residing in authigenic magnetite was reported for Permian speleothems (Elmore et al., 1987). However, the occurrence of magnetite authigenesis due to hydrocarbons does not explain the basin-wide occurrence of many CRMs, as hydrocarbons are frequently lacking.

One mechanism that could explain the common and widespread occurrence of CRMs is the diagenetic conversion of smectite during burial (Katz et al., 1998). A pervasive CRM residing in magnetite was identified in Mesozoic carbonates of southeast France only where smectite has altered to illite (Katz et al., 2000). A CRM in sedimentary rocks on the Isle of Skye in Scotland is consistent with such a clay diagenetic origin (Woods et al., 2000).

Studies dealing with CRMs and authigenic magnetite are commonly empirical in nature due to their occurrence in geologic deposits. Few laboratory studies have been conducted to decipher what mechanisms can cause the formation of secondary magnetite. Hirt et al. (1993) have shown that adsorption of iron loaded onto smectite surfaces can lead to the formation and continuous

growth of magnetite at elevated temperatures between about 250 and 500°C which are appropriate for low-grade metamorphism and moderate to greater depth of burial. Other laboratory investigations have suggested that heating to high temperature (700°C) is needed to generate a ferrimagnetic phase in nontronites, which are iron-rich smectites (Moskowitz & Hargraves, 1982; 1984). However, the possibility that naturally occurring smectites heated at lower temperatures and over prolonged periods of time can cause alteration of the magnetic signal has not been tested.

Here, results are presented of experiments conducted with several different smectites, illites, as well as an illite-smectite and a ripidolite (chlorite). The aim was to test whether changes in the magnetic signal can be observed in smectites at temperatures equivalent to low to moderate burial at which a diagenetic conversion from smectite to illite may occur. Samples were prepared in the laboratory to test for the effects on the magnetic signal for a variety of conditions including the presence of water, potassium, hydrocarbons, pyrite, and mixtures of the above at different temperatures and for prolonged time intervals up to nearly a year. The remanence-carrying magnetic minerals were identified in the clays prior to and after heating to determine whether an additional magnetic phase was created in the experiments. Understanding changes in the magnetic signal associated with alteration of clays, especially smectites, could elucidate any possible connection between clay diagenesis and the occurrence of widespread CRMs.

2.2 Materials and Methods

Several clays were purchased from the Clay Mineral Society Repository (NAu-2, SWy-2, Imt-1, IWi-1, ISCZ-1, CCa-2) and Ward's (# 49E5108) in order to set up an array of laboratory tests. The clays were mixed with water (deionized and tab water), a K^+-solution, hydrocarbons, and/or pyrite. Three smectites, namely a nontronite designated NAu-2, a Na-montmorillonite (SWy-2), and another nontronite containing iron and sodium retrieved at Cheney, Washington (# 49E5108) were chosen for the experiments. In addition, an illite-smectite (ISCZ-1), two illites (Imt-1 and IWi-1), and a chlorite (CCa-2) were tested. All clays except for the Na-montmorillonite, which arrived as a powder, were ground with mortar and pestle to about 1 – 4 mm size chunks in order to achieve some level of homogenization of the material. For the experiments involving hydrocarbons, 10 µl oil retrieved at Clearbrook, Oklahoma were added to the clays. Between 5 and 10 ml of water were added to the clays depending on the amount necessary to moisten the individual clay and, where applicable, the plaster. For the test conditions requiring pyrite, an amount between 0.050 and 0.052 g was dispersed into the samples. Samples receiving potassium were treated with a 150 mM K^+-solution adjusted to circumneutral pH.

A total of 262 samples were prepared out of which 139 were smectites, 24 were illite-smectite, 43 were illites, 43 were chlorite, and 13 were matrix control samples. The matrix samples were made of plaster of paris because of its low bulk magnetic susceptibility (χ_b) intensity and because of its magnetic stability at low temperatures. Clays were always in a 1:1 mixture (by weight) with the plaster. Between 4 and 7 g of air-dried mass for the clays were used for individual samples. The details of the experimental designs and temperatures to which the

clays were initially heated are displayed in Table 2.1. The blank matrix samples (controls) were used to subtract the effect of the plaster from the samples in the magnetic measurements. Matrix-mixed clay samples were approximately 2 cm in diameter with a length of about 2 cm.

The χ_b was measured on a Sapphire SI-2B instrument initially and periodically thereafter in order to identify and monitor changes in the magnetic mineral content throughout the duration of the experiments. The χ_b was measured immediately for samples that were prepared in vials and after 5 days of air-drying for the matrix-mixed samples. Sets of samples remained either at room temperature to serve as control samples, or were placed into one of two ovens adjusted to approximately 62 and 98°C (see Table 2.1 for details). The χ_b was measured periodically and heated samples were allowed to cool to room temperature prior to conducting the measurements.

Selected unheated and heated dry clay samples and pure matrix samples were prepared for analysis of the magnetic mineral(s) present prior to and after the experiments. Dry clay samples were bonded by either mixing only a sodium-silicate solution or the solution mixed with kaolin with the clay and allowing it to dry for approximately three days under ambient conditions. To identify the remanence-carrying magnetic minerals, isothermal remanent magnetizations (IRMs) were acquired in a stepwise increasing direct field up to 2500 mT and the remanence was recorded after each step on a 2G three-axes cryogenic magnetometer located in a magnetically shielded room. After acquiring a tri-axial IRM along perpendicular axes at direct applied fields of 120, 500, and 2500 mT, the samples underwent subsequent stepwise thermal demagnetization in a Schonstedt TSD-1 oven up to temperatures of 620°C and remanences were measured on the magnetometer after each temperature step (modified after Lowrie, 1990).

	Samples in vials	All experiments with clays mixed with matrix and H_2O (d.i., or else as indicated)													
Experiment →	**Clay with H_2O d.i.**	**Clay (plain)**			**H_2O (regular)**		**K^+-solution**			**Hydrocarbons (hc)**			**K^+solution plus hc**		**Other conditions**
Temperature [°C] →	**62**	**24**	**62**	**98**	**62**	**98**	**24**	**62**	**98**	**24**	**62**	**98**	**62**	**98**	
Clay Type ↓	↓	↓	↓	↓	↓	↓	↓	↓	↓	↓	↓	↓	↓	↓	
NAu-2:	8	2	11	1	1	1	1	1	1	1	1	1	1	1	no pyrite
Nontronite	—	1	1	1	1	1	1	1	1	1	1	1	1	1	with pyrite
SWy-2: Na-	5	1	6	1	1	1	1	1	1	1	1	1	1	1	no pyrite
Montmorillonite	—	1	1	1	1	1	1	1	1	1	1	1	1	1	with pyrite
Fe-Na-Nontronite	5	1	6	1	1	1	—	1	1	—	1	1	1	1	no pyrite
Cheney	—	1	1	1	1	1	—	1	1	—	1	1	1	1	with pyrite
ISCZ-1:	—	1	1	1	1	1	—	1	1	—	1	1	1	1	no pyrite
Illite-smectite	—	1	1	1	1	1	—	1	1	—	1	1	1	1	with pyrite
Imt-1:	—	—	1	1	1	1	—	1	1	—	1	1	1	1	no pyrite
Illite	—	—	1	1	1	1	—	1	1	—	1	1	1	1	with pyrite
Iwi-1:	5	1	5	—	—	—	1	—	—	1	—	—	—	—	no pyrite
Illite	—	1	—	—	—	—	1	—	—	1	—	—	—	—	with pyrite
CCa-2:	5	1	6	1	1	1	1	1	1	1	1	1	1	1	no pyrite
Chlorite	—	1	1	1	1	1	1	1	1	1	1	1	1	1	with pyrite
Matrix	—	1	5	1	—	—	1	—	—	1	—	—	—	—	no pyrite
(control)	—	1	—	1	—	—	1	—	—	1	—	—	—	—	with pyrite

Table 2.1: Summary of experimental designs indicating the types of clays used for a variety of conditions and temperatures. The numbers represent the amount of samples per experiment. Samples heated to 98°C are used for the χ_b figures in the results section.

2.3 Results and Interpretations

2.3.1 Bulk Magnetic Susceptibility – Initial Values

Initial values of χ_b vary with clay type (Table 2.2) with the two nontronites and the chlorite having the strongest signal. The illite-smectite has the weakest response. Variations within each clay type are generally small for strong samples but can be up to 10 % for weak clays like the Na-montmorillonite. Means for samples of the same clay type, which were subsequently heated to different temperatures are similar.

The values reflect the χ_b after subtracting the influence of the matrix material where appropriate. The initial mean χ_b of the plaster that was used as a matrix is -1.38×10^{-8} m^3/kg (standard deviation = 0.03×10^{-8} m^3/kg) and is slightly diamagnetic. Standard deviations for the individual χ_b measurements are commonly < 0.1 % of the χ_b for the two nontronites and the chlorite, < 3 % for the Na-montmorillonite, around 3 % for the illite-smectite, and < 0.2 % and < 0.5 % for the illites Imt-1 and IWi-1, respectively.

2.3.2 Bulk Magnetic Susceptibility Trends - Smectites

The χ_b results indicate that the magnetic mineral content increased in one of the nontronites (NAu-2) under all tested conditions at both temperatures (Table 2.2; Figure 2.1a, 2.2a). The change in χ_b over this time period corresponds to an approximate 15 % increase (Figure 2.1a, 2.2a) and the augmentation in the magnetic signal is significant at the 99 % confidence interval. The increase in χ_b occurs almost entirely within 10 days for the samples heated at 98°C (Figure 2.1a) and is more gradual when samples are heated at 62°C (Figure 2.2a, up to 100 days). The

more gradual increase in the χ_b in the samples heated at lower temperature could mean that the change in the magnetic signal directly relates to the time it takes for the water to be released from the samples. There are no noticeable differences between clays treated with deionized water, regular tap water, K^+-solution, K^+-solution plus hydrocarbons or only hydrocarbons or any of these conditions plus pyrite. The χ_b of the room temperature control samples reveal no significant changes in the magnetic signal with time. The results indicate that an increase in the magnetic mineral content may occur due to heating of this clay at relatively low temperatures irrespective of conditions applied.

The χ_b of heated Na-montmorillonite samples show increases with time under most conditions and both elevated temperatures (Figure 2.1b, 2.2b) but not at room temperature. Absolute values and the range of χ_b after heating are shown in Table 2.2. The increases in χ_b are observed in many pyrite-containing samples and are highest in samples to which hydrocarbon plus pyrite and tap water plus pyrite were added for samples heated to 98°C (Figure 2.1b). For Na-montmorillonite samples heated to 62°C, the greatest increases in χ_b are observed in the samples receiving potassium plus pyrite, potassium, potassium plus hydrocarbon, and hydrocarbon plus pyrite (Figure 2.2b). The increases in the magnetic signal are gradual at both temperatures and range from 0 to 15.6 % at 98°C and from 0 to 15.5 % at 62°C towards the end of the experiments. The variability of the χ_b signal in terms of percentages relative to the initial measurement (Figure 2.1b, 2.2b) could reflect the relatively low signal to noise ratio for this clay due to its low χ_b intensities. The results for the montmorillonite could indicate changes in the magnetic mineral content, which may have occurred in most of the experiments. The large range in the results

under the different conditions may indicate complex interactions between the clay and the individual treatments.

The third smectite, the Cheney nontronite, which has similar absolute values in the initial χ_b to the other nontronite, shows essentially no variation in χ_b with time during heating under any of the tested conditions or temperatures (Table 2.2; Figure 2.1c, 2.2c). The apparent slight decrease in the χ_b values with time is due to drift in the instrument as indicated by periodic measurements of a standard material (manganese dioxide). The relatively constant magnetic signal suggests that no changes take place in the magnetic mineral content at any of the applied temperatures or conditions.

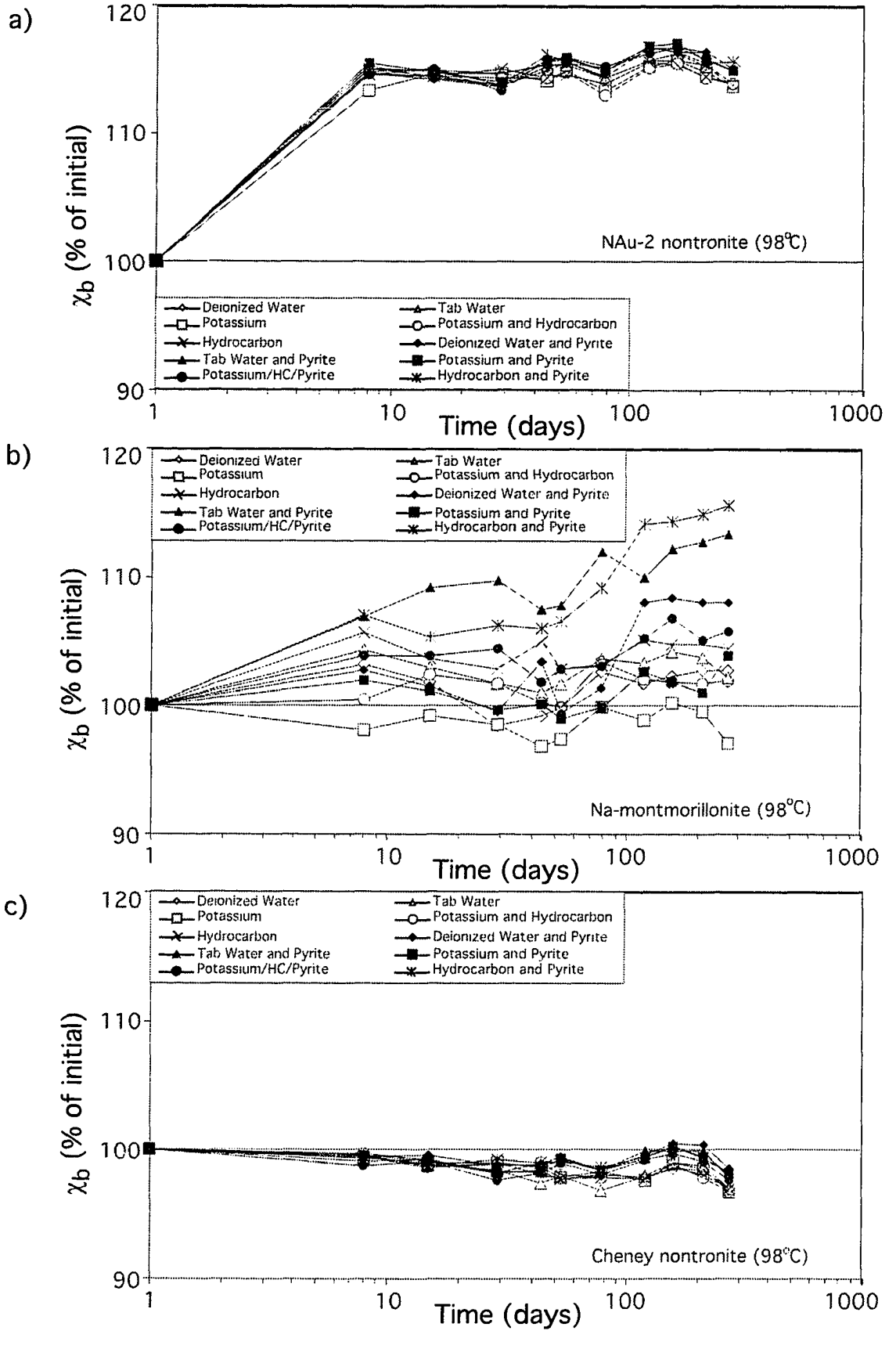
2.3.3 Bulk Magnetic Susceptibility Trends - Other Clays

The heated illite-smectite samples have χ_b values similar to the original measurements with relatively high standard deviations due to the low intensities (Table 2.2). The χ_b of the Imt-1 and IWi-1 illites show no apparent variations with time upon heating at 98 (Figure 2.1d) and 62°C (Figure 2.2d). The results indicate that there were no changes in the magnetic mineral content of the two illites under any of the experimental conditions.

The chlorite (Figure 2.1e, 2.2e; Table 2.2) shows results similar to the illites, i.e. none of the samples revealed alteration of the χ_b signal through time. At both temperatures, the values are approximately equivalent to the initial χ_b recording. The results suggest that no alteration in the magnetic mineral content occurs based on the conditions and temperatures tested herein.

Experimental Condition → / Clay Type ↓	χ_b (before heating to 98°C - initial)	χ_b (after heating to 98°C - 272 days)	χ_b (before heating to 62°C - initial)	χ_b (after heating to 62°C - 230 days)	all χ_b in: [*E^{-8} m^3/kg]
NAu-2: Nontronite	39.3 (0.57)	44.98 (0.67)	39.62 (0.69)	45.66 (0.85)	mean χ_b (std. dev.)
SWy-2: Na-Montmorillonite	4.53 (0.44)	4.04 – 5.73	4.82 (0.26)	5.09 – 5.62	mean χ_b (std. dev.)
Cheney nontronite	38.41 (1.39)	37.46 (1.45)	39.2 (0.92)	39.56 (0.9)	mean χ_b (std. dev.)
ISCZ-1: Illite-smectite	0.23 (0.08)	0.27 (0.2)	0.54 (0.1)	0.52 (0.07)	mean χ_b (std. dev.)
Imt-1: Illite	11.93 (0.34)	11.73 (0.34)	11.63 (0.32)	11.63 (0.31)	mean χ_b (std. dev.)
IWi-1: Illite	– –	– –	2.11 (0.15)	*2.16 (0.18)	mean χ_b (std. dev.)
CCa-2: Chlorite	41.32 (3.12)	41.11 (3.11)	46.8 (0.93)	46.95 (0.99)	mean χ_b (std. dev.)

Table 2.2: Absolute values for mean χ_b measurements and their corresponding standard deviations (std. dev.) prior to and after heating at designated times. Since the Na-montmorillonite showed varying results, χ_b ranges are indicated rather than mean values. *IWi-1 illite samples were heated at 62°C for 105 days.


a)
120
110
100
90
χ_b (% of initial)
NAu-2 nontronite (98°C)
Deionized Water
Potassium
Hydrocarbon
Tab Water and Pyrite
Potassium/HC/Pyrite
Tab Water
Potassium and Hydrocarbon
Deionized Water and Pyrite
Potassium and Pyrite
Hydrocarbon and Pyrite
1
10
100
1000
Time (days)
b)
Na-montmorillonite (98°C)
c)
Cheney nontronite (98°C)

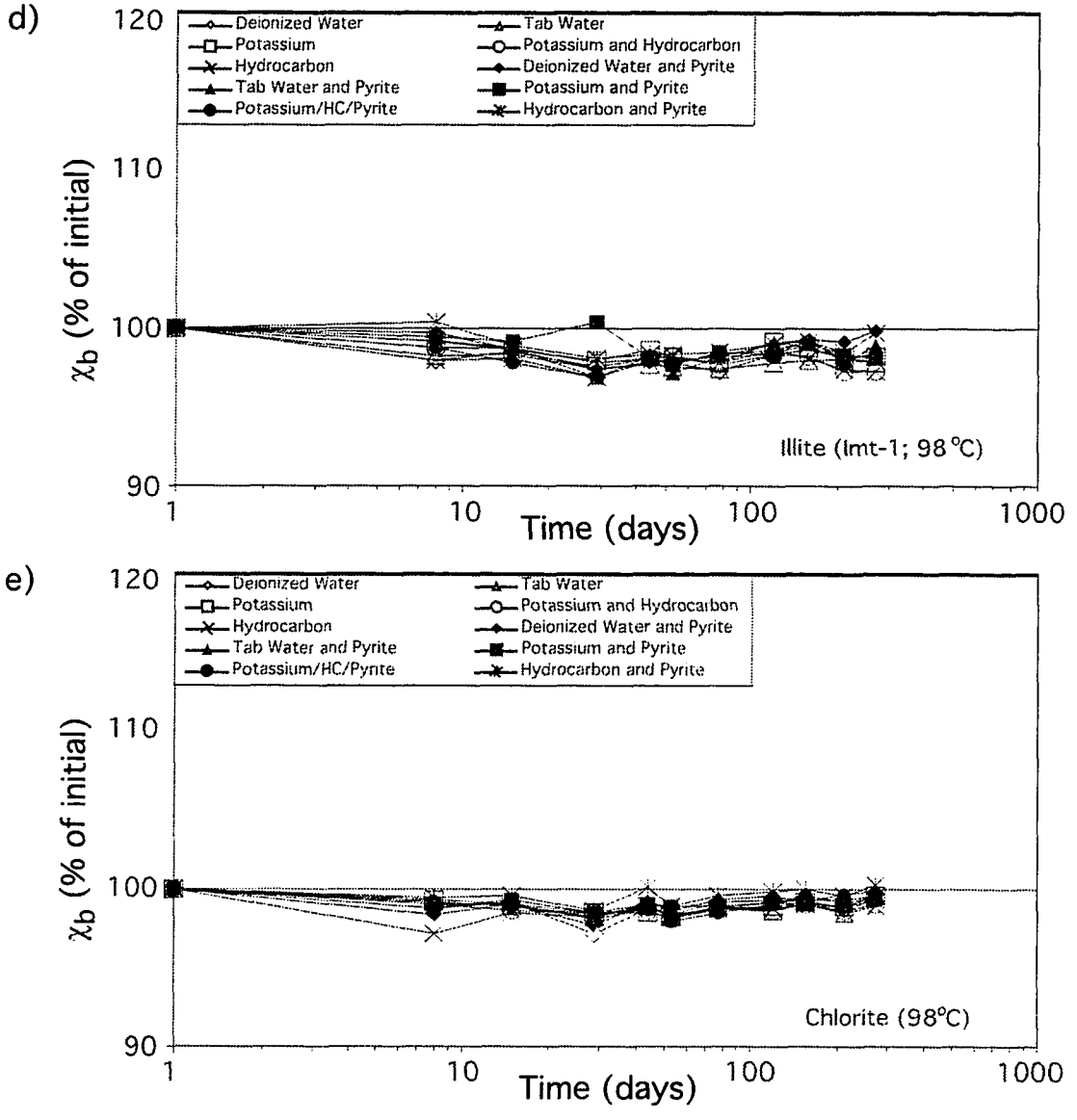
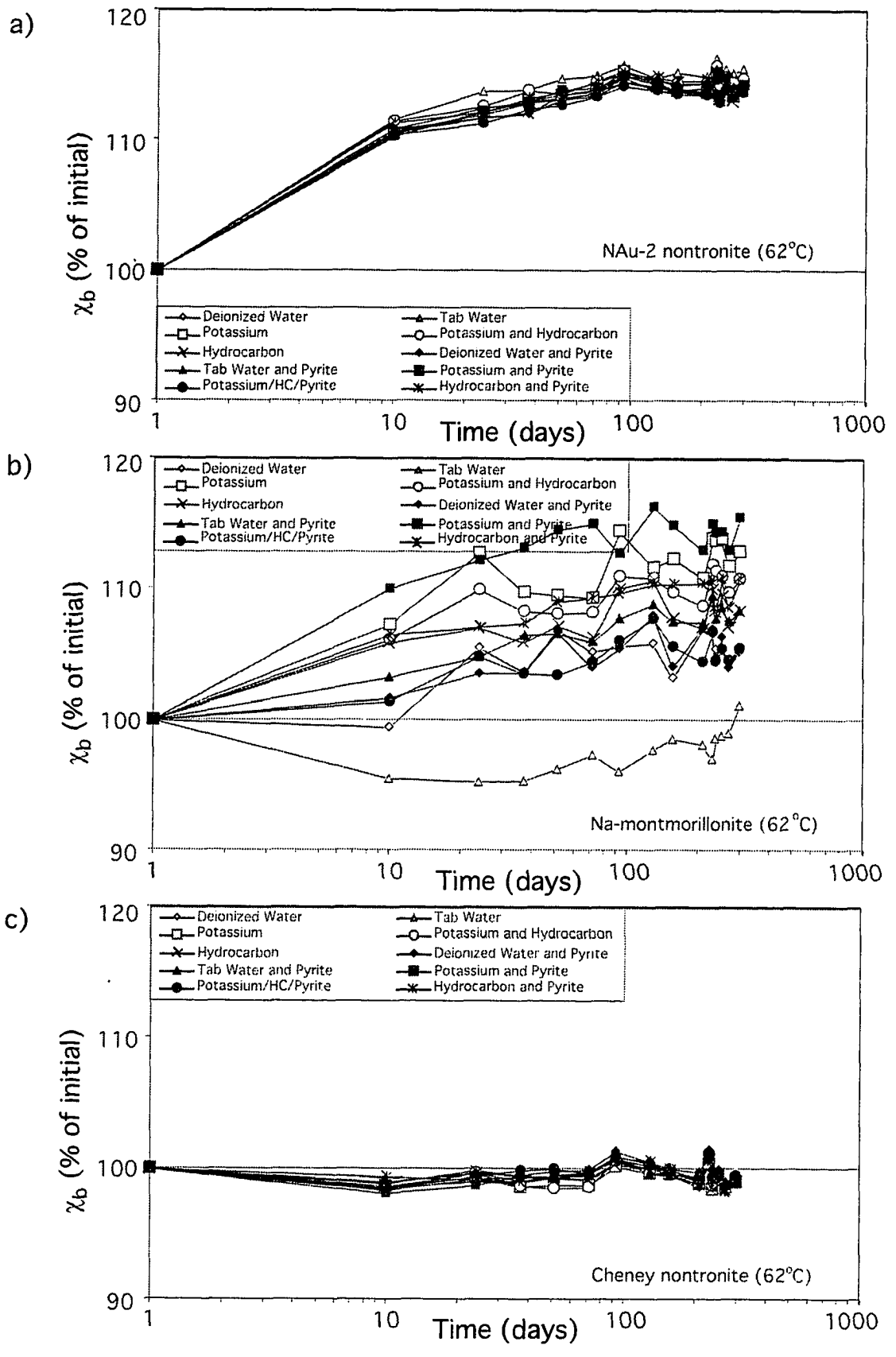


Figure 2.1: Bulk magnetic susceptibility of clays heated to 98°C over time. Three smectites: a) nontronite (NAu-2), b) Na-montmorillonite (SWy-2), and c) iron-sodium nontronite; an illite: d) Imt-1; a chlorite, e) CCa-2. The magnetic signal increased with time in one of the nontronites under all conditions (a) and under most conditions, but to varying degrees in the Na-montmorillonite (b). None of the other clays show significant variations in the susceptibility.


a)
120
110
100
90
χ_b (% of initial)
NAu-2 nontronite (62°C)
Deionized Water
Potassium
Hydrocarbon
Tab Water and Pyrite
Potassium/HC/Pyrite
Tab Water
Potassium and Hydrocarbon
Deionized Water and Pyrite
Potassium and Pyrite
Hydrocarbon and Pyrite
1
10
100
1000
Time (days)
b)
120
110
100
90
χ_b (% of initial)
Deionized Water
Potassium
Hydrocarbon
Tab Water and Pyrite
Potassium/HC/Pyrite
Tab Water
Potassium and Hydrocarbon
Deionized Water and Pyrite
Potassium and Pyrite
Hydrocarbon and Pyrite
Na-montmorillonite (62°C)
1
10
100
1000
Time (days)
c)
120
110
100
90
χ_b (% of initial)
Deionized Water
Potassium
Hydrocarbon
Tab Water and Pyrite
Potassium/HC/Pyrite
Tab Water
Potassium and Hydrocarbon
Deionized Water and Pyrite
Potassium and Pyrite
Hydrocarbon and Pyrite
Cheney nontronite (62°C)
1
10
100
1000
Time (days)

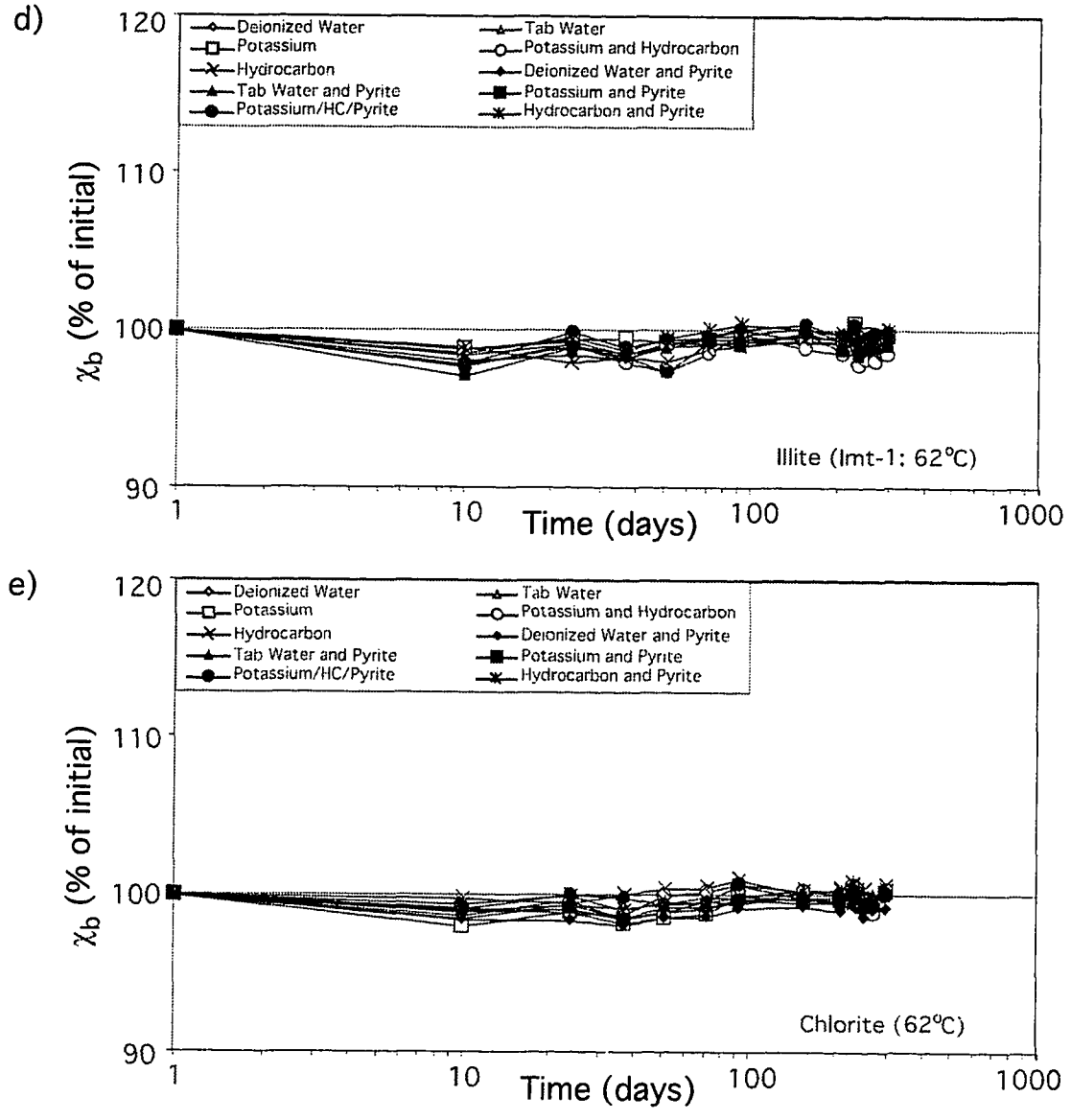


Figure 2.2: Bulk magnetic susceptibility of clays heated to 62°C over time. Three smectites, a) nontronite (NAu-2), b) Na-montmorillonite (SWy-2), and c) iron-sodium nontronite; an illite, d) Imt-1; a chlorite, e) CCa-2. The magnetic signal increased through time in one of the nontronites under all conditions (a) and under most conditions, but to varying degrees in the Na-montmorillonite (b). None of the other clays show significant variations in the susceptibility. The results are very similar to those shown for the same treatments conducted at 98°C.

2.3.4 Magnetic Mineralogy

2.3.4.1 Smectites

Acquisition patterns of IRMs indicate the presence of dominantly low coercivity material in all three smectites prior to and after heating for prolonged times (Figures 2.3a-c). This interpretation is based on the steep initial rise in remanence at applied fields below 200 mT and is also observed in the unheated clay samples. The steep initial rise is most pronounced in the NAu-2 nontronite. An intermediate to high coercivity component appears to be present as well in all three smectites as suggested by the continued rise in remanence at increasing applied fields. This component, however, is not a dominant phase in any of the smectites. The NAu-2 nontronite has a saturation magnetization of 5.98×10^{-6} Am^2/kg prior to heating which is relatively low as suggested by measurements of the matrix material. The matrix material has a saturation magnetization of 1.62×10^{-5} Am^2/kg. The mean saturation remanence is 1.64×10^{-4} Am^2/kg after the experiment for two NAu-2 nontronite samples (Figure 2.3a). The difference between these heated and unheated nontronite samples is interpreted to reflect an increase in the low coercivity phase.

The saturation magnetization for the Na-montmorillonite is 7.08×10^{-5} Am^2/kg before and 7.11×10^{-5} Am^2/kg after heating and thus, shows essentially no variations in the experiments (Figure 2.3b). The Cheney nontronite has similar magnitudes of saturation magnetization with 5.7×10^{-5} Am^2/kg before and 6.69×10^{-5} Am^2/kg after heating (Figure 2.3c).

The thermal demagnetization of tri-axial IRMs of the three smectites reveals that the low coercivity axis is the carrier of two magnetic phases. The decay occurring up to approximately 320°C is characteristic for pyrrhotite. The presence of pyrrhotite is also identified by the decay of

the intermediate coercivity axis around 320°C (Figures 2.4a-c). The remanence along the low coercivity-carrying axis continues to decay up to approximately 580°C, which indicates the presence of magnetite. A representative sample for the NAu-2 nontronite is shown in Figure 2.4a, which characterizes the clay before and after the experiment. The thermal decay patterns of a representative Na-montmorillonite and a Cheney nontronite sample are displayed in Figures 2.4b and c, respectively and the results are also representative for samples before and after heating. The NAu-2 nontronite shows hardly any decay between 320 and 560°C. The abrupt drop in remanence above 560°C suggests that magnetite of a narrow grain size range is present. Unlike in the NAu-2 clay, the Na-montmorillonite and the Cheney nontronite shows a very gradual drop in remanence above 320°C, which probably means that the magnetite in these clays is of a broader grain size distribution. The high coercivity axis appears to carry almost no remanence in any of the three smectites. Any intensity measured along this axis is probably due to minor variations in the orientation of the samples causing an interference with remanence carried by one of the other axes.

Identification of the magnetic mineralogy via IRM acquisition and the thermal demagnetization suggests that remanence-carrying minerals are present but no additional phases are formed after heating. However, intensities in remanence appear to increase in the smectite (NAu-2 nontronite) that shows significant augmentation of the χ_b signal during the experiments. The results suggest that additional magnetite is formed within the NAu-2 nontronite during the heating experiments.

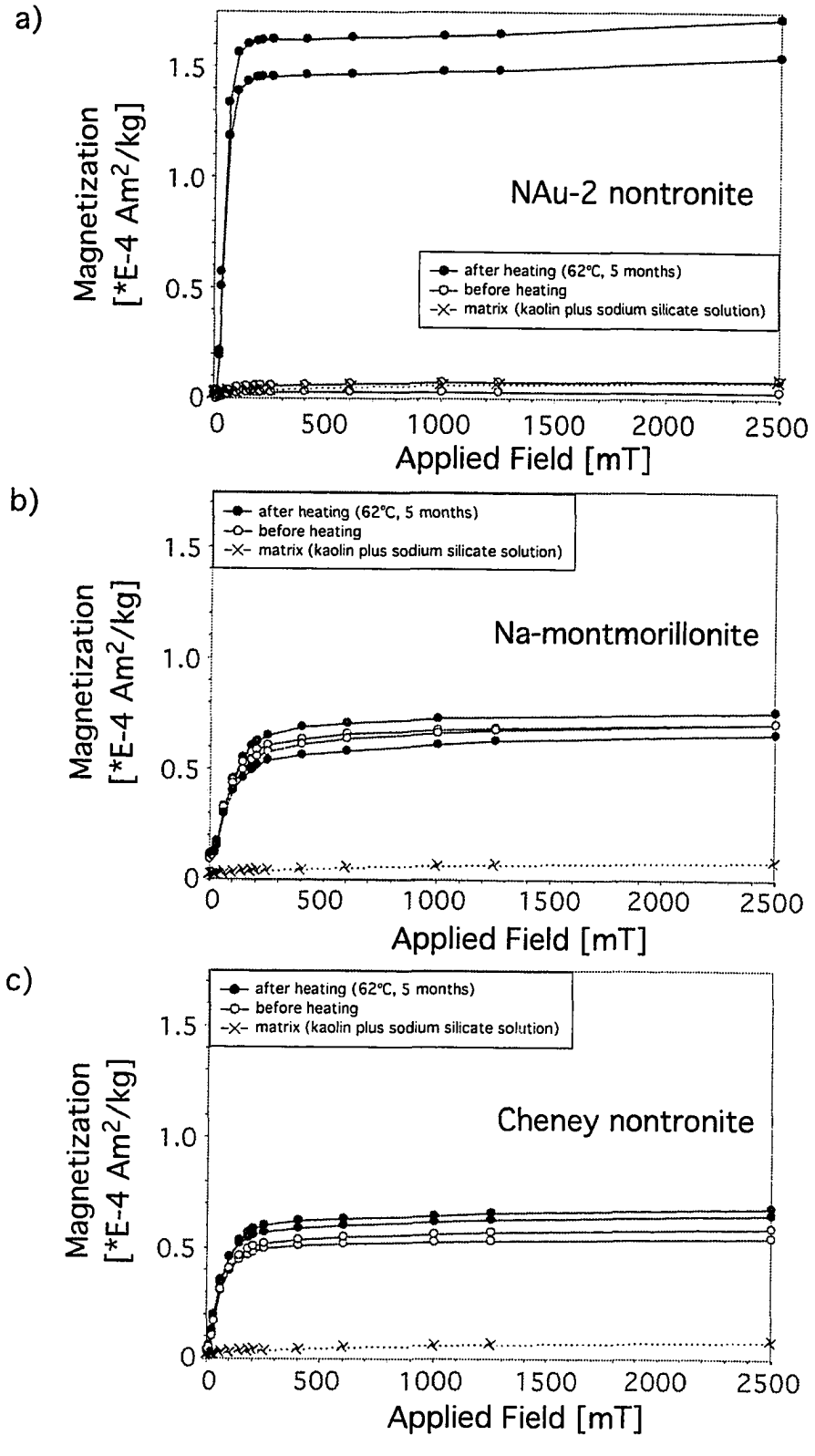
2.3.4.2 Other Clays

The IRMs for an IWi-1 illite sample (Figure 2.3d) show the dominance of a low coercivity component based on the steep initial rise in remanence at fields up to 200 mT. In addition, the presence of an intermediate to high coercivity phase is identified because of the continued rise in remanence to elevated applied fields. The saturation remanence is 2.73×10^{-5} Am^2/kg prior to and 6.06×10^{-5} Am^2/kg after heating. The increase after heating could be interpreted as growth of a remanent phase. However, the difference in SIRMs is interpreted to reflect natural variations in the initial amount of magnetite in the two samples. The absence of χ_b variations is consistent with this interpretation.

The thermal demagnetization of illite samples reveals that the low coercivity phase decays up to approximately 300°C and is thus identified as pyrrhotite (Figure 2.4d). The remanence along the intermediate axis is also carried by pyrrhotite and decays similarly around 300°C. The slightly lower temperatures for the decay in comparison to the other clays could be due to a higher Fe to S ratio (e.g., Fe_9S_{10} instead of Fe_7S_8) or impurities (Thompson & Oldfield, 1986). In addition, there is some magnetite present which was identified based on the continuous demagnetization of the low coercivity axis up to about 550°C. There are no apparent differences between the decay patterns of original clay samples and those heated in the experiments. The results indicate that no additional magnetic phases are formed with heating. This is consistent with the results from χ_b measurements. The magnetic mineralogy of the other illite, i.e. Imt-1 and the illite-smectite (ISCZ-1) were not investigated because of their low intensities.

The chlorite samples reveal the presence of magnetic minerals with a range from low to high coercivities as indicated by the brief steep initial rise followed by a more gradual and continuous increase in remanence up to the maximum applied field (Figure 2.3e). The average saturation remanence for the chlorite is relatively low in comparison to the other clays, with $1.79x10^{-5}$ Am^2/kg before heating and $1.53x10^{-5}$ Am^2/kg after the tests. These values are very similar to the matrix material (Figure 2.3d). The results suggest that there are no differences in the clay samples prior to and after the laboratory treatment.

The low coercivity phase is identified as pyrrhotite based on the drop in remanence up to 320°C (Figure 2.4e). The presence of pyrrhotite is also evident from the loss of remanence along the intermediate axis up to similar temperatures. Furthermore, minor amounts of magnetite appear to be present as suggested by the continual demagnetization of the low coercivity axis up to slightly above 500°C. There are no differences in the magnetic mineralogy of chlorite samples measured for the original clay and the heated samples.


a)
Magnetization [*E-4 Am²/kg]
1.5
1.0
0.5
0
NAu-2 nontronite
after heating (62°C, 5 months)
before heating
matrix (kaolin plus sodium silicate solution)
0
500
1000
1500
2000
2500
Applied Field [mT]
b)
Magnetization [*E-4 Am²/kg]
after heating (62°C, 5 months)
before heating
matrix (kaolin plus sodium silicate solution)
Na-montmorillonite
Applied Field [mT]
c)
Magnetization [*E-4 Am²/kg]
after heating (62°C, 5 months)
before heating
matrix (kaolin plus sodium silicate solution)
Cheney nontronite
Applied Field [mT]

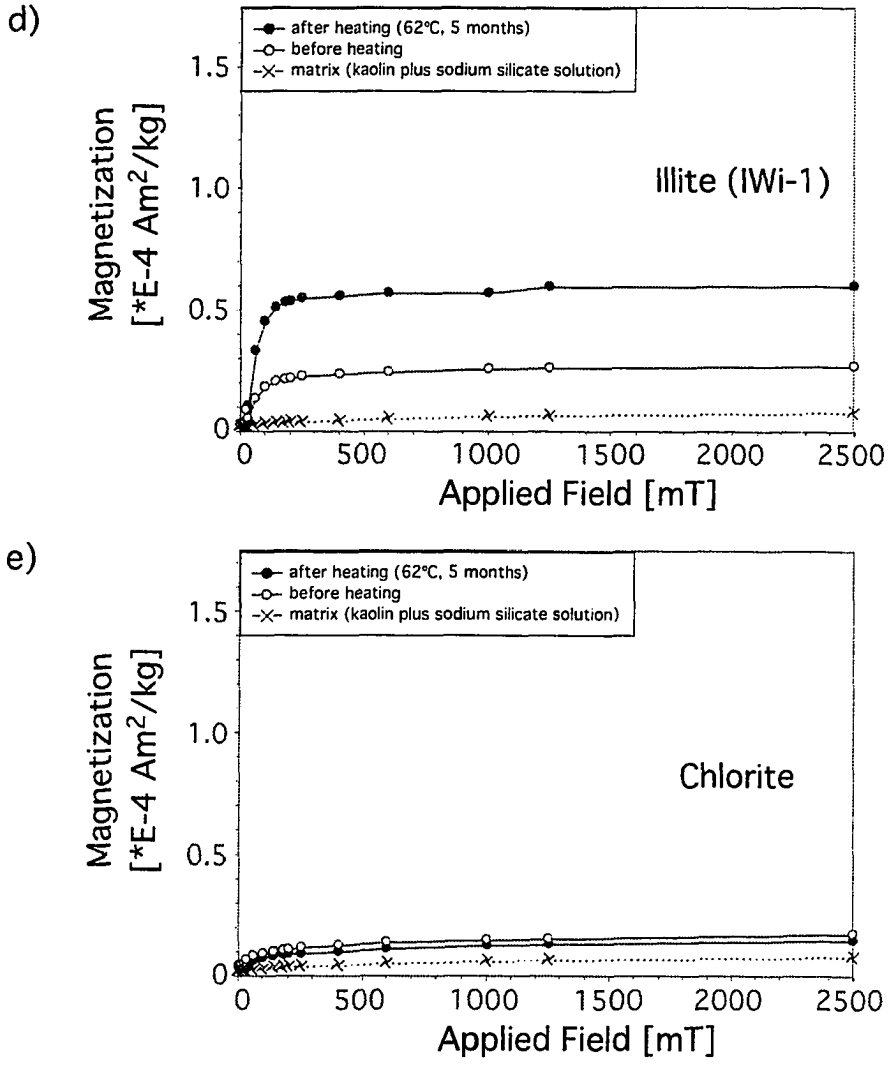
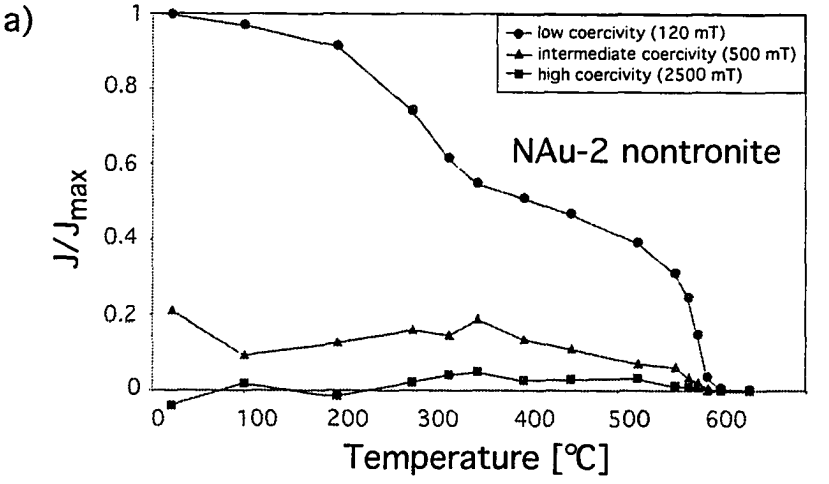
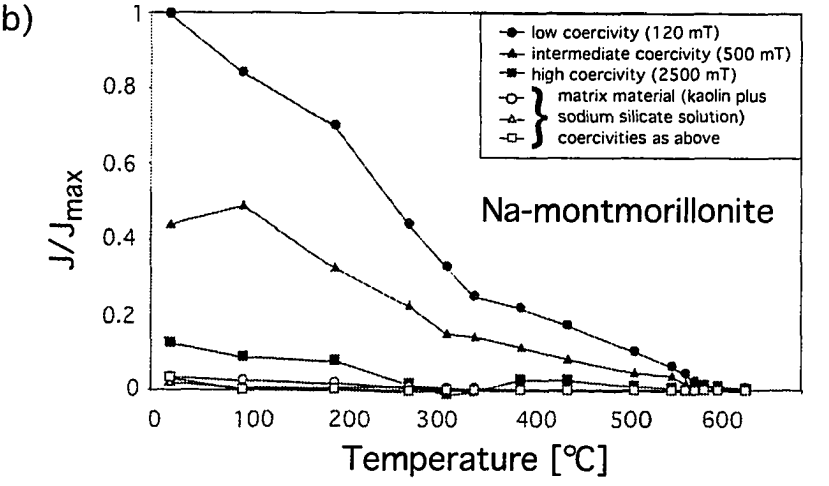
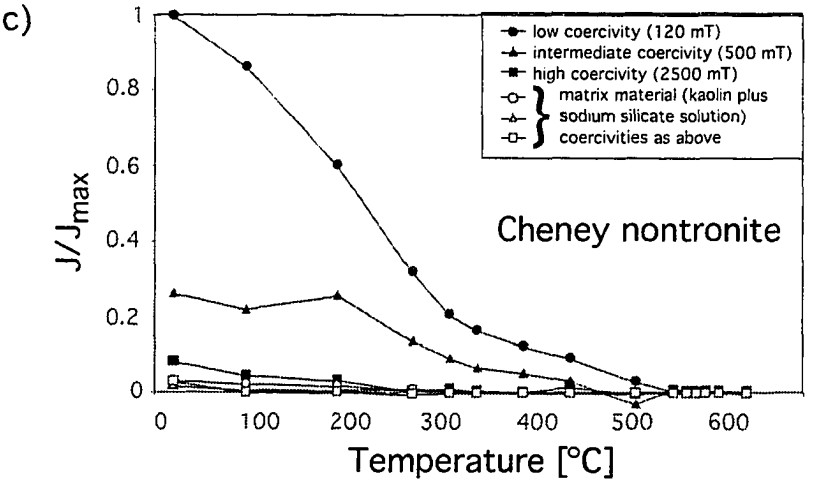


Figure 2.3: IRM acquisition patterns for five clays prior to (open circles) and after the experiments (closed circles). The curves marked by dashed lines and crosses indicate the influence of the matrix material. Acquisition of the remanence occurred dominantly at low applied fields for the three smectites (a-c) and illite (d) indicating a low coercivity phase as the major remanence-carrying factor. The continuous acquisition of remanence at higher field suggested also the presence of an intermediate to high coercivity component in a-d. The chlorite (e) acquired only a relatively small portion of its saturation remanence at low fields suggesting the dominant phase present was an intermediate to high coercivity component.


a)
low coercivity (120 mT)
intermediate coercivity (500 mT)
high coercivity (2500 mT)
NAu-2 nontronite
J/Jmax
Temperature [°C]


b)
low coercivity (120 mT)
intermediate coercivity (500 mT)
high coercivity (2500 mT)
matrix material (kaolin plus sodium silicate solution) coercivities as above
Na-montmorillonite
J/Jmax
Temperature [°C]


c)
low coercivity (120 mT)
intermediate coercivity (500 mT)
high coercivity (2500 mT)
matrix material (kaolin plus sodium silicate solution) coercivities as above
Cheney nontronite
J/Jmax
Temperature [°C]

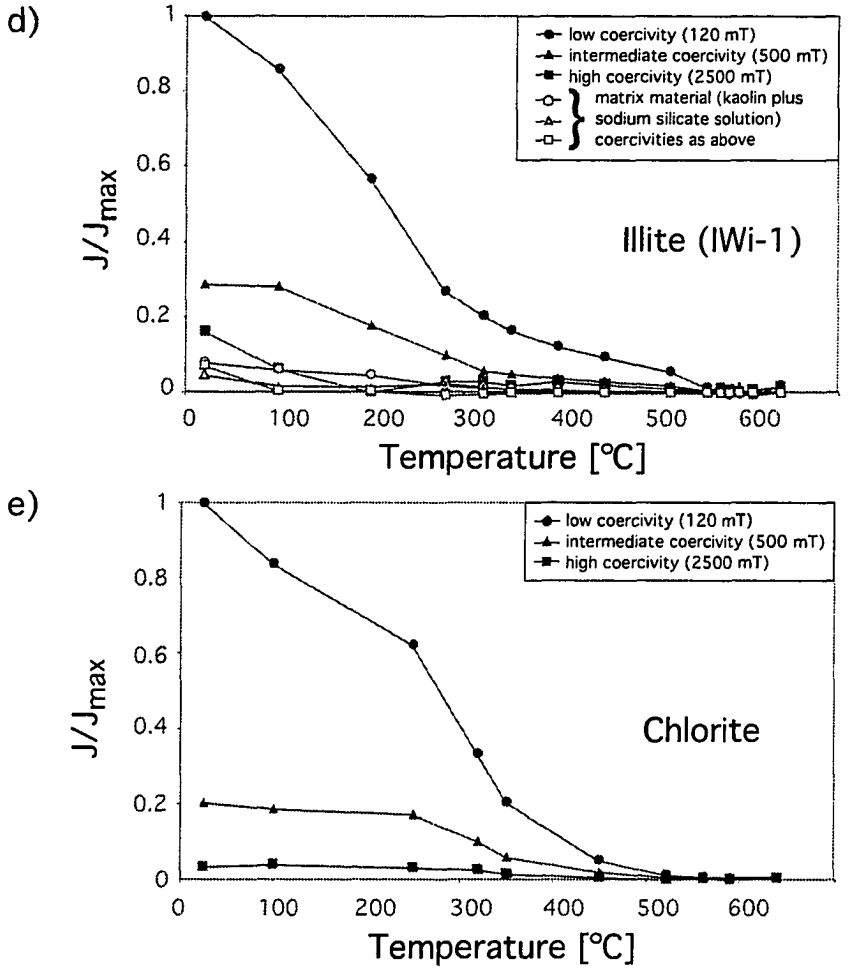


Figure 2.4: Thermal demagnetization of triaxial IRMs for representative samples of the three smectites (a-c), illite (d), and chlorite (e). All clays contained magnetite as the low coercivity phase which caused demagnetization up to around 585°C. An intermediate coercivity component decaying around 320°C was identified as pyrrhotite and was also found in all clays. The steep drop in remanence along the low coercivity-carrying axis in the NAu-2 nontronite (a) at temperatures between 560 to 590°C suggested a relatively narrow grain size range of the magnetite. For all other clays, the more gradual drop along the low coercivity axis at elevated temperatures possibly indicated a wider grain size spectrum of the magnetite present (b-e). The chlorite (e) appeared to contain very minor amounts of magnetite since it decayed at temperatures far below the magnetite Curie temperature which was consistent with its IRM acquisition behavior.

2.4 Discussion

The results suggest that a change in the magnetic signal can occur in some smectites due to heating at relatively low temperatures (62 and 98°C). One nontronite shows increases in χ_b up to 15 % under a variety of laboratory conditions. Magnetite and pyrrhotite are the only magnetic phases present and an increase in the low coercivity material is observed in this clay after heating. A Na-montmorillonite with very weak initial χ_b intensity increases between 0 and over 15 %. The study shows that other clay types such as illites are unlikely to produce increases in the magnetic signal based on the experimental treatments applied herein. Furthermore, it appears that a variety of experimental conditions, such as the presence of hydrocarbons, potassium, or pyrite, are not necessarily causing increases in the magnetic signal on their own. Instead, the presence of certain smectites together with some of the tested conditions may be conducive to alteration of the magnetic signal, as possibly suggested by the varying results for the Na-montmorillonite. Although it is possible that the augmentation of the magnetic signal in the nontronite (NAu-2) samples is partially caused by some of the tested conditions (e.g., the presence of potassium or hydrocarbons), it is not likely because the increases in the χ_b are very similar for all treatments. In addition, the untreated clay and the addition of deionized water alone causes alteration of the magnetic signal. Thus, the mere presence of some smectite types such as NAu-2 appears to be the most important factor responsible for the enhancement of the χ_b.

The reasons for alteration of the magnetic signal in some smectites (e.g., NAu-2 nontronite) but less strongly (e.g., Na-montmorillonite) or not at all in others (e.g., Cheney Fe-Na-nontronite) remains unclear. This phenomenon may be related to the availability or amount and type of iron

within the individual smectite that can be released due to the heating process. By definition, nontronites are smectites that contain ferric iron (Fe^{3+}) as the dominant cation at the octahedral sites of their structure. Thus, there is no lack of iron in the Cheney nontronite, however, all of the iron may be limited to its structural position, which may not be released during the experiments. Montmorillonites on the other hand are smectites in which Al^{3+} dominates the cation sites (e.g., Bishop et al., 1999) and thus, the low concentration of iron could explain why the magnetic signal is very low and shows greater variability than in the NAu-2 nontronite.

Magnetite is present in all smectites after heating and possibly prior to heating as well, although magnetic mineral alteration during thermal demagnetization can not be ruled out. This ferrimagnetic mineral has a strong influence on measurements of χ_b and the increases in the signal with time within the NAu-2 nontronite and the Na-montmorillonite may be caused by the creation of additional magnetite grains. Magnetite could form due to the conversion from smectite to illite. However, it is not known whether the smectite was diagenetically altered to illite and analyses including X-ray diffractometry are currently underway to investigate this possibility.

The initial presence of magnetite in the clays could be due to detrital magnetite or authigenic magnetite that formed some time during deposition of the rocks and prior to laboratory treatment. Measurements of χ_b are affected by ferrimagnetic components such as different grain sizes of magnetite ranging from superparamagnetic (SP) to multidomain-size and paramagnetic minerals such as clays. The augmentation of the χ_b, or at least part of it, could be caused by the formation of SP-size magnetite, which carries remanence below room temperature.

Another possible explanation is that some of the pyrrhotite present in the clays, could have been oxidized to form magnetite during prolonged heating under ambient atmospheric conditions. However, since pyrrhotite was identified in all of the investigated naturally occurring clays, one could expect this process to take place irrespective of clay type. This is contradictory to the observations made in the experiments presented above.

The enhancement in χ_b could also have been caused by the additional formation of pyrrhotite, particularly within the NAu-2 nontronite. Although pyrrhotite is commonly considered an intermediate coercivity component, the thermal demagnetization of tri-axial IRMs clearly indicate its strong influence on the low coercivity axis. An interpretation in terms of pyrrhotite formation, however, may be less likely because the formation of this iron sulfide requires reducing conditions, which were not provided in the experimental design. Therefore, an increase in magnetite appears to be the more reasonable explanation for the increase in the magnetic signal.

Another possible explanation for the augmentation in the χ_b in the two smectites is that the clays were altered during the heating process and form a new clay type (possibly illite) with stronger paramagnetic χ (χ_p). Generally, nontronites have larger χ_b than illites based on the examples herein and as suggested in the literature (Thompson & Oldfield, 1986). However, these data have not compared data of illites formed as a direct result from the diagenetic conversion of its precursor smectite.

The results are consistent with the creation of magnetite and have possible implications for the formation of some pervasive CRMs. The temperature ranges applied in the experiments are

equivalent to low to moderate burial conditions. The depth for such temperatures could extend from about 1.5 to 3 km based on normal thermal gradients. At such depth, smectites can undergo diagenetic conversion to illite – a process during which iron may be released (Boles & Franks, 1979). If the formation of magnetite can occur due to heat exposure of certain smectites at depth concurrent with a transformation of the clays, it is possible that, once the magnetic grains reach remanence-carrying size, the particles acquire the magnetic direction during their time of formation and could record a CRM.

Further rock magnetic analyses are needed in order to decipher the magnetic mineralogy and granulometry of the magnetic phase before and after heating. If the differences reside in the magnetic mineral grains capable of recording the magnetic field, the laboratory experiments could prove useful as an analogue to explain the mechanism of the occurrence of some pervasive CRMs such as those reported for the Vocontian trough in southeast France (Katz et al., 1998). Furthermore, analyses of the clays such as via X-ray diffractometry before and after the heating experiments may determine whether those changes in the magnetic mineralogy are directly associated with the transformation of smectite to illite and are being investigated. Alternatively, the NAu-2 nontronite may contain iron (possibly ferrous and ferric) adsorbed to the clay surface, which could be converted to ferrimagnetic phases upon prolonged heating (Hirt et al., 1993). The reasons why the Na-montmorillonite shows inconsistent results could be due to the fact that this clay appears to contain only Fe^{3+} in its octahedral structure and essentially no other iron is present in this clay (Bishop et al., 1999). Supplementary analyses such as the use of infrared

spectroscopy (Bishop et al., 1999) could aid in deciphering why alteration of the magnetic signal occurs in some smectites, but not in others.

These results are a novelty in that a connection between smectites and an associated alteration in the magnetic signal has previously only been documented for significantly higher temperatures (e.g., Hirt et al., 1993). The results of this study suggest that long-term exposure at low temperatures (< 100°C) can lead to increases in the magnetic signal.

2.5 Conclusions

The magnetic signal changes in some clays as measured via χ_b in response to heating at temperatures as low as 62°C. Alteration of the χ_b occurs in some smectites, i.e. a nontronite (NAu-2) and possibly a Na-montmorillonite, but not in another nontronite, illite-smectite, illites or chlorite. The changes in the magnetic signal are triggered by exposing the clays to elevated temperatures. Other conditions such as the addition of potassium, hydrocarbons and pyrite are not required as a cause for the increase in the magnetic signal. Magnetite and pyrrhotite are the only remanence-carrying phases present before and after the heating process and an increase in magnetite is the most likely cause for the increase in the magnetic signal, although paramagnetism of the transformed clays or authigenesis of superparamagnetic grains may be reasonable alternatives.

The results are consistent with previous studies, which identified an empirical connection between CRMs and the diagenetic conversion of smectite to illite in sedimentary rocks. The fact that the alteration of the magnetic signal occurs at low temperatures and under all tested

conditions for smectites – a common clay in sedimentary deposits, suggests that heating at temperatures equivalent to burial to low and moderate depth may be sufficient to alter the magnetic signal. Further research is necessary to decipher whether the increase in the magnetic signal is linked to authigenesis of magnetite associated with smectite alteration or to clay alteration alone.

References Chapter 2

Banerjee, S., R.D. Elmore, and M.H. Engel, Chemical remagnetization caused by burial diagenesis: Testing the hypothesis in the Pennsylvanian Belden formation, Colorado, *Journal of Geophysical Research, 102*, 24825-24842, 1997.

Bishop, J.L., E. Murad, J. Madejová, P. Komadel, U. Wagner, and A.C. Scheinost, Visible, Mössbauer and infrared spectroscopy of dioctahedral smectites Sampor, SWy-1 and SWa-1, In *Clays for our Future*, Proceeding 11th International Clay Conference, Ottawa, 413-419, 1999.

Boles, J.R., and S.G. Franks, Clay diagenesis in Wilcox sandstones of Southwest Texas; implications of smectite diagenesis on sandstone cementation, *Journal of Sedimentary Petrology, 49*, 55-70, 1979.

Elmore, R.D., M.H. Engel, L. Crawford, K. Nick, S. Imbus, and Z. Sofer, Evidence for a relationship between hydrocarbons and authigenic magnetite, *Nature, 325*, 428-430, 1987.

Elmore, R.D., and C.R. McCabe, The occurrence and origin of remagnetization in the sedimentary rocks of North America, in *Contributions in Geomagnetism and Paleomagnetism*, pp. 377-383, U.S. Nat. Rep. Int. Union Geod. Geophys. 1987-1990, 1991.

Geilmann, W., W. Klemm, K. Meisel, Das Auftreten hochmagnetischer Zwischenstufen bei der thermischen Zersetzung des Nontronits, *Naturwissenschaften, 20*, 639-640, 1932.

Hirt, A.M., A. Banin, and A.U. Gehring, Thermal generation of ferromagnetic minerals from iron-enriched smectites, *Geophysical Journal International, 115*, 1161-1168, 1993.

Jackson, M., C. McCabe, M.M. Ballard, and R. Van der Voo, Magnetite authigenesis and diagenetic paleotemperatures across the northern Appalachian Basin, *Geology, 16*, 592-595, 1988.

Jackson, M., Diagenetic sources of stable remanence in remagnetized Paleozoic cratonic carbonates: a rock magnetic study, *Journal of Geophysical Research, 95*, 2753-2761, 1990.

Katz, B., R.D. Elmore, M. Cogoini, and S. Ferry, Widespread chemical remagnetization: Orogenic fluids or burial diagenesis of clays? *Geology, 26*, 603-606, 1998.

Katz, B., R.D. Elmore, M. Cogoini, M.H. Engel, and S. Ferry, Associations between burial diagenesis of smectite, chemical remagnetization, and magnetite authigenensis in the Vocontian trough, SE France, *Journal of Geophysical Research, 105*, 851-868, 2000.

Lowrie, W., Identification of ferromagnetic minerals in a rock by coercivity and unblocking temperature properties, *Geophysical Research Letters, 17*, 159-162, 1990.

Lu, G., C. McCabe, J.S. Hanor, and R.E. Ferrell, A genetic link between remagnetization and potassic metasomatism in the Devonian Onondaga formation, Northern Appalachian basin, *Geophysical Research Letters, 18*, 2047-2050, 1991.

Machel, H.G., and E.A. Burton, Chemical and microbial processes causing anomalous magnetization in environments affected by hydrocarbon seepage, *Geophysics, 56*, 598-605, 1991.

Machel, H.G., Magnetic mineral assemblages and magnetic contrasts in diagenetic environments - with implications for studies of palaeomagnetism, hydrocarbon migration and exploration, in

Palaeomagnetic applications in hydrocarbon exploration and production, edited by P. Turner, and A. Turner, pp. 9-29, Geological Society Special Publication, 1995.

McCabe, C., and R.D. Elmore, The occurrence and origin of late Paleozoic remagnetization in the sedimentary rocks of North America, *Reviews of Geophysics, 27*, 471-494, 1989.

McCabe, C., M. Jackson, and B. Saffer, Regional patterns of magnetite authigenesis in the Appalachian Basin; implications for the mechanism of late Paleozoic remagnetization, *Journal of Geophysical Research, 94*, 10, 429-10,443, 1989.

Miller, J.D., and Kent, D.V., Regional trends in the timing of Alleghanian remagnetization in the Appaclachians, *Geology, 16*, 588-591, 1988.

Moskowitz, B.M., and R.B. Hargraves, Magnetic changes accompanying the thermal decomposition of nontronite (in air) and its relevance to Martian mineralogy, *Journal of Geophysical Research, 87*, 10115-10128, 1982.

Moskowitz, B.M., and R.B. Hargraves, Magnetic cristobalite (?): A possible new magnetic phase produced by thermal decomposition of nontronite, *Science, 225*, 1152-1154, 1984.

Oliver, J., Fluids expelled tectonically from orogenic belts: Their role in hydrocarbon migration and other geologic phenomena, *Geology, 14*, 99-102, 1986.

Oliver, J., The spots and stains of plate tectonics, In *Metamorphic fluids*, edited by W.S. Fyfe, pp. 77-106, Elsevier, Amsterdam, Netherlands, 1992.

Stamatakos, J., A.M. Hirt, and W. Lowrie, The age and timing of folding in the central Appalachians from paleomagnetic results, *Geological Society of America, 108*, 815-829, 1996.

Thompson, R., and F. Oldfield, Environmental magnetism, London, Allen and Unwin Ltd., pp. 227, 1986.

Woods, S.D., R.D. Elmore, and M.H. Engel, The occurrence of pervasive chemical remanent magnetizations in sedimentary basins: Implications for dating burial diagenetic events, *Journal of Geochemical Exploration, 69/70*, 381-386, 2000.

CHAPTER 3

Rock Magnetic Evidence for the Authigenesis of Remanence-Carrying Magnetite in Thermally Treated Smectite – An Analogy to Low Burial Conditions

3 Abstract

Bulk magnetic susceptibility (χ_b) results of three smectites heated for prolonged times at 62°C confirm previously reported increases in χ_b in a nontronite (NAu-2) and, with greater variability, in a moistened Na-montmorillonite (SWy-2) but not in a nontronite from Cheney, Washington. Hysteresis measurements combined with thermal demagnetization of low-temperature saturation isothermal remanent magnetization (SIRM) analyses, room temperature IRMs, and anhysteretic remanent magnetization (ARM) of the NAu-2 nontronite indicate that the increase in χ_b is at least partially caused by the formation of ferrimagnetic material and not only by changes in the paramagnetism of the heated clay. The authigenic phase is interpreted as magnetite and is of superparamagnetic (SP) as well as remanence-carrying grain size. The Na-montmorillonite showed weak intensities in all remanence measurements and hence, the origin of the augmentation of the χ_b in this clay could not be determined. The reasons for the unchanged Cheney nontronite remain unclear but could be related to a lack of easily releasable iron in this clay. Although pyrrhotite is also present in all three smectites, it is less likely created in the experiments because results suggested the authigenesis of a lower coercivity magnetic mineral and conditions provided were not conducive for the creation of a reduced phase such as pyrrhotite. X-ray diffraction analysis of the NAu-2 nontronite suggest that illitization of the smectite did not take place. The findings suggest that a smectite diagenetic process other than the formation of illite triggered by temperatures equivalent to low burial can cause authigenesis of magnetic phases like magnetite of grain sizes sufficient to carry remanence and acquire a chemical remanent magnetization (CRM). This laboratory study provides supporting genetic

evidence for a potential connection between some clay diagenetic processes and the formation of some widespread CRMs.

3.1 Introduction

Chemical remanent magnetizations (CRMs) are common in sedimentary rocks (e.g., Elmore & McCabe, 1991). Many of these secondary magnetizations are caused by the formation and growth of magnetite crystals. The reasons for the post-depositional creation of additional magnetic phases on regional scales are a matter of debate. It is important to understand the origin of CRMs because they can be used to date the processes responsible for their formation.

Previous research has shown an empirical connection between chemical remanent magnetizations (CRMs) and burial diagenesis of smectites (e.g., Katz et al., 1998, 2000). The CRM in those rocks commonly resides in magnetite. A laboratory study revealed that iron loading onto the surface of a montmorillonite resulted in the formation of magnetite at temperatures above 250°C (Hirt et al., 1993). Hirt et al. (1993) also suggested that unidentified magnetic nanophases developed at lower temperatures on the clay surface as precursors of the magnetite, which was created at higher temperatures. In previous work, factors like the presence of potassium, hydrocarbons, and pyrite were tested as potential agents for magnetic signal enhancement (see Chapter 2). The study revealed that some smectites showed increases in the bulk magnetic susceptibility (χ_b) when they were heated to 62 and 98°C – temperatures equivalent to low burial conditions – for prolonged times and that different boundary conditions (e.g., presence of hydrocarbons or potassium) were not of importance. Magnetite and pyrrhotite

were identified in the study as the only magnetic phases present before and after the heating experiments. Since no additional phase was identified, it remains unresolved whether the increases in χ_b values were caused by authigenesis of magnetite or, alternatively, by an increase in the paramagnetic susceptibility (χ_p) due to alteration of the clays or by the formation of additional pyrrhotite. Furthermore, it needs to be investigated whether the alteration in the magnetic signal occurred within grain sizes that are capable of acquiring a stable remanent magnetization. Rock magnetic techniques can result in the identification and characterization of such magnetic minerals.

This study presents research conducted in the laboratory on three smectites in the presence and absence of deionized water. The clays were heated to 62°C to test for reproducibility and statistical significance of magnetic alteration at low temperature. In order to identify the origin of possible changes in the magnetic signal as determined via χ_b, several rock magnetic analytical techniques were applied, including investigations at and below room temperature. The paramagnetic component was also determined using hysteresis measurements (e.g., Housen et al., 1996) in order to understand whether increases in the χ_b could be caused by alteration of the clays alone. If the origin of the augmentation of the magnetic signal is found in authigenic magnetite, this study could confirm smectite diagenesis as a viable mechanism for many of the extensive CRMs occurring in sedimentary basins. Smectites are ubiquitous in sedimentary rocks and an association between their alteration and the formation of CRMs during heating of the clays at temperatures equivalent to low to moderate burial conditions could provide a reasonable explanation for many widespread secondary magnetizations.

3.2 Materials and Methods

Two smectites, a nontronite from Australia with high iron content designated NAu-2 and a Na-montmorillonite (SWy-2) from Crook County in Wyoming (U.S.A.) were purchased from the Source Clay Minerals Repository. A third smectite, a nontronite from Cheney, Washington (49E5108) was obtained from Ward's Natural Science Establishment, Inc. The three clays were ground with mortar and pestle (maximum fragment size of 3 mm) where necessary in order to obtain homogenous samples for the experiments.

For the NAu-2 nontronite, 10 air-dried samples were weighed into glass tubes (either 5 or 6 g) and 10 samples were mixed with deionized water (5 or 6 ml) dispersed in a slightly diamagnetic matrix (plaster of paris). The amounts of matrix material added were equal to those of the individual clays (ranging from 5 to 6 g) and the cylindrical shaped samples were about 2 cm in height and 2 cm in diameter. The samples treated with deionized water will be referred to as wet samples. Five air-dried samples of the Na-montmorillonite (4.5 g) and the Cheney nontronite (6 g) were placed into glass tubes and another 5 samples (same mass as for dry samples) of each clay type were prepared like the wet NAu-2 samples. For the wet samples, 10 and 7 ml water were used for the Na-montmorillonite and the Cheney nontronite, respectively. Six matrix samples (5 g) bound with deionized water (5 ml) were used as control samples and their mass normalized magnetic signal was subtracted from the appropriate clay samples. Those samples mixed with the matrix were allowed to dry for several days at ambient temperatures under dust free conditions.

The mass normalized bulk magnetic susceptibility (χ_b) was measured for all samples on a Sapphire SI-2B instrument prior to heating to 62°C. The χ_b was periodically remeasured and the samples remained at elevated temperatures for over 100 days. Subsets of samples were prepared only from clays that were not mixed into a matrix, except for a few Na-montmorillonite samples, and were used for further rock magnetic analyses. To prepare subsamples of the clays for a variety of rock magnetic measurements, the clays were dispersed in a sodium silicate solution (or sodium silicate solution and kaolin) and allowed to solidify for several days.

Selected samples underwent hysteresis experiments, which were conducted using a Vibrating Sample Magnetometer (Micro VSM) at the Institute for Rock Magnetism, University of Minnesota. The hysteresis of each of the samples was measured 5 times and data reported herein are based on the calculated averages. Since the strong paramagnetic nature of the clays causes relatively high noise level in the signal and problems such as poorly centered loops, shifting corrections were applied to the loops. A total of 12 samples (6 NAu-2 nontronite, 2 Na-montmorillonite, and 4 Cheney nontronite) were measured. Hysteresis measurements were taken in order to determine the contribution of the ferrimagnetic (χ_f) and paramagnetic (χ_p) material to the χ_b signal in the original clays as compared to their heated equivalents. A comparison of saturation magnetization (Ms) for unheated and heated samples of each clay type was used to identify whether changes in the total magnetic content have occurred. Hysteresis characteristics also assist in the identification of the magnetic phases of the different smectites before and after the experiments for example by providing information about the coercivity ranges necessary to reach saturation.

In order to determine the presence of superparamagnetic (SP) and coarser magnetite grains, the thermal demagnetization patterns of low-temperature SIRMs acquired at 10°K were measured on a Magnetic Property Measurement System (MPMS) at the Institute for Rock Magnetism. The cooling patterns to 10°K for room temperature SIRMs were also recorded for 10 NAu-2 nontronite (before/after heating: 4/6), 3 Na-montmorillonite (1/2), and 2 Cheney nontronite samples (1/1). Usually, the remanence of most samples is stronger than the induced magnetization, which is caused by imperfect magnetic shielding. However, there was a strong induced component due to the paramagnetism of the clays and the effects of the induced magnetization were estimated and corrected. After modeling the effects of several magnetic fields between 5 and 10 A/m, a field of 7 A/m was assumed to be present. The assumption was based on the fact that none of the measured samples should have negative magnetizations after the corrections were applied. A field of 7 A/m was the smallest field strength resulting in only positive remanence values for the temperature ranges. In order to calculate the contribution of the induced magnetization, the following relationship was used: $M_i = C*H/T$, where M_i is the induced magnetization, C is the Curie constant, H is the implied residual magnetic field, and T is the temperature (e.g., O'Reilly, 1984; Dunlop & Özdemir, 1997). The Curie constant was calculated for each sample by multiplying the χ_p, as determined in the hysteresis measurements, by 300°K, i.e. the estimated temperature at which the hysteresis was acquired. The calculated induced magnetization was then added to the original low-temperature measurements at each temperature, since the residual field apparently opposed the applied SIRM.

The amount of SP grains in samples from the NAu-2 nontronite was estimated by calculating the difference between the magnetization at 25°K and room temperature. Commonly, the proportion of SP grains is calculated by subtracting the SIRM from the remanence at 300°K and excluding the effect of the Verwey transition if present (Hunt et al., 1995). However, since the drop in remanence below 25°K could be due to an ordering of the clay in the smectite samples and because corrections were applied to the measured data, the method for estimating the SP grains was altered and hence, the comparison could only be used for relative comparison.

The total anhysteretic remanent magnetization (ARM) was produced by exposing samples to a 0.1 mT direct field while applying an alternating field (AF) of 100 mT using a 2G Automated Degaussing System. The remanence was subsequently recorded on a 2G, three-axes, cryogenic magnetometer located in a magnetically shielded room. The ARMs were measured for 22 (6 before and 16 after heating) NAu-2 nontronite, 15 (5 before, 10 after heating) Na-montmorillonite, and 18 (3 before, 15 after heating) Cheney nontronite samples. Variations in ARMs are commonly interpreted to reflect differences in the abundance of magnetite in the remanence-carrying fraction, i.e. single domain (SD) and coarser grain size (e.g., Hunt et al., 1995).

Afterwards, most of the ARM samples were demagnetized by AF demagnetization and subsequently exposed to direct fields of 200 and 2500 mT in an impulse magnetizer. The isothermal remanent magnetization was measured at both steps (IRM_{200} and SIRM, respectively) to determine the relative contribution of low and high coercivity magnetic.

In order to identify whether the NAu-2 smectite underwent diagenetic alteration such as a conversion to illite, X-ray diffraction analyses were conducted on a sample prior to heating and another one after the experiments (approximately 100 days of heating at 62°C). Intact fragments of the samples were prepared by adding water to an aliquot of solid material, mixing thoroughly, allowing to settle for 1-5 minutes, then pipetting the liquid onto a 2.54 cm diameter glass slide. The clay-sized particles suspended in the liquid settled onto the glass slide as the water evaporated forming an air-dried, oriented mount, which was suitable for clay mineral analysis. Samples were reanalyzed following expansion with ethylene glycol. The glass slides holding the air-dried clay suspensions were placed in a desiccator containing EGME which was subsequently maintained at 30°C for 24 hours. This procedure expands the smectite basal spacing allowing confirmation of its presence. Powders of the whole rock were scanned from 4 to 60° 2θ at two degrees per minute, air-dried clay separates were scanned from 2 to 30° 2θ at two degrees per minute, and glycolated samples were scanned from 2 to 20° 2θ at two degrees per minute. X-rays were generated from a copper filament maintained at 40 mA and 40 kV. X-ray tube slits were 2 mm and 1 mm and detector slits were 0.5 mm and 0.3 mm. The detector is a Peltier cooled, solid state Theta-Theta diffractometer, Scintag, Inc., XPDS 2000).

3.3 Results and Interpretations

3.3.1 Bulk Magnetic Susceptibility

Table 3.1, Figures 3.1 and 3.2 indicate that the NAu-2 nontronite had the highest initial absolute χ_b values in comparison to the other two smectites. The NAu-2 nontronite also showed

significant increases in the bulk magnetic susceptibility with time in both wet and dry samples that were heated to 62°C (Figure 3.1 = dry clays, Figure 3.2 = wet clays). The dry NAu-2 nontronite showed an augmentation of the χ_b within the first approximately 20 days and values remained relatively unchanged during continued heating (Figure 3.1). The wet NAu-2 nontronite increased in χ_b within only 10 days and remained at steady levels afterwards (Figure 3.2). The magnetic signal was augmented by approximately 9.5 % for the dry clays and 12.5 % for the wet clays. The corresponding averaged absolute values prior to and after heating and a summary of the statistical analysis of all clays are displayed in Table 3.1. Probabilities < 0.05 indicate statistically significant differences existed between the initial χ_b and periodic χ_b measurements thereafter based on student t tests (e.g., Sall & Lehman, 1996). The results for this clay confirmed those of previous experiments conducted with the NAu-2 nontronite (see chapter 2) and possibly suggested an increase in the magnetic material due to heating.

The Na-montmorillonite had very weak average χ_b values (on average 61.4 *E-9 m^3/kg) and the dry version of the clay appeared to remain constant even after prolonged heating times (Table 3.1, Figure 3.1). The statistical analysis, however, indicated the tendency of the magnetic signal of this smectite to drop slightly, but significantly (Table 3.1). These variations are obvious in the inset of Figure 3.1, which shows an enlarged scale for the samples of the montmorillonite. Though this loss of χ_b appeared to be significant, measurements of a standard material (manganese dioxide) conducted each measurement day suggested that the apparent drop was caused by a machine induced drift with time of a similar amount. Thus, the results of the dry Na-montmorillonite were interpreted to reflect that no changes occurred in the magnetic signal. The

addition of water to this smectite caused a slight augmentation of the χ_b, which dominantly occurred during the early stages of the experiment (Table 3.1, Figure 3.2 inset). The statistical analysis (Table 3.1) revealed these results were significant at the 95 % confidence interval. The increases in χ_b in the wet samples were, on average, 5.4 % of the initial value and indicate additional magnetic material may have formed during the heating process. These results were consistent with those previously reported for this clay.

The Cheney nontronite had relatively high initial χ_b values, which were slightly below those of the previously described nontronite. Both the dry and wet Cheney nontronite samples (Figures 3.1 and 3.2, respectively) showed a small decrease in the χ_b with time during heating. The magnitude of the reduction in the magnetic signal was similar to those observed for the standard material. Thus, the results were interpreted to reflect that no changes in the magnetic signal occurred. An unchanged χ_b of this smectite was in accordance with observations reported previously.

Clay Type	Initial mean (std) χ_b [*E^{-9}m^3/kg]	Desig-nation	60°C 3 days	60°C 6 days	60°C 9 days	60°C 17 days	60°C 26 days	60°C 38 days	60°C 50 days	60°C 72 days	60°C 104/105 days
NAu-2 (dry)	[1] 403.7 (5.1) [2] 438.6 (6.9) [1+2] 421.2 (19.3)	Δ mean χ_b std. dev. Prob > |t| n		+ 20.96 9.65 < 0.0001 10	+ 32.83 8.48 < 0.0001 10	+ 41.59 3.81 < 0.0001 10	+ 37.86 3.24 < 0.0001 10	+ 39.05 3.63 < 0.0001 10	+ 38.77 3.09 < 0.0001 10	+ 42.7 7.34 < 0.0001 10	+ 39.73 9.75 < 0.0001 10
NAu-2 (wet)	[1] 447.8 (4.2) [2] 481.8 (6.8) [1+2] 464.8 (18.7)	Δ mean χ_b std. dev. Prob > |t| n	+ 32.73 7.27 < 0.0001 10	+ 51.97 4.51 < 0.0001 10	+ 49.96 3.62 < 0.0001 10	+ 57.42 3.51 < 0.0001 10	+ 60.97 4.21 < 0.0001 10	+ 59.19 4.08 < 0.0001 10	+ 63.64 3.82 < 0.0001 4	+ 58.74 4.19 < 0.0001 8	+ 57.51 4.42 < 0.0001 8
Na-Mont. (dry)	61.4 (3.2)	Δ mean χ_b std. dev. Prob > |t| n		-0.45 0.42 0.0765 5	-0.67 0.35 0.0131 5	-0.37 0.38 0.0979 5	-1.37 0.41 0.0017 5	-1.35 0.39 0.0015 5	-1.06 0.27 0.0009 5	-1.16 0.6 0.0127 5	-1.51 0.38 0.0009 5
Na-Mont. (wet)	55.1 (10.2)	Δ mean χ_b std. dev. Prob > |t| n	+ 2.17 1.72 0.0476 5	+ 3.03 1.66 0.015 5	+ 2.28 1.18 0.0125 5	+ 3.58 1.39 0.0045 5	+ 3.43 1.92 0.0163 5	+ 3.29 1.4 0.0063 5	+ 2.68 0.7 0.1171 2	+ 2.92 1.61 0.036 4	+ 2.65 1.23 0.0228 4
Cheney Nontr. (dry)	373.4 (6.1)	Δ mean χ_b std. dev. Prob > |t| n		-3.75 2.3 0.022 5	-3.45 1.86 0.0144 5	-3.35 1.93 0.0179 5	-6.0 1.51 0.0009 5	-5.72 1.99 0.003 5	-5.66 1.88 0.0025 5	-1.24 5.84 0.6608 5	-4.82 6.48 0.1716 5
Cheney Nontr. (wet)	406.8 (4.3)	Δ mean χ_b std. dev. Prob > |t| n	-6.71 1.21 0.0002 5	-3.39 1.13 0.0026 5	-7.49 1.58 0.0004 5	-2.69 0.92 0.0028 5	-2.31 0.86 0.0039 5	-5.67 1.65 0.0015 5	-9.84 0.12 0.00562 5	-14.0 1.14 0.0001 4	-14.71 0.81 0.0001 4

[1,2] Two different orders NAu-2 nontronite were used.

Table 3.1: Summary of statistics for the three smectites left as delivered and mixed with deionized water. All χ_b as values *E-9. Statistics were performed for the two sets of NAu-2 together. Delta mean values reflect differences to the initial χ_b. Probabilities that are < 0.05 indicate the differences are statistically significant.

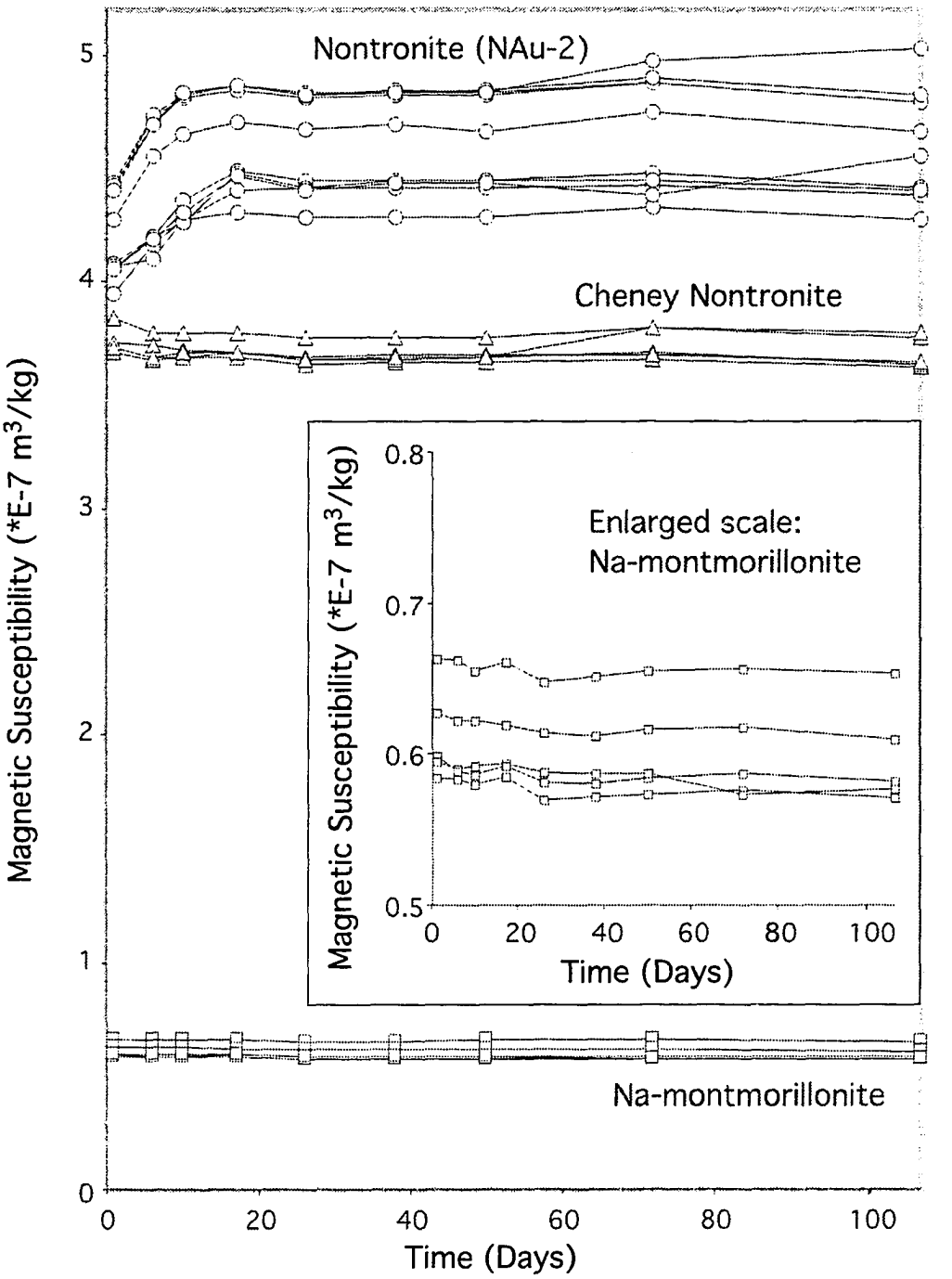


Figure 3.1: The χ_{lf} of representative dry clay samples for the NAu-2 nontronite (circles), the Cheney nontronite (triangles), and the Na-montmorillonite (squares) measured periodically during treatment. The NAu-2 nontronite showed significant increases in all samples which occurred dominantly within the first 20 days, suggesting possible changes in the magnetic mineral content of this clay. Samples for both other clay types appeared to remain at their original intensities indicating no alteration of the magnetic mineral. Small decreases through time are due to instrumental drift.

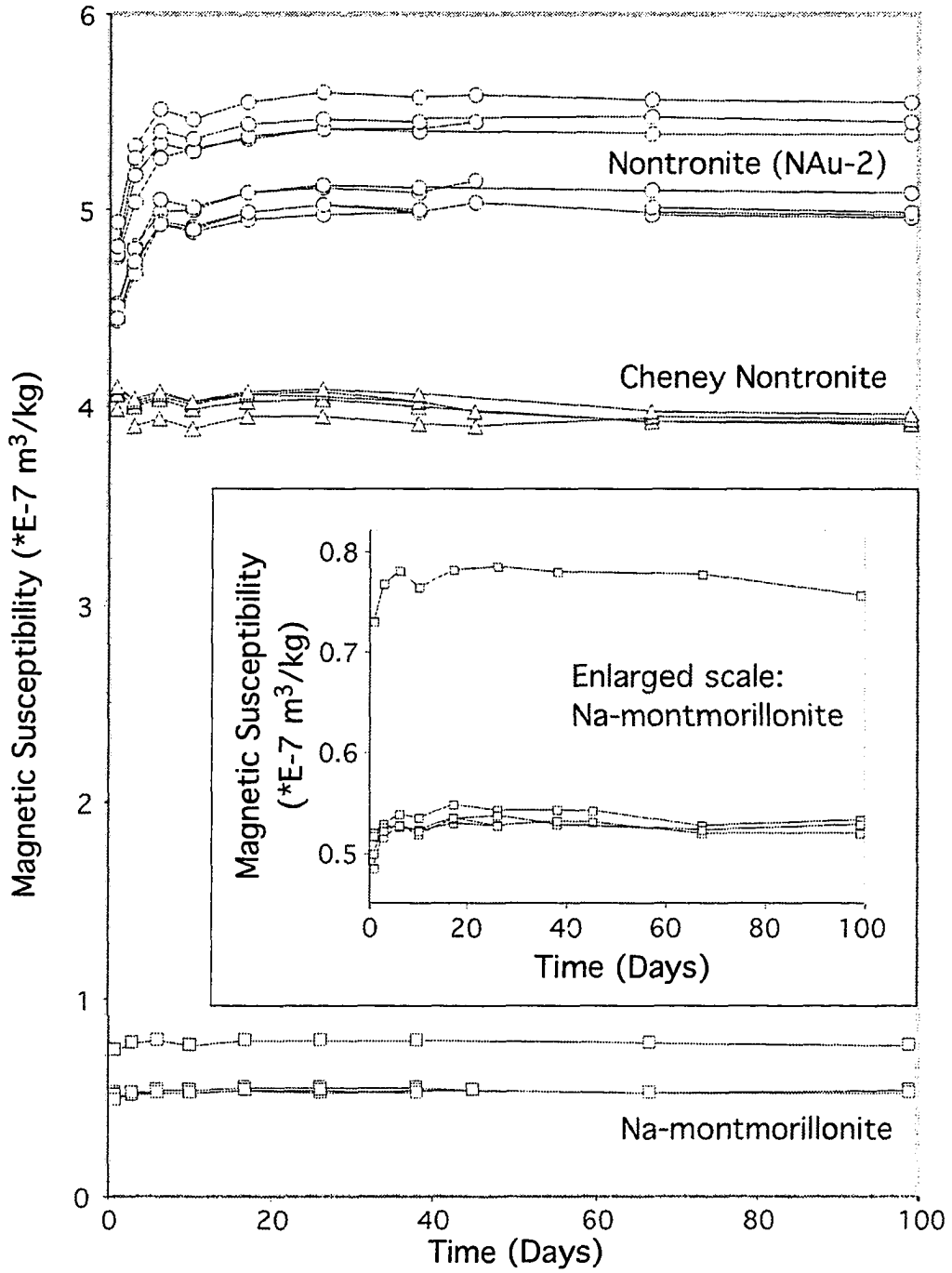


Figure 3.2: Absolute χ_{lf} of NAu-2 (circles) and Cheney nontronite (triangles), and Na-montmorillonite (squares) samples heated at 62°C in deionized water. The NAu-2 nontronite showed increases in all samples occurring within only about 10 days - much faster in comparison to the dry clay (Figure 1) - suggesting changes in the magnetic signal can occur more rapidly when abundant water was present. The Na-montmorillonite showed minute increases in χ_{lf} which are visible on the enlarged scale shown for the inset, which indicate possible alteration of the magnetic signal due to heating in the presence of water. A slight decrease in the χ_{lf} observed particularly for Cheney nontronite samples, was caused by instrument drift determined by measurements of a standard (MnO_2) and the values for this smectite are considered to remain unchanged.

3.3.2 Hysteresis

The strong influence of the paramagnetism of the clays was responsible for the tendency of the loops to be noisy, positioned off-center (prior to applying corrections), and indisputable closure of the loops was in some cases not evident. The paramagnetic influence of the clays dominated the hysteresis loops for all three smectite types based on strong intensities and almost straight-line behavior (Figure 3.3 a-c, smaller graphs on the right side). When the paramagnetic component was eliminated from the data by applying a slope correction, the resulting hysteresis loops revealed that ferrimagnetic material was also present in each of the clays (Figure 3.3 a-c, left side). The presence of low coercivity material was evinced by a more rapid initial increase in intensities at low applied fields up to about 200 mT. Furthermore, the continuous and more gradual augmentation of the magnetization at higher applied fields was indicative of the presence of intermediate to high coercivity magnetic material. There were no significant differences between the shapes of the hysteresis loops for the original and the heated clay samples. These results were consistent with previous IRM acquisition and thermal demagnetization experiments, which identified the two components as magnetite and pyrrhotite (Chapter 2).

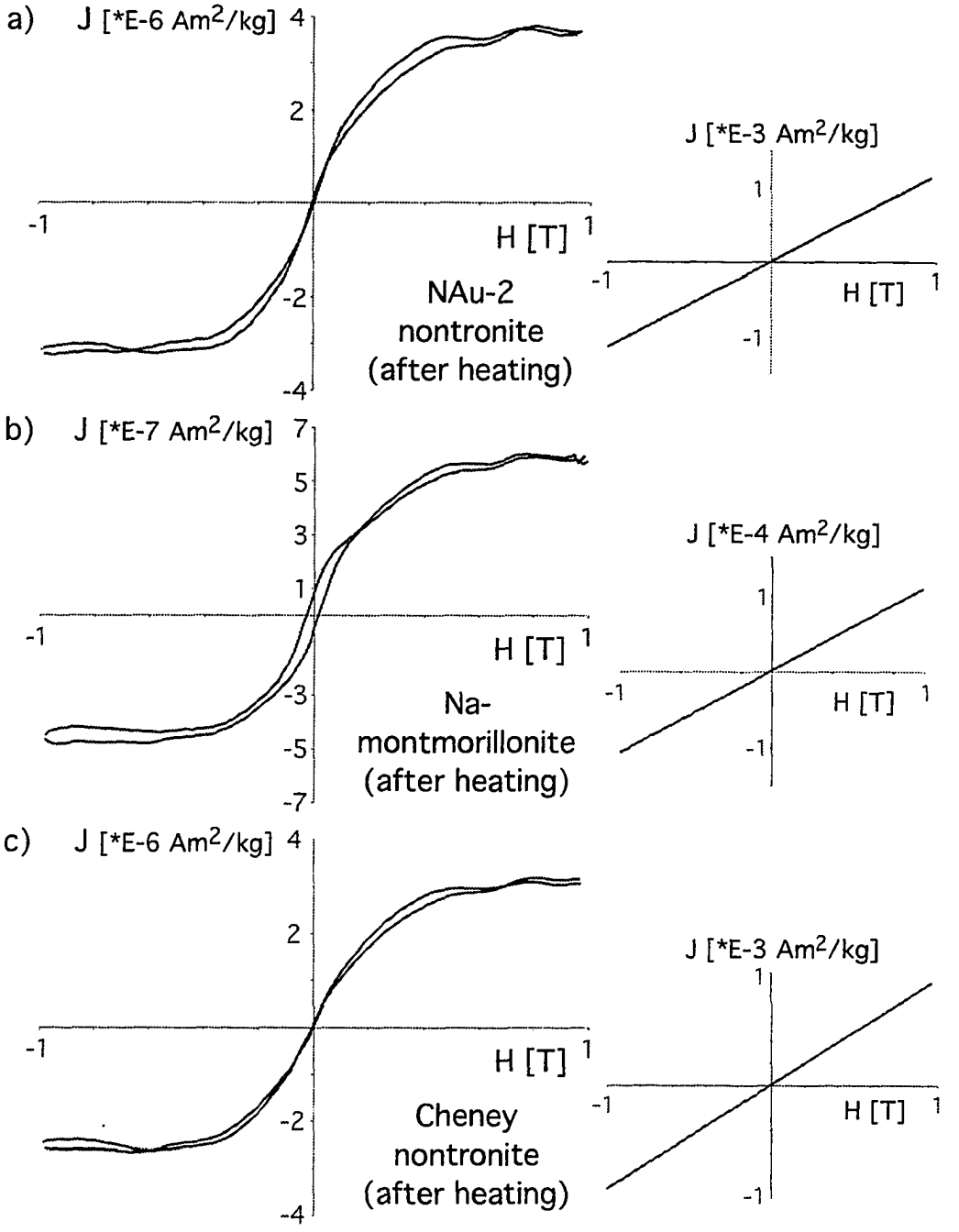


Figure 3.3: Hysteresis loops for the three smectites after heating. The data shown on the left were slope corrected, i.e. the influence of paramagnetic material was subtracted from the measured signal. The original data is displayed on the right and indicated the strong paramagnetic component in each clay type. The two nontronites (a and c) had similar intensities in both - slope corrected and uncorrected data. The Na-montmorillonite had weaker intensities and hysteresis measurements were somewhat difficult to achieve because of the low J values. Hysteresis loops also indicated the presence of low and intermediate coercivity material. J = magnetization; H = applied field.

The hysteresis results were also used to calculate the χ_f for the three clay types prior to and after heating. Concurrent with an increase in χ_b was an increase in the ferrimagnetic contribution to the signal for the NAu-2 nontronite (Figure 3.4). The original clay shows a very small portion of the χ_b was carried by ferrimagnetic material with an average of 2.9 % (standard deviation = 1.2 %). After the heating process, the χ_f increased to make up a mean of 12.1 % (standard deviation = 3.7 %) of the χ_b (Figure 3.4). It should be noted that the absolute values for the χ_b were slightly higher compared to those measured on the SI2B Sapphire instrument (Figures 3.1, 3.2; Table 3.1). This was interpreted to be due in part to differing sensitivities of the measurement devices and/or, different frequencies (e.g., Hunt et al., 1995). Collateral with the enhanced χ_f after heating of the clays was a general increase in the saturation magnetization (Ms) from an average of 2.7 *E-6 Am^2/kg to 3.34 *E-6 Am^2/kg (Figure 3.4). The augmented contribution of the χ_f to the χ_b and the increase in Ms were interpreted to indicate the formation of additional ferrimagnetic material, both in remanence-carrying and in SP grains. The χ_p also increased in the heated NAu-2 nontronite samples by an average of 12.1 % from 5.15 to 5.78 *E-7 m^3/kg. This increase suggests that clay diagenetic processes cause not only the formation of ferrimagnetic components but also an augmentation in the paramagnetic character of the altered clay.

As for the Na-montmorillonite, the intensity of χ_b was very small and the proportion of χ_f was determined as < 1 %. However, these results were based on only two samples (Figure 3.4). The difference before and after heating was very small and was similar to the observations from the measurements on the SI2B Sapphire instrument. The Ms for the two samples was 0.48 and 0.53 *E-6 Am^2/kg prior to and after heating, respectively. The small increase in Ms – although only

determined for one sample pair – was consistent with χ_b results of the wet clays. Due to the low intensities, however, it remains uncertain whether the increase in χ_b was caused by the addition of ferrimagnetic grains or an augmented paramagnetic signal.

The two investigated Cheney nontronite samples had χ_b similar to the initial values of the NAu-2 nontronite, but showed no changes in the contribution of the χ_f to the bulk signal before and after heating (Figure 3.4). The proportion of the χ_f to the χ_b was on average 13.6 % and the Ms was 1.95 *E-6 Am^2/kg before heating and 2.58 *E-6 Am^2/kg after the heating process. This difference was probably due to natural variations within the clay and was not considered to be significant. A strong but unchanging contribution of the χ_f before and after heating agreed with a strong χ_b signal, both of which were similar in magnitude to the NAu-2 samples prior to heating.

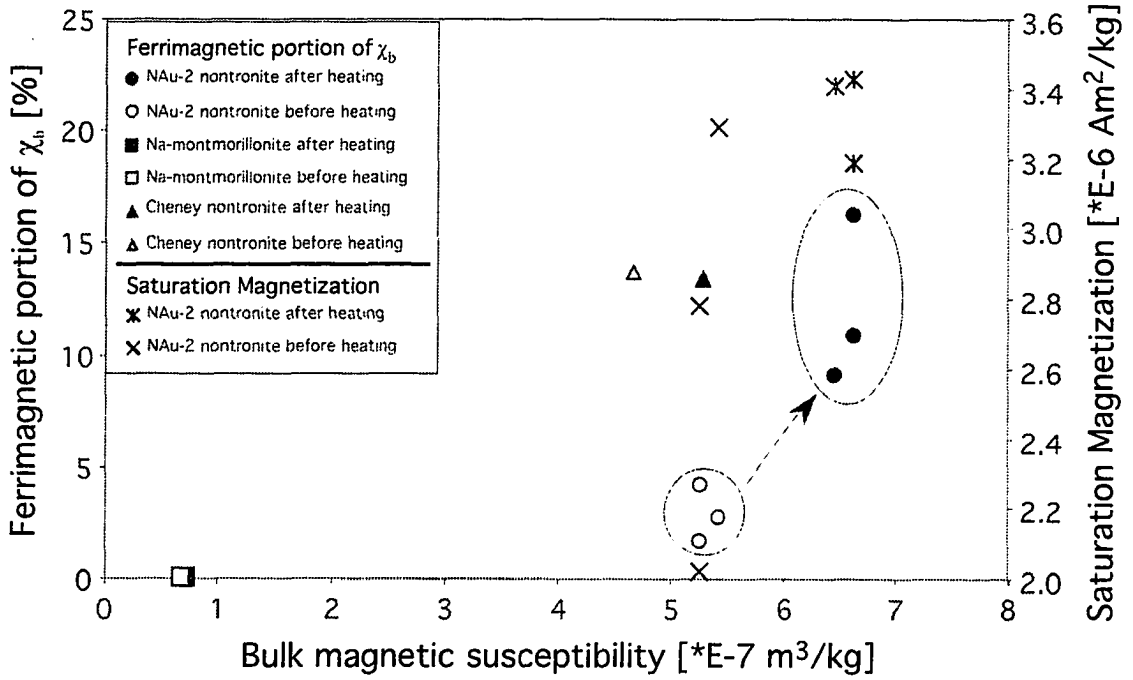


Figure 3.4: Proportion of ferrimagnetic material of the χ_b for clay samples prior to (open symbols) and after heating (closed symbols) in relation to χ_b. The increase in χ_f is concurrent with the increase observed in χ_b for the heated NAu-2 nontronite samples suggesting the additional formation of ferrimagnetic material. There are not sufficient measurements for the other two smectites, but results may indicate only a very small amount of ferrimagnetic material present within the Na-montmorillonite and no changes in the ferrimagnetic content occurred due to heating. The two Cheney nontronite samples showed no significant variations between the unheated the heated sample. An apparent increase in the saturation magnetization (Ms) for the NAu-2 nontronite samples from before heating (×) to after heating (*) is consistent with an increase in ferrimagnetic material.

3.3.3 Low-Temperature Analyses

Thermal demagnetization of low temperature SIRMs for NAu-2 nontronite samples showed a steep initial decrease in remanence up to 20°K (Figure 3.5a). Upon further heating, the remanence continued to decrease slightly up to 300°K. The rapid initial drop was probably due to an ordering of the clay and may not reflect a ferrimagnetic phase. The remaining intensity at 300°K and the fact that the acquisition of a room temperature SIRM resulted in an increase in remanence suggested the presence of magnetic material capable of carrying remanence at room temperature. The observation was consistent with previous magnetic mineral identification and IRM acquisition and decay measurements (Chapter 2), and hysteresis results. However, neither the Verwey transition (a loss of remanence occurring during heating at 110-120°K due to a temperature dependent crystallographic change in magnetite) nor the magnetite isotropic point (a loss in remanence occurring in magnetite during cooling below about 120°K caused by a change in the magnetocrystalline anisotropy energy) were observed in any of the measurements.

Figure 3.5b shows a representative thermal demagnetization curve of an SIRM acquired at 10°K and a cooling curve for a room temperature SIRM for the Na-montmorillonite. The gradual decay of the remanence upon heating was interpreted to reflect the presence of SP grains, which were probably magnetite (e.g., Hunt et al., 1995). The remanence that remained at room temperature and the higher SIRM suggested that magnetic minerals capable of carrying remanence at 300°K were present. The relatively weak remanence intensity was consistent with the findings of other rock magnetic methods such as IRM acquisition (Chapter 2) and hysteresis measurements. There were no significant differences between heat treated and original clay

samples. Similar to the NAu-2 nontronite, the Verwey transition and the isotropic point for magnetite were not observed for the Na-montmorillonite.

The thermal demagnetization pattern of the Cheney nontronite was similar to that of the Na-montmorillonite and suggested the presence of what was probably SP magnetite (Figure 3.5c). The room temperature remanence of the thermally demagnetized sample and the SIRM indicated that magnetic minerals were present, which are capable of carrying remanence at room temperature. The results confirmed findings of other rock magnetic identification and characterization techniques. The Cheney nontronite samples before and after heating remained essentially unchanged and there was no indication of a Verwey transition or the isotropic point for magnetite.

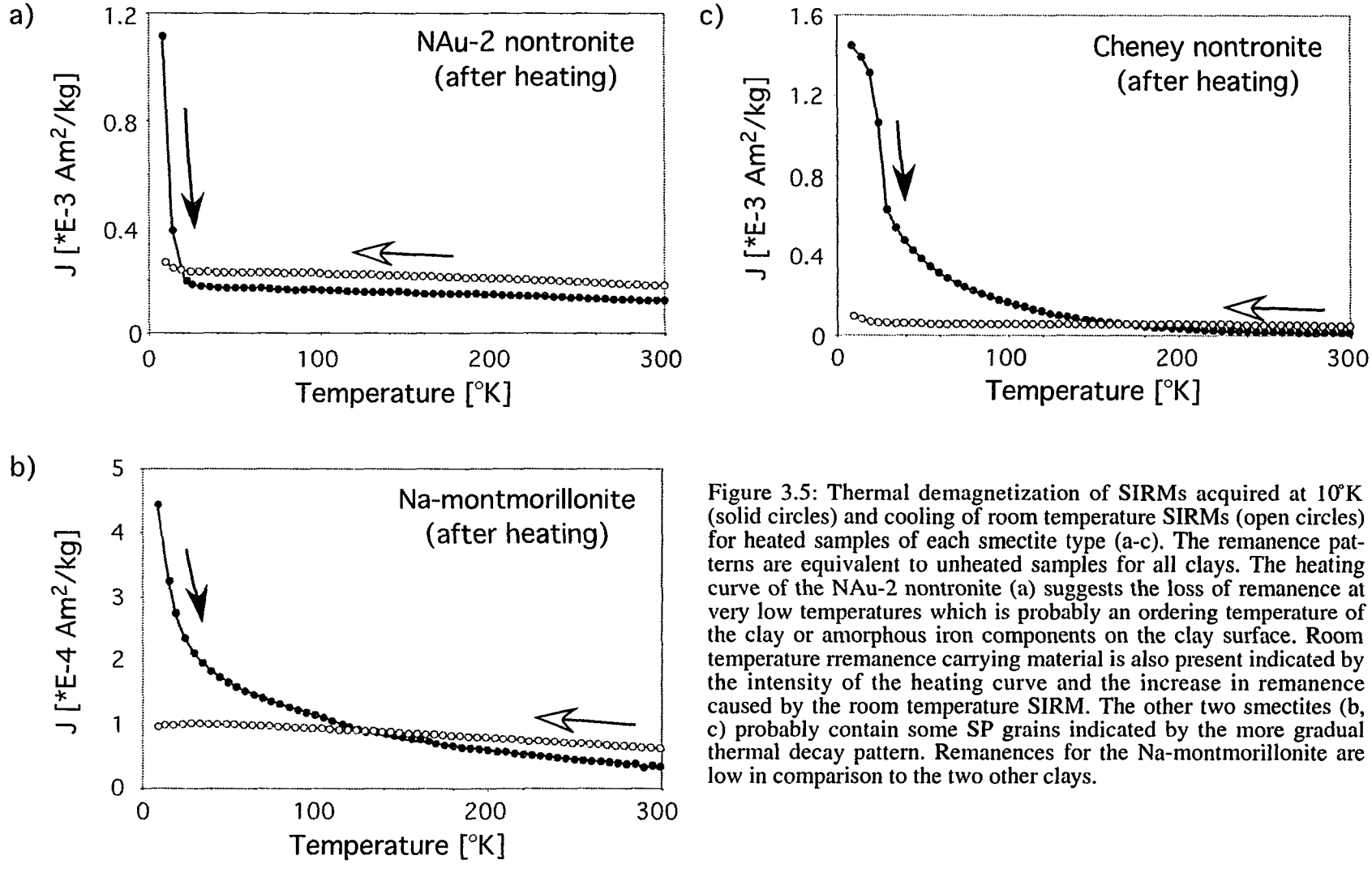


Figure 3.5: Thermal demagnetization of SIRMs acquired at 10°K (solid circles) and cooling of room temperature SIRMs (open circles) for heated samples of each smectite type (a-c). The remanence patterns are equivalent to unheated samples for all clays. The heating curve of the NAu-2 nontronite (a) suggests the loss of remanence at very low temperatures which is probably an ordering temperature of the clay or amorphous iron components on the clay surface. Room temperature rremanence carrying material is also present indicated by the intensity of the heating curve and the increase in remanence caused by the room temperature SIRM. The other two smectites (b, c) probably contain some SP grains indicated by the more gradual thermal decay pattern. Remanences for the Na-montmorillonite are low in comparison to the two other clays.

There were no differences in the shape of the heating and cooling curves for the heated and unheated samples of the NAu-2 nontronite or in the other smectites. However, a comparison of remanences between the thermally demagnetized samples at 300°K and their corresponding room temperature SIRM revealed a clustering of values prior to heating with relatively low values for the NAu-2 nontronite. After the heating process, samples showed significant increases and a greater variability in both remanences (Figure 3.6). The enhanced intensities of the remanence and SIRM at room temperature indicated the addition of ferrimagnetic material capable of carrying remanence which was caused by exposure of the clay to elevated temperatures for prolonged times. These observations were in accordance with findings in the previously described rock magnetic analyses. The SP content in the NAu-2 nontronite prior to heating was probably relatively low (Figure 3.6), although due to the corrections applied, results could only serve as a proxy. Concurrent with an increase in the room temperature remanence was also an increase in SP grains for the heated samples (Figure 3.6). The results suggest that authigenesis of both grains that are capable of carrying remanence at room temperature and SP grains occurred due to heating of the NAu-2 nontronite.

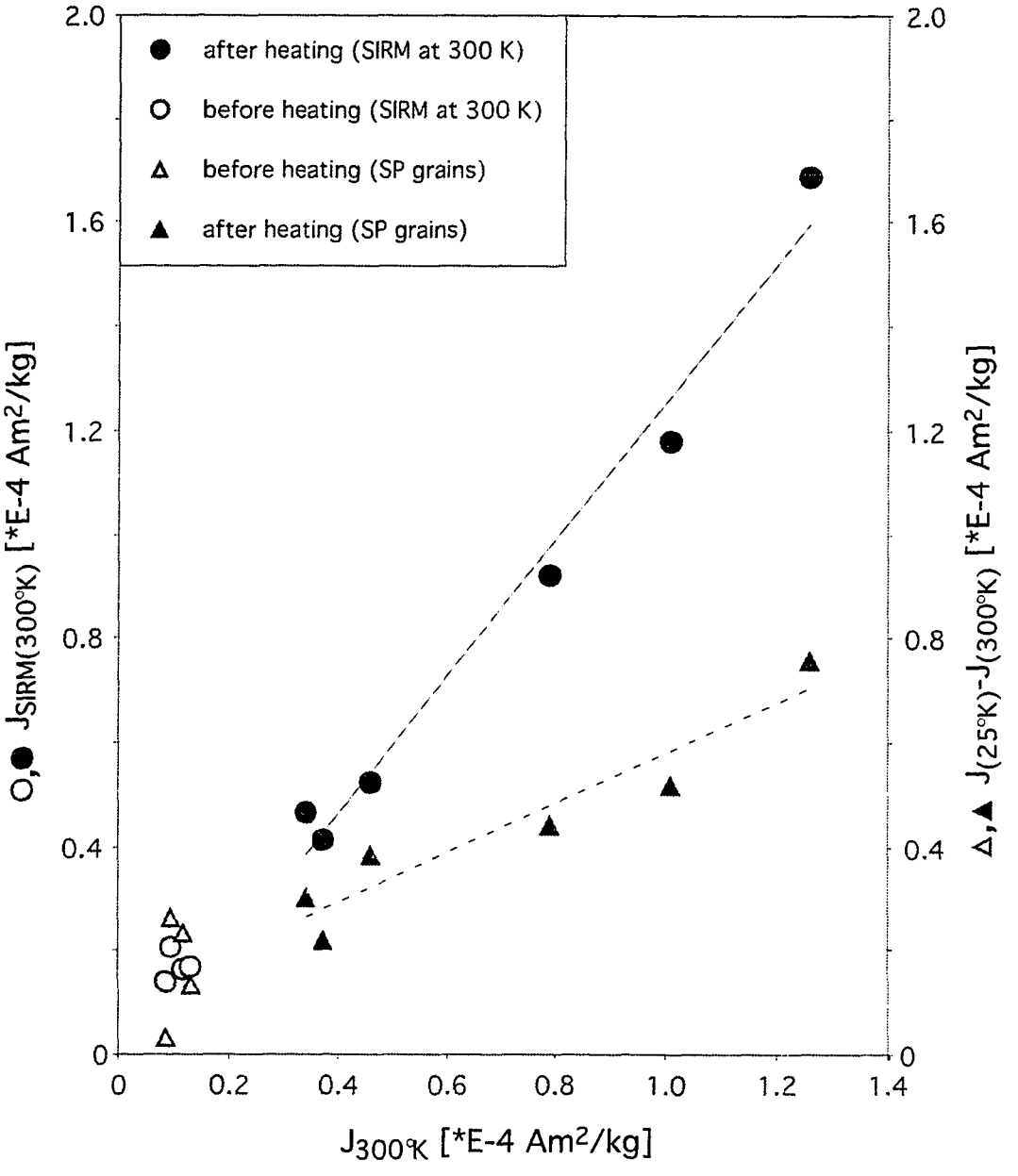


Figure 3.6: Remanences after thermal demagnetization of SIRMs acquired at low temperature versus SIRMs acquired at room temperature for NAu-2 nontronite samples prior to (open circles) and after heating (solid circles, solid trendline). Remanences of samples prior to heating have a narrow intensity range and those after heating show a larger range of remanences and increases relative to the original clay samples indicating the amount of magnetic material capable of carrying remanence at room temperature increased due to heating of the NAu-2 nontronite. In addition, an approximation of SP grains indicates that the content of ultra-fine grains also increased in the heated samples (solid triangles, dashed trendline) compared to their unheated equivalents (open triangles). Note: the SP content is only an estimate because corrections were applied for the induced magnetization.

3.3.4 IRM_{200}, SIRM, ARM

The mass specific IRM_{200} increased from 0.19 *E-4 Am^2/kg in samples prior to heating to mean values of 1.37 *E-4 Am^2/kg in heated samples which also showed greater variability (Figure 3.7a). This increase suggested the addition of a low coercivity magnetic mineral. Concurrent with the augmentation of the IRM_{200} was an increase in the SIRM in heated samples of the NAu-2 nontronite with intensities of 0.21 *E-4 Am^2/kg before heating and 1.47 *E-4 Am^2/kg after heating. The isothermal remanence that was carried by high and intermediate coercivity mineral was estimated by subtracting IRM_{200} from the SIRM. The contribution from high coercivity material to the remanence in heated and unheated samples was very minor (Figure 3.7b). The results indicated a dominance of low coercivity material and that the increase in the SIRM was due to the addition of low coercivity material. There were two magnetic phases present in the clay which were previously identified as magnetite and pyrrhotite. While pyrrhotite has a wide range of coercivities, magnetite is a low coercivity phase and is interpreted to be the material that was formed in the heating process. The fact that the experiments were conducted under ambient atmosphere conditions also favors the interpretation that magnetite was added rather than pyrrhotite.

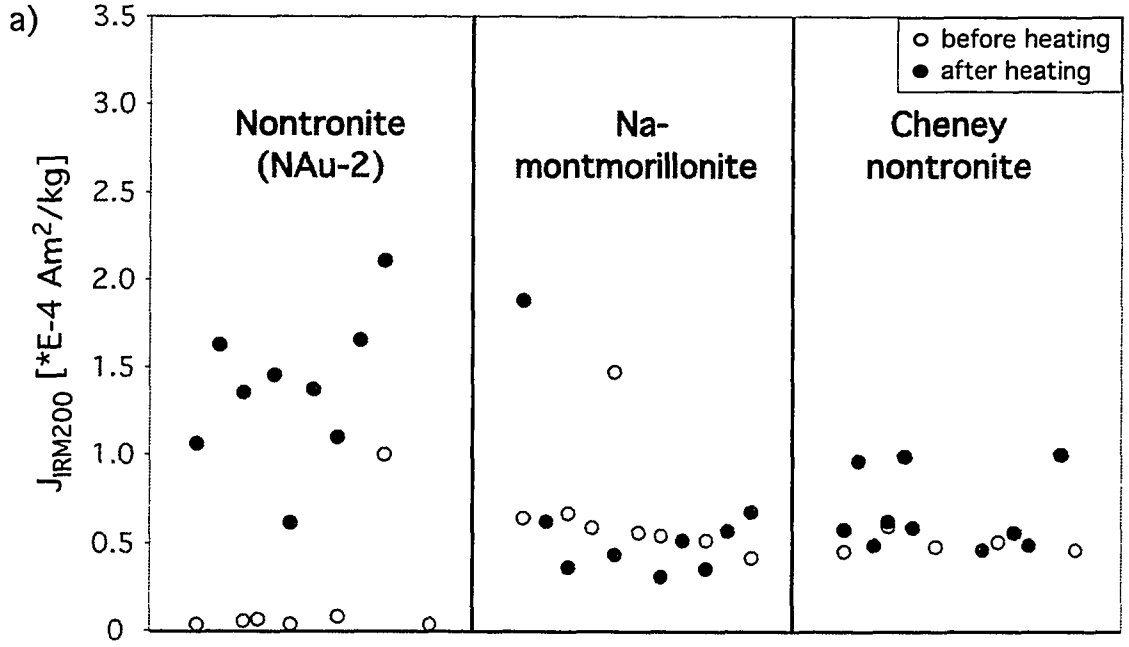
Values of ARM were, on average, higher for heated NAu-2 nontronite samples and showed generally a greater variability in comparison to their unheated equivalents (Figure 3.7c). The average ARM for original samples was 0.54 *E-6 Am^2/kg and increased to a mean of 1.11 *E-6 Am^2/kg after the heating experiments. The increases in the ARM for the heated samples also suggested the addition of low coercivity material. The fact that the IRM_{200} increased much more

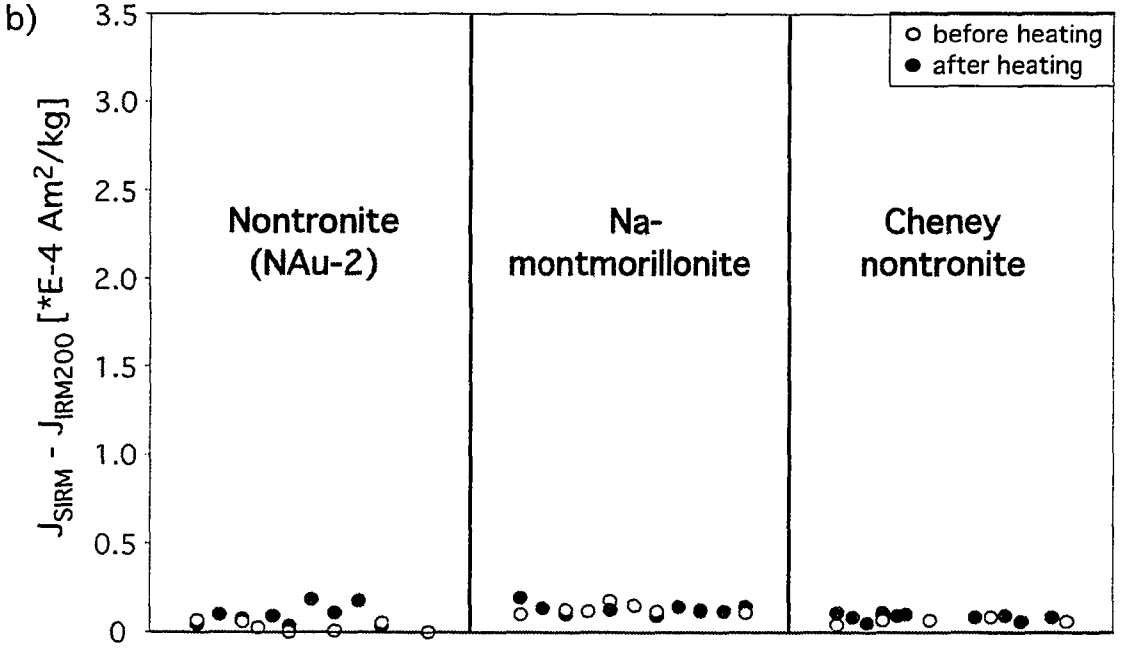
than the total ARM, is interpreted to indicate that the dominant remanence-carrying magnetite formed during heating was MD magnetite. The results of increasing remanences were consistent with those found in the χ_b measurements and support an interpretation that increases in the χ_b were caused by an authigenic ferrimagnetic phase.

The IRM_{200} values of the Na-montmorillonite were similar for unheated and heated samples with averages of 0.68 *E-4 Am^2/kg and 0.64 *E-4 Am^2/kg, respectively (Figure 3.7a). The SIRMs for original Na-montmorillonite samples averaged 0.80 *E-4 Am^2/kg and remained essentially unchanged after heating with a mean of 0.77 *E-4 Am^2/kg and the contribution of the high coercivity phase to the SIRM was very minor (Figure 3.7b). The total ARM values for the Na-montmorillonite indicated only minor variations existed between the clay prior to (0.82 *E-6 Am^2/kg) and after heating (1.0 *E-6 Am^2/kg) (Figure 3.7c). The fact that neither of the three remanence parameters showed major variations prior to and after heating of the Na-montmorillonite suggested that the magnetic mineral content was unaffected by the heating process, variations were not significant or the concentrations were below the detection limit of the instrument. Like the NAu-2 smectite, the montmorillonite also contained dominantly a low coercivity phase. Previous analyses of the magnetic mineralogy showed that magnetite was this dominant phase although some pyrrhotite was present in the clay, as well. However, remanence-detecting techniques were not capable of providing information on the influence of ferrimagnetic minerals on the small increase of the χ_b observed in the wet clay samples.

The IRM_{200} values for the original Cheney nontronite samples were, on average, 0.50 *E-4 Am^2/kg and were 0.68 *E-4 Am^2/kg after heating (Figure 3.7a). Measurements of SIRM were

similar to the IRM_{200}, with 0.56 *E-4 Am^2/kg and 0.76 *E-4 Am^2/kg before and after heating, respectively. The results indicated the dominance of the low coercivity phase on the remanence as shown by the low contribution of high coercivity material in Figure 3.7b. Earlier investigations identified the magnetic phases present to be magnetite and pyrrhotite. The former was probably the remanence-determining mineral, but there were no apparent variations caused by heating of the clay in the experiments. The Cheney nontronite samples had relatively high total ARMs, with 1.35 *E-6 Am^2/kg prior to heating and 1.50 *E-6 Am^2/kg after prolonged heating (Figure 3.7c). None of the differences in any of the parameters was considered to be significant for this clay type.


a)
3.5
3.0
2.5
2.0
1.5
1.0
0.5
0
J_{IRM200} [*E-4 Am^2/kg]
Nontronite (NAu-2)
Na-montmorillonite
Cheney nontronite
before heating
after heating


b)
3.5
3.0
2.5
2.0
1.5
1.0
0.5
0
J_{SIRM} - J_{IRM200} [*E-4 Am^2/kg]
Nontronite (NAu-2)
Na-montmorillonite
Cheney nontronite
before heating
after heating

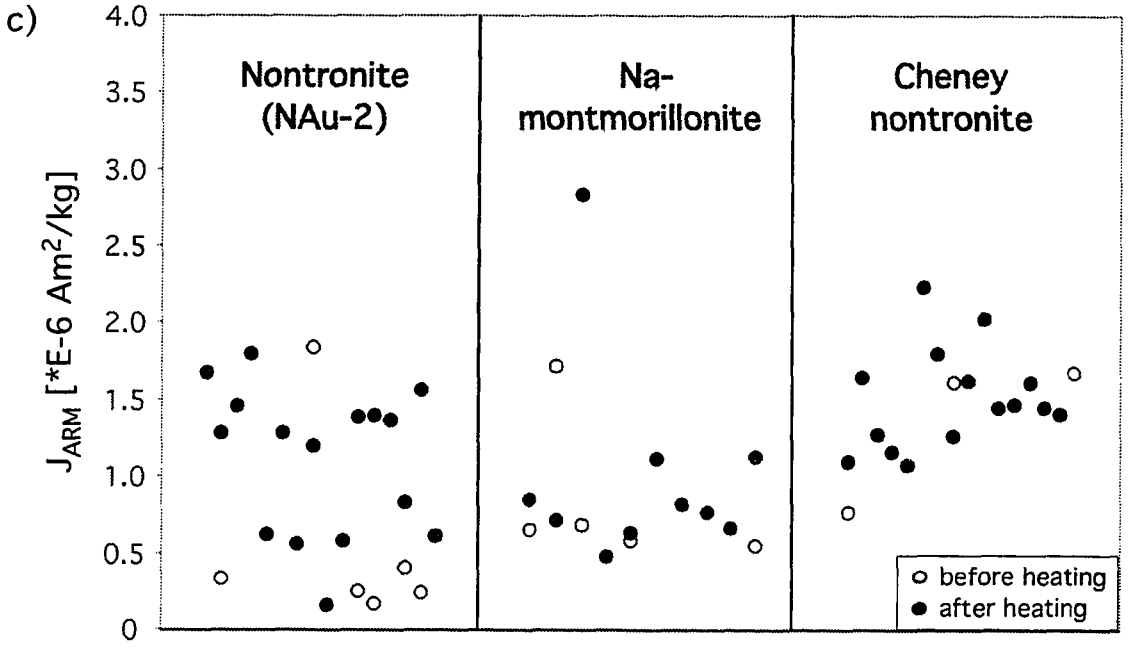


Figure 3.7: IRM acquired at 200 mT (a), high coercivity content (b), and total ARMs (c) for the three smectites. Samples were measured prior to (open circles) and after heating for prolonged times (solid circles). The remanence increased dominantly in the low coercivity phase, suggesting an increase in magnetite (a and b). Although the total ARM increased (c), the relatively low intensity may suggest that the magnetite formed is dominantly in the multi-domain and weak single-domain grain size. Values of the three parameters remain essentially unchanged for the two other clays.

3.3.5 X-ray Diffraction

The X-ray diffraction patterns of the NAu-2 nontronite samples before and after heating indicate some variation in the degree of dehydration apparent in the air-dried diffractograms (Figure 3.8a). The broad peak area with shoulders on the high 2 θ side indicated the nontronites were collapsed to variable interlayer spacings. However, upon glycolation, both the original smectite and the heated NAu-2 samples, expanded to a 17 Å basal spacing (Figure 3.8b). Thus, any collapse in the air-dried samples was reversible and did not indicate the irreversible formation of illite-type layers in the heated nontronite sample.

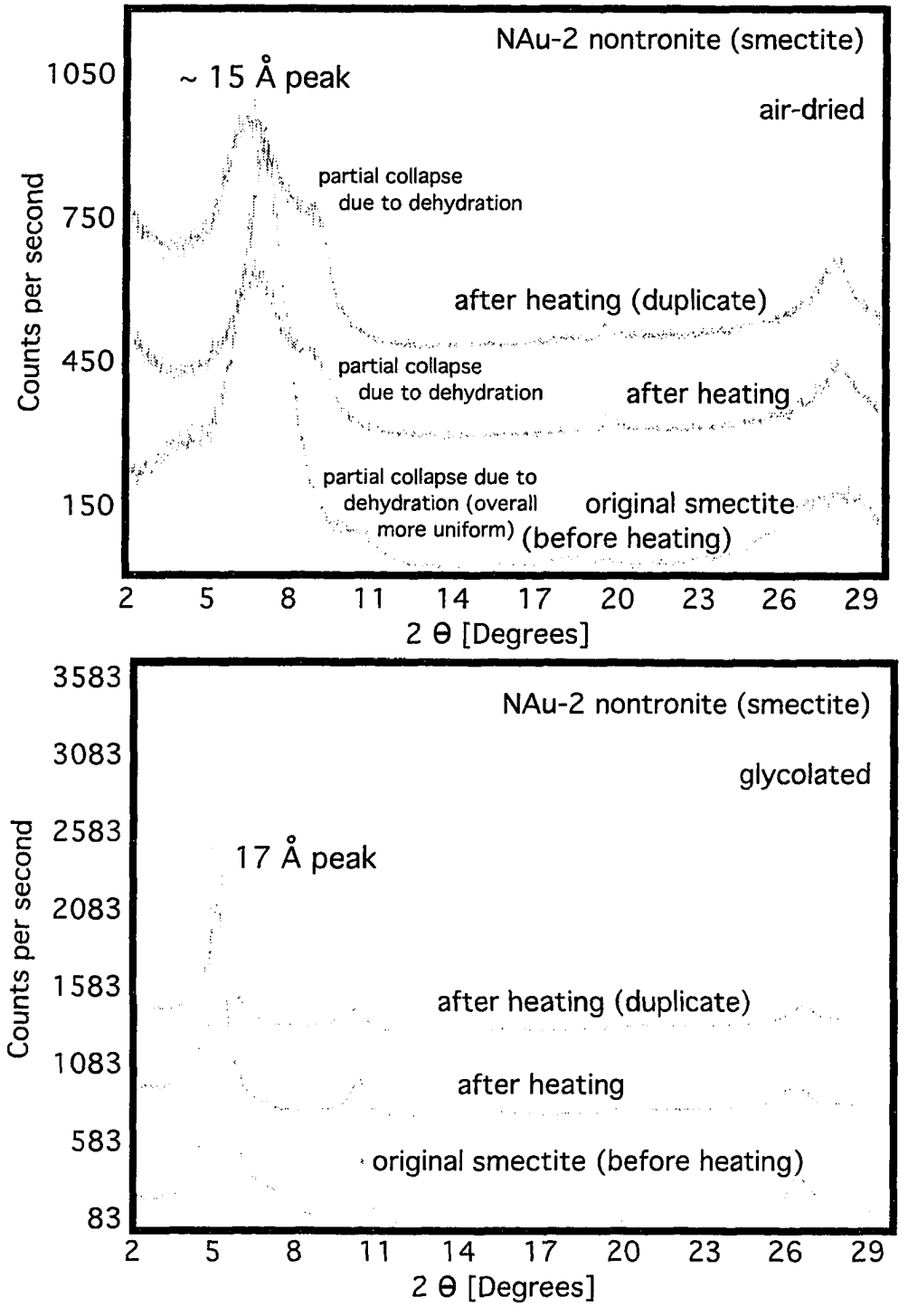


Figure 3.8: X-ray diffraction patterns for an air-dried, oriented original and a heated (with duplicate measurement) NAu-2 nontronite sample (a) and the same samples after glycolation (b). The analyses of the air-dried samples showed some variation in the degree of dehydration between the original and the heated sample. Upon glycolation the samples expand to a 17 Å basal spacing indicating that the collapse of interlayer space was reversible and that no illitization occurred due to the heating in the experiments.

3.4 Discussion

The rock magnetic investigations presented above confirm previously reported experimental results on three smectites that showed increases in the χ_b for one of the nontronites (NAu-2) and a wet Na-montmorillonite (SWy-2) and no variations in another nontronite (Cheney) after heating at 62°C for prolonged times. The analyses support an interpretation that the augmentation of the magnetic signal in the NAu-2 nontronite was partially caused by authigenesis of a ferrimagnetic phase. Both SP and remanent magnetic phases increased after heating and the carrier of the neoformed magnetic mineral is interpreted to be mainly MD magnetite although additional magnetite of all grain sizes was formed. The findings of this study suggest that the creation of magnetite sufficiently large to acquire remanence can occur due to exposure of some smectites to temperatures equivalent to low burial. The results support the possibility of clay diagenesis as a viable mechanism for the formation of some pervasive CRMs as has been suggested to have occurred in some sedimentary rocks (e.g., Katz et al., 1998). The conversion of smectite to illite has been reported to occur at temperatures between 50 and 100°C for sediments in the Gulf of Mexico area (e.g., Pusch, 1998). However, a transformation from smectite to illite was not detected by X-ray diffraction analyses in the NAu-2 nontronite suggesting that another clay diagenetic process must be responsible for the formation of magnetite associated with this particular clay.

Hysteresis experiments suggested that, although the paramagnetic character of the clays was responsible for the major portion of the χ_b signal and the χ_p increases due to clay heating, there was a significant increase in the contribution of a ferrimagnetic mineral in the heated samples.

Low-temperature analyses indicate that there are more SP grains present in the heated nontronite samples. Hunt et al. (1995) state that SP material commonly identified in low-temperature analysis are either magnetite or maghemite. However, there is no evidence for the presence of maghemite and thus, the SP grains are interpreted to be ultra-fine magnetite. In addition, a comparison of low-temperature analyses, IRM_{200}, SIRM, and ARM measurements of heated and unheated samples of the NAu-2 nontronite indicate that dominantly magnetite of remanence-carrying grain size is the authigenic ferrimagnetic phase formed due to heating. Pyrrhotite, which is also present in the nontronite, is not considered to have formed in the experiments based on the fact that it commonly has intermediate to high coercivity ranges and the atmospheric conditions provided in the tests would not favor the formation of this reduced form.

The reasons as to why there is no evidence for a Verwey transition or the magnetite isotropic point in the low-temperature analyses remain unresolved. The Verwey transition is commonly caused by MD and/or equi-dimensional SD magnetite (e.g., Özdemir et al., 1993). Either the magnetite formed is dominantly in the SD size range, or both transitions are suppressed due to oxidation of the magnetite present. An attenuation of the Verwey transition caused by surface oxidation of magnetite to maghemite has been described in Özdemir et al. (1993). However, the complete masking of the transition seems somewhat unusual and a preferential explanation might be that the paramagnetic nature of the clays also tends to mask the transitions.

The rapid initial drop at low temperatures up to 20°K was interpreted as being probably caused by an ordering of the clay itself. Alternatively, SP magnetite or ferric-oxyhydroxides could cause this phenomenon. If amorphous ferric-oxyhydroxides were present, they would not

be detected in most other analysis techniques. Since the shape of the cooling curves are similar for unheated and heated curves, the amorphous compound could be assumed to be present prior to the experiments and they could possibly be the result of iron adsorption onto the clay surface. Hirt et al. (1993) demonstrated that artificial surface loading of iron onto a montmorillonite may cause the formation of iron-nanophases. Such amorphous phases apparently served as precursors of authigenic magnetite created upon heating of the clay to above 250°C. Similarly, the presence of an amorphous iron phase in the NAu-2 nontronite could have triggered the formation of magnetite during heating. In contrast to previous research (e.g., Moskowitz & Hargrave, 1984; Hirt et al., 1993), the temperatures applied in this study resulting in authigenesis of a ferrimagnetic phase were significantly lower. If an amorphous iron phase were present in the NAu-2 nontronite, this could provide an explanation for the differences in results between this and the Cheney nontronite. The variability in the results for the two nontronites – which both contain structural iron – possibly resides in an additional availability of iron within the NAu-2 nontronite. Further analyses are necessary to elucidate this issue.

The Na-montmorillonite appears to require water for any alteration to occur based on the χ_b increases, which were only observed in wet samples. The rock magnetic methods applied are not successful in determining the cause for the changes in the magnetic signal, probably due to the extremely weak magnetic intensities of this clay type. The significantly weaker intensities in comparison to the nontronites could at least partially be explained by the fact that montmorillonites contain essentially no iron but aluminum ions instead. If magnetite formed in the Na-montmorillonite, it would provide supporting evidence for a connection between clay

diagenesis, perhaps the alteration of smectite to illite, and the potential formation of CRMs. However, with current knowledge, it remains unclear as to whether authigenesis of magnetite occurred in this clay type during heating.

To further investigate the type(s) of iron present, its location (structural versus adsorbed onto the surface) and fate, analyses via infrared spectroscopy are currently underway. In particular, the differences of the NAu-2 nontronite prior to and after heating will be explored as well as a comparison with the Cheney nontronite, the latter of which did not result in authigenesis of magnetite upon heating.

3.5 Conclusions

Heating of a nontronite (NAu-2) and a wet Na-montmorillonite to temperatures of 62°C results in an increase of the χ_b. Rock magnetic analyses argue for the formation of remanence-carrying magnetite in the NAu-2 nontronite. The heating conditions chosen are equivalent to low burial and this study indicates that exposing some smectite types to such surroundings may result in the formation of magnetic phases capable of recording a CRM. Thus, the results provide supporting evidence for a previously proposed empirical connection between smectite diagenesis and some widespread CRMs although some process other than the conversion from smectite to illite must be responsible for the formation of magnetite in the experiments.

Several questions remain unresolved, e.g., what specific clay diagenetic process is responsible for the authigenesis of magnetite and whether formation of magnetite caused the increase in the magnetic signal in the moistened Na-montmorillonite. The reasons for the varying responses of

the two nontronites are unclear, but may be related to differences in the availability of releasable iron. Developing a better understanding of smectite diagenesis and associated processes such as authigenesis of magnetic phases can assist in explaining the occurrence of some pervasive CRMs. In turn, paleomagnetic methods can be used to identify CRMs and provide a dating tool for smectite diagenesis and related processes.

References Chapter 3

Dunlop, D.J., and Ö. Özdemir, Rock magnetism - Fundamentals and frontiers, editor: D. Edwards, Cambridge University Press, pp. 573, 1997.

Elmore, R.D., and C. McCabe, The occurrence and origin of remagnetization in the sedimentary rocks of North America, in: Contributions in geomagnetism and paleomagnetism, U.S. National Report 1987-1990, edited by Shea, M.A. and Kodama, K. eds., Reviews in Geophysics, Supplement, pp. 377-383, 1991.

Hirt, A.M., A. Banin, and A.U. Gehring, Thermal generation of ferromagnetic minerals from iron-enriched smectites, *Geophysical Journal International, 115*, 1161-1168, 1993.

Housen, B.A., S.K. Banerjee, and B.M. Moskowitz, Low-temperature magnetic properties of siderite and magnetite in marine sediments, *Geophysical Research Letters, 23*, 2843-2846, 1996.

Hunt, C.P., S.K. Banerjee, J. Han, P.A. Solheid, E. Oches, W. Sun, and T. Liu, Rock-magnetic proxies of climate change in the loess-palaeosol sequences of the western Loess Plateau of China, *Geophysical Journal International, 123*, 232-244, 1995.

Katz, B., R.D. Elmore, M. Cogoini, and S. Ferry, Widespread chemical remagnetization: Orogenic fluids or burial diagenesis of clays? *Geology, 26*, 603-606, 1998.

Katz, B., R.D. Elmore, M. Cogoini, M.H. Engel, and S. Ferry, Associations between burial diagenesis of smectite, chemical remagnetization, and magnetite authigenesis in the Vocontian trough, SE France, *Journal of Geophysical Research, 105*, 851-868, 2000.

Moskowitz, B.M., and R.B. Hargraves, Magnetic cristobalite (?): A possible new magnetic phase produced by thermal decomposition of nontronite, *Science, 225*, 1152-1154, 1984.

Özdemir, Ö., D.J. Dunlop, and B.M. Moskowitz, The effect of oxidation on the Verwey transition in magnetite, *Geophysical Research Letters, 20*, 1671-1674, 1993.

O'Reilly, W., Rock and mineral magnetism, Blackie and Son Ltd., pp. 220, 1984.

Pusch, R., Transport of radionuclides in smectite clay, in: Environmental interactions of clays – Clays and the environment, edited by A. Parker and J.E. Rae, pp. 271, Springer, Berlin, 1998.

Sall, J., and A. Lehman, JMP Start statistics – A guide to statistics and data analysis using JMP® and JMP In® software, SAS Institute Inc., Duxbury Press – an imprint of Wadsworth Publishing Company, pp. 521, 1996.

CHAPTER 4

Contrasting Rock-Magnetic Characteristics of Two Upper Paleozoic Loessite-Paleosol Profiles

4 Abstract

Rock magnetic results from paleosols in two North American Paleozoic loessite sequences, the Maroon Formation (Colorado) and the lower Cutler beds(Utah), indicate that bulk magnetic susceptibility (χ_b) variations can be complex. In Maroon Formation profiles, χ_b increases with increased pedogenic intensity and the major contributor to the augmentation of the χ_b signal is the ferrimagnetic susceptibility (χ_f). These trends are consistent with previous studies in which χ_b has been linked to climatically controlled pedogenesis. Thermal demagnetization of low-temperature saturation isothermal remanent magnetizations (SIRMs) indicates this increase correlates to a greater abundance of superparamagnetic (SP) grains, most likely magnetite, within the paleosols. The presence of coarser magnetite is indicated by the Verwey transition. In contrast, paleosols in the lower Cutler beds show a less predictable pattern in the χ_b signal. The paramagnetic χ (χ_p) and χ_f contribute to varying degrees to the χ_b within the loessite-paleosol couplets. Thermal demagnetization of low-temperature SIRMs indicates that both SP and coarser magnetite is present. There are no consistent patterns and often no significant variations in the amount of SP material within loessite-paleosol couplets. The thermal demagnetization curves for samples of the lower Cutler beds display a gradual decay of remanence and a weakly developed Verwey transition, both of which probably relate to maghemitization. Most paleosol and loessite samples differ in that there is more remanence-carrying material, predominantly hematite and some magnetite and maghemite, in the loessite. Rock-magnetic differences among loessite-paleosol couplets of the lower Cutler beds may relate to the heterogeneous distribution of pedogenic carbonate and/or to the presence of abundant hematite. This study shows that combining rock-

magnetic techniques with sedimentologic evidence is important for deciphering the origin and preservation of χ_b patterns in ancient strata.

4.1 Introduction

Recent research has established that magnetic susceptibility (χ_b) variations in some Quaternary-Pliocene loess-paleosol sequences track changes in paleoclimate (e.g., Heller and Liu, 1984; Kukla et al., 1988). For example, studies of χ_b variations in Plio-Pleistocene loess-paleosol sequences in China have linked χ_b increases in paleosols to pedogenic formation of fine-grained magnetite and maghemite during warm, wet interglacials, whereas lower χ_b values in loess reflect deposition during cooler, drier glacials (e.g., Maher and Taylor. 1988; Zhou et al., 1990; Heller et al., 1991; Liu et al., 1992). In contrast, several studies (Begét et al., 1990; Oches et al., 1998; Rutter and Chlachula, 1995; Vlag et al., 1999) on loessite-paleosol sequences in other regions report the opposite χ_b trend. Depletion of χ_b has been related to (1) loss or absence of ferrimagnetic minerals in excessively arid, wet or acidic (i.e., gleyed and leached) modern soils (Maher, 1998; Nawrocki et al., 1999), and (2) detrital source controls such as variability in magnetic mineral content related to wind intensity (Begét et al., 1990).

Based on these studies, χ_b trends alone do not necessarily provide information on paleoclimate. Establishing a connection between χ_b and paleoclimate requires an understanding of the controls on the χ_b signal. The objective of this study is to contrast χ_b with other rock-magnetic and sedimentologic data from two upper Paleozoic loessite-paleosol sequences, the Maroon Formation (Colorado) and the lower Cutler beds (Utah). Loessite-paleosol units of the

Maroon Formation consistently display an increase in χ_b with increasing pedogenic intensity (Soreghan et al., 1997; Tramp et al., in review), whereas the lower Cutler beds show a more complex relationship. This study illustrates the necessity of integrating analyses of magnetic behavior at low temperatures with other types of rock-magnetic and sedimentologic data in order to assess the origin and preservation of χ_b variations in loess(ite)-paleosol sequences and their possible paleoclimatic significance.

4.2 Geologic Setting

For this study, loessite-paleosol sequences were targeted in upper Paleozoic (Pennsylvanian-Permian) deposits exposed in the Eagle basin of northwestern Colorado and the Paradox basin of southwestern Utah (Figure 4.1). Both basins are part of the Ancestral Rocky Mountains system (Kluth and Coney, 1981) and developed at near-equatorial latitudes (Scotese, 1997) of western Pangea. Coeval eolian dune fields of each basin presumably supplied the silt for these loessite accumulations (Johnson, 1989; Murphy, 1987; Condon, 1997) and both deposits consist of uniform parent material, i.e. quartzose siltstone.

Johnson (1987, 1989) first suggested a loessitic origin for the Maroon Formation of the southeastern Eagle basin near the towns of Basalt and Aspen, Colorado. Within this region, the nearly 900 m of the Maroon Formation consist of red-orange (10R 6/6 to 10R 7/4 Munsell colors) loessite (massive siltstone) beds up to several m thick that are commonly separated from one another by paleosols. Paleosols consist of darker red (10R 4/6 to 10R 3/4) intervals ranging from several cm to nearly 2 m thickness that bear sedimentologic evidence for pedogenesis such

as root traces, peds, pedogenic dolomite, and cutans. Nearly all the paleosols of this section are relatively weakly developed and constitute "protosols" in Mack et al.'s (1993) classification (Tramp, 2000).

Murphy (1987) first recognized the loessitic origin of the lower Cutler beds of the southwestern Paradox basin near the town of Mexican Hat, Utah. The lower Cutler beds in this area consist of approximately 200 m of red-orange (10R 5/4) loessite (massive siltstone) beds up to a few m thick, which are commonly separated by paleosols. Analogous to the Maroon Formation loessite, local structures (planar and ripple cross-laminae) record the influence of minor water reworking. Paleosols consist of moderate (5R 5/4) or dark red (e.g., 10R 3/4) to locally gleyed (5GY 6/1 to 5GY 8/1) intervals ranging from several cm to a few m thick that exhibit calcified rhizoliths, peds, calcite nodules, and cutans. Local gleying appears to be the result of burial gleization rather than groundwater or surface-water gley (cf. Retallack, 1997). In marked contrast to the Maroon Formation loessite, many paleosols of this section are well-developed calcisols (cf. Mack et al., 1993).

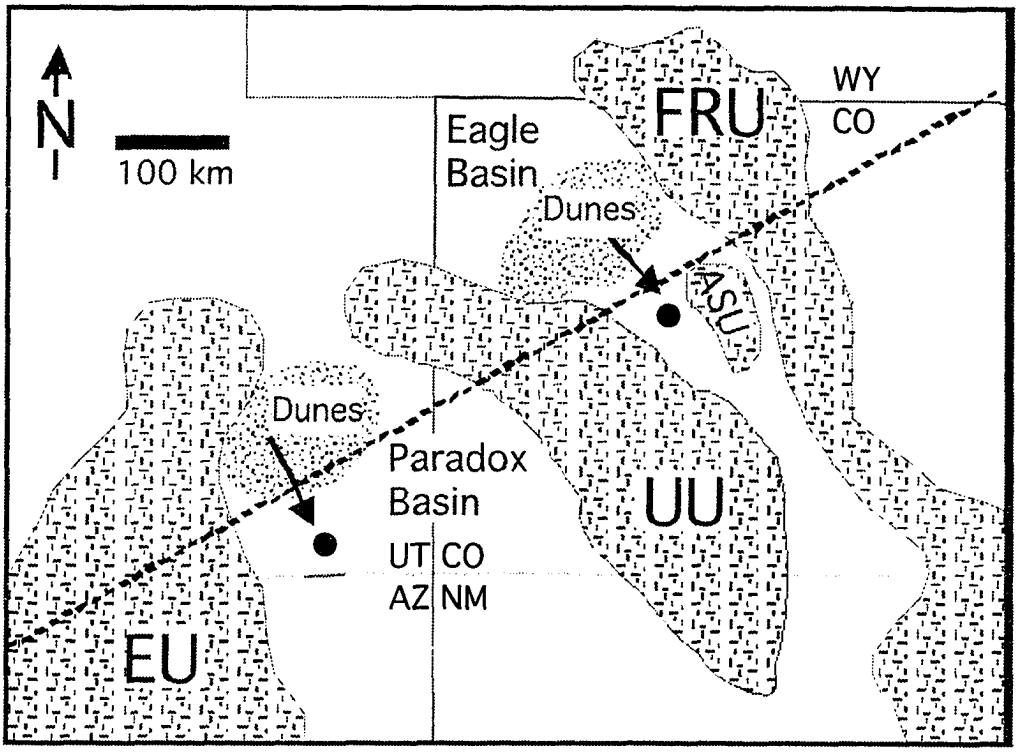


Figure 4.1: Location and paleogeographic map for the Eagle and Paradox basins. Study locations are indicated by dots. Diagonal line is approximate 5-10° north paleolatitude line for latest Pennsylvanian-early Permian time (Scotese and Golonka, 1992). Arrows indicate inferred wind directions, and stipples indicate inferred eolian dune fields (Johnson, 1989; Condon, 1997). Uplifts shown are: Uncompahgre (UU), Front Range (FRU), Ancestral Sawatch (ASU), and Emery (EU). Modified from Johnson et al. (1992).

4.3 Methods

Utilizing a gasoline powered drill, cores were collected from vertical transects in loessite-paleosol couplets of the Maroon Formation and the lower Cutler beds. The cores were cut to standard length, and mass-normalized χ_b was measured on a Sapphire SI-2 Instrument. Rock-magnetic data were collected from one representative couplet in the Maroon Formation and three couplets in the lower Cutler beds. The natural remanent magnetizations (NRMs) of several samples from each loessite-paleosol couplet were measured on a 2G three-axes cryogenic magnetometer located in a magnetically shielded room and were then used for stepwise acquisition of isothermal remanent magnetizations (IRMs) using an Impulse Magnetizer. Subsequently, these specimens were thermally demagnetized up to 700°C.

The thermal decay patterns of low-temperature SIRMs were recorded on a Magnetic Property Measurement System (MPMS) at the Institute for Rock Magnetism, University of Minnesota, for several samples from the selected loessite-paleosol couplets at each study section. These data were used to estimate the amount of SP grains, which is the difference in remanence between 10°K (in some cases 19°K) and 300°K, and subtracting the influence of the Verwey transition (Hunt et al., 1995). Hysteresis properties were measured using a 'Micromag' alternating gradient force magnetometer at the Institute for Rock Magnetism. The paramagnetic susceptibility (χ_p) was determined using the high-field part of the hysteresis loops. The ferrimagnetic susceptibility (χ_f) is the calculated difference between χ_b and χ_p. The χ_f was normalized by dividing it by the room-temperature saturation magnetization (Ms) determined from the hysteresis loops. Differences in this parameter reflect concentration-independent variations in the proportions of

ultra-fine-grained material (Hunt et al., 1995). Curie temperature measurements were performed on samples from the lower Cutler beds using a Vibrating Sample Magnetometer, and two samples were analyzed in a Mössbauer spectroscope at the Institute for Rock Magnetism. Several samples from both locations were investigated using reflected- and transmitted-light microscopes.

4.4 Results and Interpretations

4.4.1 Bulk Magnetic, Paramagnetic, and Ferrimagnetic Susceptibility

In the studied Maroon Formation loessite-paleosol couplet, χ_b increases from approximately 2.0-3.3 x 10^{-8} m^3/kg in the loessite to 4.2-6.5 x 10^{-8} m^3/kg at the top of the paleosol (Figure 4.2a). The tops of some paleosols range up to 1.0-2.0 x 10^{-7} m^3/kg (Soreghan et al., 1997). The χ_p increases but the χ_f shows a greater increase from the loessite into the paleosol, indicating that it exerts the more dominant control on the up-profile increase in χ_b (Figure 4.2a). The χ_f/Ms is also higher for the paleosol than the loessite, which is consistent with a higher amount of ultra-fine-grained material in the paleosol. These results are consistent with what Soreghan et al. (1997) found in other Maroon loessite-paleosol couplets.

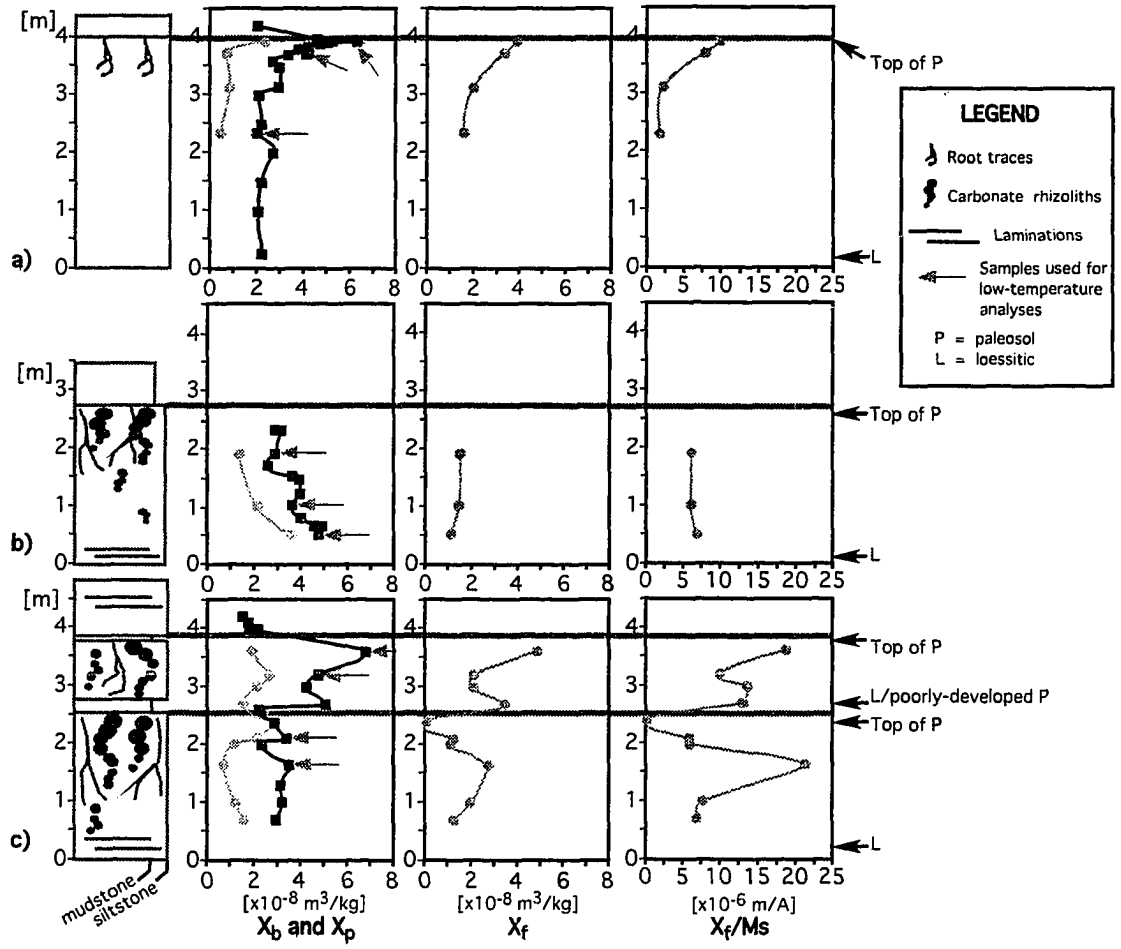


Figure 4.2: Selected profiles from the Maroon Formation (a) and the lower Cutler beds (b and c). From left to right: stratigraphic column, χ_b (squares) and χ_p (circles), χ_f, and χ_f/Ms. In the Maroon Formation (a) χ_p values increase, but χ_f increases more significantly up-profile, suggesting the increase in χ_b is mainly controlled by χ_f. Samples from three couplets of the lower Cutler beds (b, c) show high variability in the χ_b pattern as well as in the contribution of both χ_p and χ_f to the χ_b signal.

In contrast, χ_b patterns from the three loessite-paleosol couplets of the lower Cutler beds examined in this study are more variable. Figure 4.2b, for example, shows that χ_b decreases from the base to the top of the paleosol whereas χ_b increases upward (upper couplet) or exhibits no clear trend (lower couplet) in Figure 4.2c. Furthermore, whereas χ_p tracks χ_b in some cases (Figure 4.2b), no obvious correlation exists in other loessite-paleosol couplets (Figure 4.2c). The χ_f and χ_f/Ms do not vary between the studied loessite and paleosol displayed in Figure 4.2b, whereas both χ_f and χ_f/Ms exhibit either an upward increase or a variable pattern in Figure 4.2c. These results suggest that χ_p and χ_f contribute in varying amounts to the χ_b signal in the loessite and paleosol samples.

4.4.2 Low-Temperature Analyses

Patterns of thermal demagnetization of low-temperature SIRMs were recorded for the four couplets to test for the presence of magnetite and to investigate the contribution of SP grains to the χ_b signal. Thermal demagnetization of low-temperature SIRMs for samples from the Maroon Formation couplet exhibit a steeper initial drop in remanence for the paleosols relative to the more loessitic samples (Figure 4.3a). This rapid decrease in remanence at low temperatures (< 50-300°K) is commonly caused by SP grains (Hunt et al., 1995). The approximate contribution of SP grains ranges from 3.24-4.94 x 10^{-4} Am^2/kg (3 specimens) with the greater values found in the top part of the paleosol. Calculated absolute values of SP material for these samples are underestimated because the increase in remanence at temperatures >150°K was not considered. Despite the underestimate of SP material, the results suggest a greater abundance of ultra-fine-

grained magnetic material, presumably magnetite, in the paleosol relative to the loessite. These results are consistent with the results of Soreghan et al. (1997).

The presence of the Verwey transition at around 118°K is indicative of mostly multidomain (md) magnetite and is found in all samples from this couplet. In addition, all samples show varying degrees of remanence increases upon heating above about 150°K, which is interpreted to reflect the presence of hematite.

Compared to the Maroon Formation samples, the thermal demagnetization of low-temperature SIRMs for samples from the lower Cutler beds exhibit a more gradual decay of remanence up to 300°K and a weakly developed Verwey transition (Figure 4.3b, c, and d). This is particularly clear in samples that acquired the low-temperature SIRM at 19°K (Figure 4.3b), which is equivalent to the temperature used to apply the SIRM in the Maroon Formation samples. Özdemir et al. (1993) suggested that suppression of the Verwey transition reflects oxidation and maghemitization of magnetite. A gradual decay of magnetic remanence upon heating, such as that observed in specimens from the lower Cutler beds, is comparable to the demagnetization pattern for maghemite (Özdemir et al., 1993). Based on the attenuated Verwey transition and the gradual decay of remanence in the lower Cutler beds couplets, these paleosols are interpreted to contain both maghemite and magnetite.

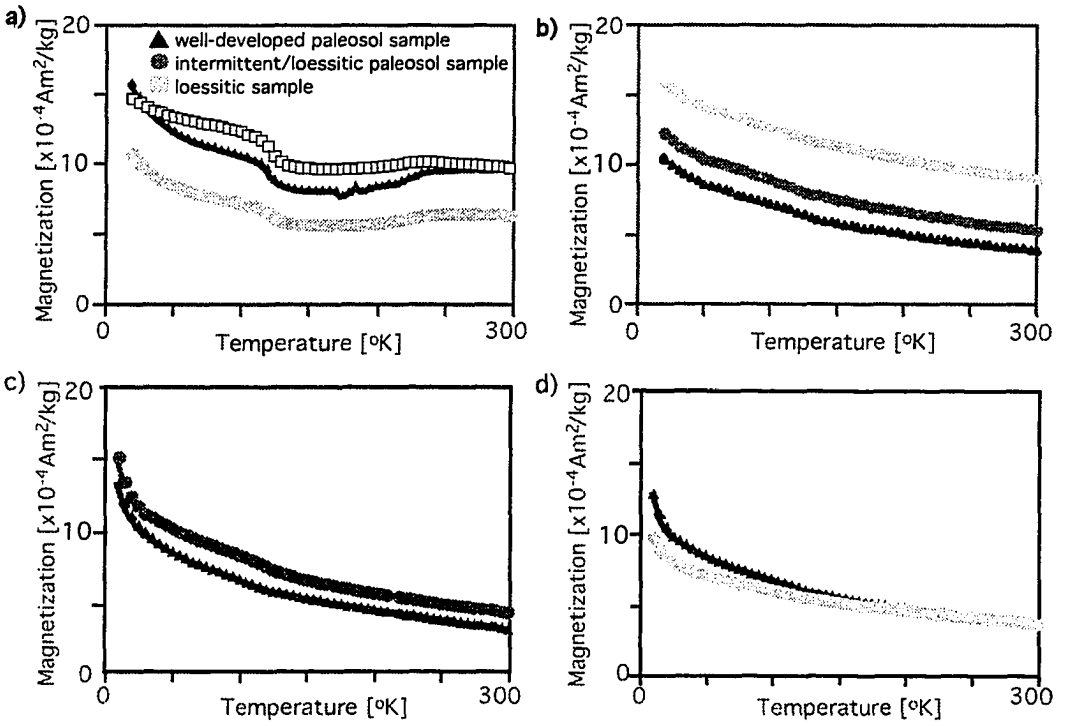


Figure 4.3: Thermal demagnetization patterns of low-temperature SIRMs for loessitic and paleosol samples. The SIRMs were acquired at 19°K (a, b) and at 10°K (c, d). Triangles (black) = well-developed paleosol, circles (medium gray) = intermittent to loessitic paleosol, squares (light gray) = loessitic. a) Analysis of samples from the Maroon Formation profile indicating the presence of SP grains and coarse (mainly md) magnetite (Verwey transition). b-d) Samples from the lower Cutler beds show an overall more gradual thermal decay pattern and an attenuated Verwey transition, indicating the presence of maghemite and magnetite. Calculation of SP contents indicate that the differences in the curves between a loessitic or poorly-developed paleosol and a well-developed paleosol are caused by magnetic minerals that carry remanence at room temperature (b, c) or, in case d, by SP grains.

The demagnetization patterns of the decay curves are very similar for both loessite and paleosol samples in Figure 4.3b, and absolute values for the SP material are between 6.16 x 10^{-4} and 6.37 x 10^{-4} Am^2/kg. Magnetic minerals that carry remanence at room temperature therefore cause the difference in the curves and they are more abundant in the loessitic samples than the paleosols. A similar pattern of remanence loss upon heating exists for the samples displayed in Figure 4.3c. The absolute values for SP grains of these samples (9.8 x 10^{-4} Am^2/kg and 10.3 x 10^{-4} Am^2/kg, Figure 4.3c) are similar. In contrast, Figure 4.3d shows a different pattern wherein the SP content is lower (5.74 x 10^{-4} Am^2/kg) in the loessite relative to the paleosol (8.64 x 10^{-4} Am^2/kg).

4.4.3 IRM Acquisition and Thermal Decay of IRM

Acquisition curves of IRMs for samples from the Maroon Formation couplet show a rapid rise by 100 mT and then a more gradual rise up to 2500 mT. This suggests the presence of a low-coercivity phase, but the remanence is dominated by a high-coercivity phase, which is in accordance with results reported in Soreghan et al. (1997). Subsequent stepwise thermal demagnetization reveals a slight drop in remanence at approximately 580°C, indicating the presence of magnetite, and a steep drop to approximately zero remanence between 680°C and 695°C, which is indicative of hematite. The IRM acquisition and decay curves for couplets in the lower Cutler beds are similar to those from the Maroon Formation, except for a more gradual decay in remanence during thermal demagnetization. The results from both units indicate the

magnetic minerals contributing to the remanence are dominantly hematite and subordinate magnetite.

4.4.4 Curie Balance, Mössbauer Spectroscopy, Petrography

Curie balance analyses and Mössbauer spectroscopy of several samples from the lower Cutler beds reveal the presence of hematite, but no other magnetic mineral was identified with these methods. This result likely stems from the low concentration of magnetite and/or maghemite present in the samples. Both macroscopic and thin-section observations of the lower Cutler bed paleosols confirm the presence of variable amounts of detrital, authigenic, and predominantly pedogenic carbonate. Detrital and diagenetic hematite are also present in the lower Cutler beds.

4.5 Discussion and Summary

Bulk χ and rock-magnetic data from the Maroon Formation loessite-paleosol couplet covary with pedogenic intensity and support previous interpretations (Soreghan et al., 1997) that χ_b patterns relate to an increase in SP material (probably magnetite). The minor increase of χ_p from the loessite into the paleosol may be caused by the high-field χ characteristics of hematite (Collinson, 1983), which could indicate that hematite constitutes a small portion of the overall increase in χ_p from the loessite into the paleosol. The fact that the χ_b is elevated due to an increase in SP material in the paleosol is consistent with results published by other researchers on Quaternary-Pliocene paleosols developed in the Chinese Loess Plateau (e.g., Heller and Liu, 1984; Kukla et al., 1988; Hunt et al., 1995).

In contrast, χ_b does not exhibit a consistent vertical pattern and SP material is not as important in controlling χ_b in the three couplets from the lower Cutler beds. In the couplet shown in Figure 4.2b, χ_p comprises a relatively high fraction of the χ_b and is probably influenced by the high-field χ of hematite (Collinson, 1983) as well as clays. The results of the low-temperature experiments are consistent with the presence of more remanence-carriers, predominantly hematite and subordinate magnetite and maghemite, in the loessite (Figure 4.3b). The reason for the greater abundance of remanence-carrying grains within the loessite compared to the paleosol remains unclear. The upper couplet illustrated in Figure 4.2c has consistent trends in terms of χ_b, χ_f, and χ_f/Ms compared to the results from the Maroon Formation. The low-temperature curves (Figure 4.3c), however, provide contradictory evidence, i.e. they do not indicate differences in the SP content. The differences in the low-temperature results appear to be caused by remanence carriers as it is the case with the couplet shown in Figure 4.2b. The third lower Cutler beds couplet (Figure 4.2c, lower couplet) does not exhibit a vertical pattern of χ_b variation although the low-temperature analyses indicate higher SP material near the top of the paleosol. The lack of consistency in the rock-magnetic data in the two loessite-paleosol couplets shown in Figure 4.2c is puzzling but may relate to heterogeneous samples, perhaps as a result of pedogenic carbonate. The paleosols in the lower Cutler beds contain variable amounts of pedogenic carbonate, which could produce a selective dilution of the rock-magnetic signals. Testing this particular hypothesis, however, will require further analysis that is currently underway.

The SP magnetite in the Maroon Formation and the lower Cutler beds is interpreted as pedogenic, whereas the coarser magnetite is authigenic and/or detrital in origin. The maghemite

interpreted to be present in the lower Cutler beds probably formed due to oxidation of magnetite (Özdemir et al., 1993), perhaps as a result of weathering. This maghemitization process may have masked or destroyed part of the χ_b signal, which was possibly carried by pedogenic (SP) magnetite. Detrital and diagenetic hematite are present in both units.

In summary, the results from the Maroon Formation loessite-paleosol couplet are similar to those reported for the Chinese loess-paleosol sequences and suggest that χ_b variations track climatically-controlled pedogenesis and can be preserved in ancient strata (Soreghan et al., 1997; Tramp, 2000). In contrast, the nearly coeval lower Cutler beds, which formed in similar loess deposits, exhibit more variable χ_b patterns, which are not controlled by SP magnetite. It is likely that the SP material was created during pedogenesis but has not been preserved, perhaps as a result of oxidation. This study shows the value of using an integrated rock-magnetic and sedimentologic approach in addition to χ_b to develop a better understanding of the controls on χ_b, and to assess the origin (magnetic carriers), preservation, and possible paleoclimatic significance of ancient loess-paleosol sequences.

References Chapter 4

Begét, J.E., Stone, D.B., and Hawkins, D.B., Paleoclimatic forcing of magnetic susceptibility variations in Alaskan loess during the late Quaternary, *Geology, 18*, 40-43, 1990.

Collinson, D.W., Methods in Palaeomagnetism and Rock Magnetism, *Chapman and Hall*, London, 500 pp., 1983.

Condon, S.M., Geology of the Pennsylvanian and Permian Cutler Group and Permian Kaibab Limestone in the Paradox Basin, southeastern Utah and southwestern Colorado, *U. S. Geological Survey Bulletin 2000-P*, 46 pp., 1997.

Heller, F., and Liu, T.S., Magnetism of Chinese loess deposits, *Geophys. J. R. Astr. Soc., 77*, 125-141, 1984.

Heller, F., Liu, X.M., Liu, T.S., and Xu, T.C., Magnetic susceptibility of loess in China, *Earth Planet. Sci. Lett., 103*, 301-310, 1991.

Hunt, C.P., Banerjee, S.K., Han, J., Solheid, P.A., Oches, E., Sun, W., and Liu, T.S., Rock-magnetic proxies of climate change in the loess-paleosol sequences of the western Loess Plateau of China, *Geophys. J. Int., 123*, 232-244, 1995.

Johnson, S.Y., Stratigraphic and sedimentologic studies of Late Paleozoic strata in the Eagle basin and northern Aspen subbasin, northwest Colorado, *U.S. Geological Survey Open-File Report 87-286*, 82 pp., 1987.

Johnson, S.Y., Significance of loessite in the Maroon Formation (Middle Pennsylvanian to Lower Permian), Eagle Basin, northwestern Colorado, *J. Sedim. Petrol., 59*, 782-791, 1989.

Johnson, S. Y., Chan, M. A., and Konopka, E. A., Pennsylvanian and early Permian paleogeography of the Uinta-Piceance Basin region, northwestern Colorado and northeastern Utah: *U. S. Geological Survey Bulletin 1787-CC*, 35 pp., 1992.

Kluth, C.F., and Coney, P.J., Plate tectonics of the Ancestral Rocky Mountains, *Geology, 9*, 10-15, 1981.

Kukla, G., Heller, F., Liu, X.M., Xu, T.C., Liu, T.S., and An, Z.S., Pleistocene climates in China dated by magnetic susceptibility, *Geology, 16*, 811-814, 1988.

Liu, X.M., Shaw, J., Liu, T.S., Heller, F., and Yuan, B., Magnetic mineralogy of Chinese loess and its significance, *Geophys. J. Int., 108*, 301-308, 1992.

Mack, G.H., James, W.C., and Monger, H.C., Classification of Paleosols, *Geol. Soc. Am. Bull., 105*, 129-136, 1993.

Maher, B.A., Magnetic properties of modern soils and Quaternary loessic paleosols: paleoclimatic implications, *Paleogeogr., Paleoclimatol., Paleoecol., 137*, 25-54, 1998.

Maher, B.A., and Taylor, R.M., Formation of ultra-fine-grained magnetite in soils, *Nature, 336*, 368-371, 1988.

Murphy, K., Eolian origin of upper Paleozoic red siltstones at Mexican Hat and Dark Canyon, southeastern Utah, *M.S. Thesis, University of Nebraska*, 128 pp., 1987.

Nawrocki, J., Bakhmutov, V., Bogucki, A., and Dolecki, L., The paleo- and petromagnetic record in the Polish and Ukrainian loess-paleosol sequences, *Phys. Chem. Earth (A), 24*, 773-777, 1999.

Oches, E.A., Banerjee, S.K., Solheid, P.A., Frechen, M., High-resolution proxies of climate variability in the Alaskan loess record, *in* A. Busacca (ed.), Dust Aerosols, Loess Soils and Global Change (conference proceedings), Washington State University, 167-170, 1998.

Özdemir, Ö., Dunlop, D.J., Moskowitz, B.M., The effect of oxidation on the Verwey transition in magnetite, *Geophys. Res. Lett., 20*, 1671-1674, 1993.

Retallack, G.J., A color guide to paleosols: Chichester, *Wiley and Sons*, 175 pp., 1997.

Rutter, N.W., and Chlachula, J., Magnetic susceptibility and remanence record of the Kurtak Loess, southern Siberia, Russia, *Terra Nostra, 2*, 235, 1995.

Scotese, C.R., Paleogeographic Atlas, PALEOMAP Progress Report 90-0497, Department of Geology, *University of Texas at Arlington*, Arlington, Texas, 45 pp., 1997.

Scotese, C.R., and Golonka, J., Paleogeographic Atlas, PALEOMAP Project, Department of Geology, *University of Texas at Arlington*, Arlington, Texas, 34 pp., 1992.

Soreghan, G.S., Elmore, R.D., Katz, B., Cogoini, M., and Banerjee, S., Pedogenically enhanced magnetic susceptibility variations preserved in Paleozoic loessite, *Geology, 25*, 1003-1006, 1997.

Tramp, K.L., Integrated sedimentologic, geochemical, and rock-magnetic records of pedogenesis in the Pennsylvanian Maroon Formation loessite (Colorado), *M.S. Thesis, University of Oklahoma*, 212 pp., 2000.

Vlag, P.A., Oches, E.A., Banerjee, S.K., and Solheid, P.A., The paleoenvrionmental-magnetic record of the Gold Hill Steps loess section in central Alaska, *Phys. Chem. Earth (A), 24*, 779-783, 1999.

Zhou, L.P., Oldfield, F., Wintle, A.G., Robinson, S.G., and Wang, J.T., Partly pedogenic origin of magnetic variations in Chinese loess, *Nature, 346*, 737-739, 1990.

Concluding Remarks

The results of the studies presented herein reveal some of the complex pathways by which magnetic minerals like magnetite can form. Biological factors are shown to be responsible for the formation of magnetite in a hydrocarbon-contaminated soil under a variety of laboratory conditions. The findings indicate that biological processes may be important controls on authigenesis of magnetic minerals in some soils. In many sedimentary rocks, CRMs are a common occurrence and the studies on clay diagenesis at low burial temperatures indicate that heating of some smectites results in the precipitation of magnetite. In both studies at least a portion of the magnetite produced is large enough to carry remanence at room temperature and thus provide viable mechanisms for authigenesis of magnetic minerals which may be preserved in the rock record. The study presented in the last chapter provides insight into the complexity of the magnetic mineralogy in one type of geologic deposits – loessite-paleosol sequences, which are often thought to reflect climatic changes. The results indicate that a variety of rock magnetic techniques combined with sedimentologic analyses are useful in deciphering the origin, preservation, and possibly any paleoclimatic significance of geologic deposits.